Abstract

The characteristics of quasi-periodic (QP) ELF-VLF emissions with periods of 3–150 s and their relationships to magnetic pulsations are studied by using data obtained from Syowa and Mizuho Stations in Antarctica and Husafell in Iceland which is located near the geomagnetic conjugate point of Syowa Station. From the relations of QP emissions to magnetic pulsations, QP emissions are classified into two types, Type 1 and 2 QP emissions, according to whether the emissions are clearly associated with magnetic pulsations or not.

The typical characteristics of Type 1 QP emissions are as follows. The intensity and period of QP emissions change concurrently with variations in the intensity and period of magnetic pulsations. From the coherency analysis between QP emissions and Pc 3–4 magnetic pulsations it is found that the coherency between the D component of magnetic pulsations and the intensity fluctuations of QP emissions is much higher than that between the H component of magnetic pulsations and QPs. It is also found that the propagation time of magnetic pulsations (HM waves) from the interaction region between magnetic pulsations and QPs in the magnetosphere to the ground is 20–30 s. These properties are observed at conjugate-pair stations with good conjugacy. The results strongly suggest that Type 1 QP emissions are modulated by compressional mode Pc 3–4 magnetic pulsations near the equatorial plane in the outer magnetosphere.

On the other hand, QP emissions are categorized as the Type 2 QP emissions when the period of concurrent pulsations is entirely different from that of QP emissions or the amplitude of pulsations is too small to determine the periodicity. The most striking feature of Type 2 QP emissions are their very regular periodicity as compared with that of Type 1 QP emissions, and the Q value of the spectral peak usually attains to more than 10. In most cases magnetic variations during Type 2 QP events, which occur under magnetically quiet condition, have no spectral peak corresponding to the peak in QP's spectrum. However, a small but significant peak in pulsation spectrum is occasionally noted, when the Type 2 QP event occurs in modelate disturbed condition. The peak value of magnetic spectrum, in such a case, is generally two order of magnitude less than the maximum power of background magnetic fluctuations. The amplitude of magnetic pulsations is in the

order of 0.001 nT/s. The H component of magnetic pulsations tends to be more correlated with the VLF intensity variations than that the D component. These properties are observed at conjugate-pair stations with good conjugacy. It is suggested that weak magnetic pulsations, correlated with the Type 2 QP, are produced by wave induced particle precipitations. As to the periodicity of Type 2 QP emissions, either the period is controlled by compressional magnetic waves which are usually not detected on the ground, or the period of QPs is controlled by some other modulation mechanism which is unknown at present.

The frequency-time (f-t) spectra of QP emissions are classified into five types. A phenomenological model to explain the f-t spectra is proposed, that is, the rising-tone type of QP emission is generated by compressional mode Pc 3 magnetic pulsations which propagate in radial direction toward the earth, while the non-dispersive type is generated by standing oscillations of the magnetic field which have effective compressional components.

1. Introduction

1.1. General introduction

The magnetosphere is a complex system of energetic particles, thermal plasma, electromagnetic waves, magnetic and electric field. The main geomagnetic field, roughly a dipole, is influenced by the flow of charged particles known as the solar wind (PARKER, 1967), which causes the geomagnetic field to be confined within a boundary called the magnetopause. Outside the magnetopause on the sunward side exists a bow shock, where the supersonic flow of charged particles is interrupted and slowed down. Between the magnetopause and the bow shock, there exists a magnetosheath where the compressed and disordered interplanetary magnetic fields are contained.

On the dayside, the magnetopause lies at about $10\,R_E$. On the nightside, the magnetic field is drawn into a long tail which extends definitely to the moon's orbit at $\sim 60\,R_E$. The pattern of field lines within the tail is still largely unknown. A region of somewhat enhanced plasma density exists in the tail, and contains a thin neutral sheet in which the magnetic field is very weak and across which the field reverses in direction.

Within the magnetosphere, there exists an approximately donut-shaped region with relatively high plasma density, called the plasmasphere. The boundary between the outer magnetosphere and plasmasphere is called the plasmapause. The position of the plasmapause depends on local time and geomagnetic conditions.

The magnetosphere is permeated by hydromagnetic waves and electromagnetic ELF-VLF radiation, which have provided a great deal of information about its physical condition. For example, whistlers, produced by lightning discharges, propagate from hemisphere to hemisphere along the geomagnetic line of force and provide a powerful tool for studies of the structure and dynamics of the inner magnetosphere. The nose whistler, discovered by HELLIWELL *et al.* (1956), led to the discovery of the plasmapause (CARPENTER, 1962, 1963, 1966). Whistlers have recently been used to measure the magnetospheric convection electric field and coupling fluxes of the ionization between the ionosphere and the plasmasphere.

ELF-VLF emissions also carry information about solar-terrestrial relation-

ships. BRICE (1964a) divided VLF emissions into two broad categories, discrete emissions and hiss. Detailed descriptions of ELF-VLF emissions can be found in HELLIWELL's monograph (1965). VLF emissions with fairly regular periods, longer than the two-hop whistler delay, are known as quasi-periodic (QP) emissions (HELLIWELL, 1965) or long period VLF emissions (CARSON *et al.*, 1965). Among many the natural emissions, QP emissions are perhaps still not understood. They are the main subject matter of this study.

1.2. Historical background on ELF-VLF emission study

L.R.O. STOREY presented his pioneering work on the whistler atmospherics in 1953 (STOREY, 1953). In his experimental study, he found a systematic relation between the whistler train and the preceding atmospheric click and he contributed also to the theoretical study of whistler by showing the existence of a low-frequency electromagnetic mode traveling very nearly along the direction of earth's magnetic field in the exosphere. With these observations and theoretical results, he concluded that electromagnetic energy originating in a lightning discharge echoes back and forth approximately along the line of force of the earth's magnetic field.

STOREY also mentioned other types of audio frequency atmospherics. These include 'dawn chorus', steady hiss and others which are now categorized into VLF emissions. Emissions of all these types were found to be associated with magnetic activity. The earlier work for such phenomena was done by BURTON (1930) and BURTON and BOARDMAN (1933). The description in their work that quasi-musical sounds were observed between 500 to 1500 cps, is now thought to correspond to the 'polar chorus' (HELLIWELL, 1965).

During the IGY many systematic observations for ELF-VLF natural waves were carried out all over the world. Data recorded on magnetic tape were analyzed by a high speed spectrum analyzer. A variety of shapes of frequency-time spectra were obtained, and were classified (GALLET, 1959). These works were extended by HELLIWELL (1965). The frequency-time spectral features of the emissions have been stimulating theoretical work.

Since 1962, most of the important informations on ELF-VLF emission phenomena from the outer space have been provided by satellite-borne instruments. Direct observations have given a variety of features of wave phenomena in the space plasma.

ELF-VLF chorus is one of the most common intense naturally occurring electromagnetic emissions found in the terrestrial magnetosphere. These emissions have been detected from the ground (BURTON, 1930; STOREY, 1953; ALLCOCK, 1957; GALLET, 1959; POPE, 1963; UNGSTRUP and JACKEROTT, 1963; EGELAND *et al.*, 1965), at ionospheric altitudes (TAYLOR and GURNETT, 1968; BARRINGTON *et al.*, 1971; THORNE *et al.*, 1977), and in the outer magnetosphere, the region where chorus is believed to be generated (RUSSELL *et al.*, 1969; DUNCKEL and

HELLIWELL, 1969; TSURUTANI and SMITH, 1974, 1977; BURTON and HOLZER, 1974; BURTIS and HELLIWELL, 1976). The above studies have shown that chorus is present at L values between the plasmapause and the magnetopause at all local times but predominantly in the dayside magnetosphere. Emission frequencies are found to be related to the local electron gyrofrequency. For a review of magnetospheric ELF-VLF wave observations, see RUSSELL *et al.* (1972) and GENDRIN (1975).

The study of ELF-VLF chorus is important from a magnetospheric physics point of view. The pitch angle scattering as a result of a cyclotron resonance between chorus and trapped electrons leads to the loss of the electrons by precipitation (BRICE, 1964b; KENNEL and PETSCHEK, 1966; KIMURA, 1967; HOLZER *et al.*, 1974). The precipitation causes ionospheric phenomena such as bremsstrahlung X-rays, diffuse aurora, riometer absorption, magnetic pulsation, 5–10 s quasi-periodic aurora and X-ray pulsations (MCPHERRON *et al.*, 1968; ROSENBERG *et al.*, 1971).

1.3. Historical background on quasi-periodic ELF-VLF emission study

A type of ELF-VLF radio noise generated in the earth's magnetosphere is observed as a series of bursts with some regularity and relatively long time separation. The bursts are known as quasi-periodic (QP) ELF-VLF emissions. QP emissions were first reported by WATTS *et al.* (1963), and a summary of early work on this phenomenon can be found in HELLIWELL (1965).

The period of QP emission ranges from 10 s to 2 min or more, and typically from 20 to 40 s at high latitudes (EGELAND *et al.*, 1965; KITAMURA *et al.*, 1969; SATO *et al.*, 1974). EGELAND *et al.* (1965) found that the signal strength of QP emissions with a period of 20–30 s often changes in association with magnetic pulsations with approximately the same period. CARSON *et al.* (1965) also observed that the QP period falls into the general range of magnetic pulsation periods. They suggested on this basis that hydromagnetic waves could be the source of oscillations for QP emissions. KOKUBUN (1971) also suggested that QP emissions associated with magnetic pulsations mostly occurred in the outer magnetosphere beyond the plasmapause.

QP emissions have been recorded at stations ranging in geomagnetic latitude from $\sim 50°$ to $\sim 80°$. On occasion they have been observed simultaneously over a wide range of latitudes (say, from $L=3.2$ to $L=6.8$) and longitudes (CARSON *et al.*, 1965). BRICE and SMITH (1965) reported QP activity on board the Alouette satellite extending over ~ 1700 km at an altitude of 1000 km. Recently, CORNILLEAU-WEHRLIN *et al.* (1978) reported that QP emissions are observed simultaneously at the GEOS-1 satellite and at approximately geomagnetic conjugate stations on the ground.

The geomagnetic conjugacy of QP emissions was examined by CARSON *et al.*

(1965), KITAMURA *et al.* (1969) and KOROTOVA *et al.* (1975). CARSON *et al.* (1965) reported that the periodic components recorded in the north alternate in time with those observed in the south. In this study we also observed QP conjugacy.

Recent studies have revealed that QP emissions are not always associated with concurrent corresponding magnetic pulsations and that there are significant differences in the emission properties of QP emissions associated with magnetic pulsations, compared with those having no corresponding pulsation (KITAMURA *et al.*, 1969; SATO *et al.*, 1974; see review KIMURA, 1974). It is also found that QP emissions not associated with magnetic pulsations are more often observed at Eights ($L\sim4$) than at Byrd ($L\sim6.8$). HO (1973) has reported that QP emissions observed at Eights is strongly modified by whistlers and other whistler mode signals, and it was also reported that the emission frequency tends to decrease with increasing observing latitude. These results indicate that the characteristics of QP emissions change with latitude and that the generation of QP emissions may be controlled by different physical processes in different magnetospheric regions.

Theoretical discussions to explain the characteristics of QP emissions have been presented (CORONITI and KENNEL, 1970; KIMURA, 1974; CHEN, 1974; HAUGSTAD, 1975, 1976; BESPALOV and TRAKHTENGERTS, 1976; SAZHIN, 1977; BESPALOV, 1977). However, it is hard to solve the complex features of QP's spectra.

2. Instrumentation and Observations

The data of ELF-VLF emissions, magnetic pulsations and related phenomena, used in this study, were obtained during five observation periods, i) February 1970–January 1972 at Syowa Station, ii) February 1972–January 1973 at Syowa Station, iii) February 1974–January 1975 at Syowa Station, iv) September 1976–September 1977 at Syowa and Mizuho Stations, Antarctica, and v) July 29, 1977–September 18, 1977 at Husafell, Iceland.

Coordinated observations of polar disturbance phenomena, ELF-VLF emissions, geomagnetic variations, auroral activities and others, have been carried out at Syowa Station. ELF-VLF signals below 4 kHz have been recorded almost continuously at Syowa Station since 1969, using a magnetic tape recorder with an automatic reverse device. It enabled us to examine frequency-time spectra as required for most of the emission events by reproduction from magnetic tapes. Emission signal strengths of five selected bands below 2 kHz together with magnetic pulsation signals have also been recorded on a strip chart. These records were mainly used in calculating the statistics of QP emission occurrences. Six-channel chart records of narrow band ELF-VLF intensities in the frequency range of 0.5–2 kHz together with magnetic pulsations were examined for the 2 year period from February 1970 to February 1972. Statistical results for this period will be shown in Section 3. Wide-band signals from 0.2 kHz to 10 kHz and the three components of magnetic pulsations were simultaneously recorded on magnetic tapes using a 4-tracks data recorder, during January 1973. This record is most useful for examining the relative phase relation, power spectra, and correlation between QP emissions and magnetic pulsations. The relationship between QP emissions and magnetic pulsations based on this data will be discussed in Section 8.

2.1. Outlines of observation system

The outlines of QP emission and related phenomena observed in the periods iii), iv) and v) are as follows;

2.1.1. Observation period from February 1974 to January 1975

The data obtained are;

1) Variations of geomagnetic field in north-south (H), east-west (D) and vertical (Z) components measured by a fluxgate magnetometer (chart speed, 5 cm/h and sensitivity 10 γ/mm).

2) Three components of magnetic pulsations ($\dot{H}$, $\dot{D}$ and $\dot{Z}$) measured by an induction magnetometer. Both a magnetic tape and a 35 mm scratch film record (film speed, 10 mm/min) are used here. The frequency range is below 3 Hz with a sensitivity of 0.01 γ/s/mm on the scratch film record.

3) ELF-VLF natural radio waves

i) Continuous recordings of ELF-VLF signals in the frequency range 0.2–20 kHz using a magnetic tape recorder.

ii) Intensities of ELF-VLF emissions in narrow frequency bands recorded on strip chart (speed, 30 cm/h) at 0.4, 0.7, 1.0, 1.5, 2.0 kHz, with a band width of 40 Hz.

iii) Continuous records of arrival direction (N_x, N_y) polarization and emission intensity at three frequency bands, 0.75, 2.5 and 8 kHz. Details will be discussed in a later section.

4) Correlation records

i) Simultaneous records of intensities in ELF-VLF wave at the frequency bands of 0.75 kHz, 2.5 kHz and magnetic pulsations in the $\dot{D}$ component on strip chart (speed, 3 cm/min).

ii) Simultaneous record of luminosity of the auroral green line, the H component of magnetic field variations, the $\dot{H}$ component of magnetic pulsations, cosmic noise absorption and intensities of ELF-VLF emissions in frequency bands at 0.75, 1.5, 8, 32 kHz on an 8-channel strip chart (speed, 15 cm/h).

2.1.2. Observation period from September 1976 to September 1977

Observations of ELF-VLF emissions, magnetic variations and auroras have been carried out at Syowa Station (geographic lat. −69.03, long. 39.69, geomagnetic lat. −70.03, long. 79.39) and Mizuho Station (geographic lat. −70.70, long. 44.33, geomagnetic lat. −72.32, long. 80.62). Mizuho Station is located about 270 km poleward from Syowa Station on the same magnetic meridian. Details of observation systems in this period were described by MAKITA *et al.* (1978). Characteristics of ELF-VLF emissions and QP emissions observed simultaneously at Syowa and Mizuho Stations will be shown in Section 7.

2.1.3. Observation period from July 29, 1977 to September 18, 1977 at geomagnetic conjugate-pair stations

The coordinated observations of ELF-VLF emissions, magnetic pulsations and auroras have been carried out at Syowa and Mizuho Stations in Antarctica and Husafell, Iceland from July 29, 1977 to September 18, 1977. Locations of Husafell, Reykjavik and the calculated conjugate point of Syowa and Mizuho Stations are shown in Fig. 1. As seen in the figure Husafell is located about 60 km

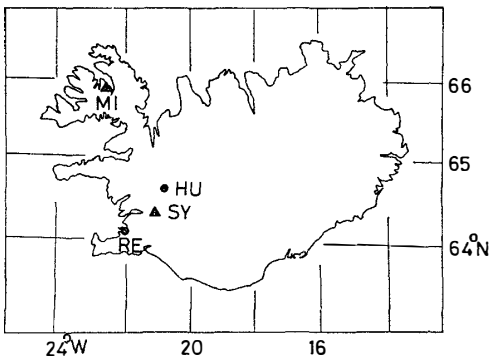

Fig. 1. Locations of Husafell, Reykjavik and the geomagnetic conjugate points of Syowa and Mizuho Stations.

Table 1. Geographic and geomagnetic coordinate.

Stations	Geographic		Geomagnetic	
	Latitude	Longitude	Latitude	Longitude
Syowa Station	−69.03	39.69	−70.03	79.39
Mizuho Station	−70.70	44.33	−72.32	80.62
Reykjavik, Iceland	64.14	−21.88	69.87	72.41
Husafell, Iceland	64.70	−20.90	70.19	74.24

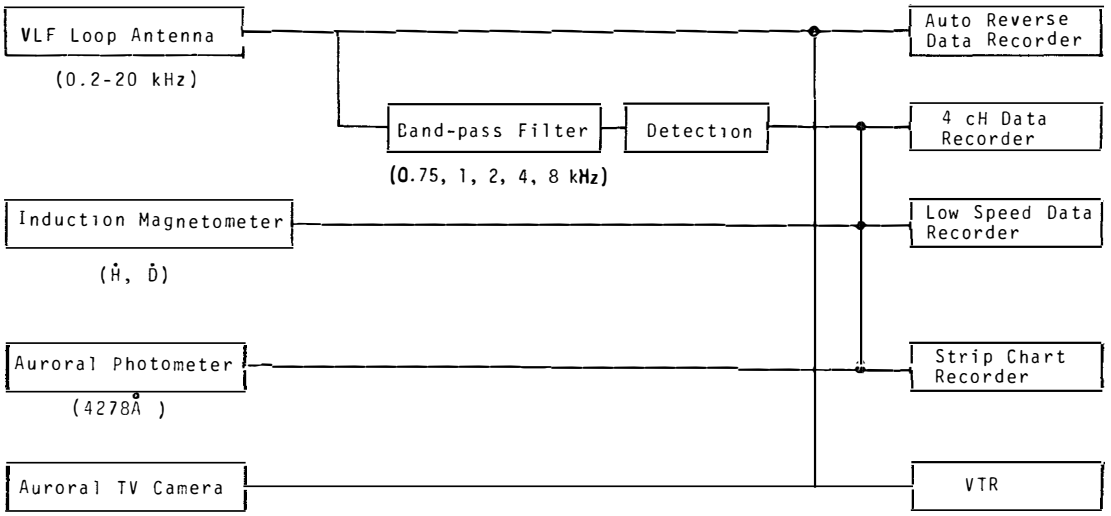

Fig. 2. Block diagram of the observation system at Husafell.

north of the geomagnetic conjugate point of Syowa Station. Geographic and geomagnetic coordinates of these stations are listed in Table 1. The block diagram of observation system at Husafell is shown in Fig. 2. The observation system at Husafell is as follows;

1) Two horizontal components ($\dot{H}$ and $\dot{D}$) of magnetic pulsations in the frequency range below 3 Hz were measured with an induction magnetometer of which the frequency response is the same as that at Syowa Station and were recorded on magnetic tape and on a strip chart (speed, 30 cm/h).

2) ELF-VLF natural emissions

i) Continuous record of wide band signals in the frequency range of 0.2–20 kHz using a magnetic tape recorder.

ii) Intensity of emission at selected frequency bands, 0.75, 1.0, 2.0, 4.0, 8.0 kHz, with a Q value of 40, recorded on a strip chart (speed, 30 cm/h).

3) Correlation records

i) Simultaneous records of wide band (0.3–10 kHz) ELF-VLF emissions, the $\dot{H}$ and $\dot{D}$ components of magnetic pulsations and auroral luminosity (4278 Å) on the same magnetic tape. These records were obtained only during the occurrence of QP emissions.

ii) Simultaneous records of ELF-VLF emissions in narrow bands (0.75, 1.0, 2.0 kHz), and the $\dot{H}$ and $\dot{D}$ components of magnetic pulsations. These records were obtained for this observation period, continuously from July 29 to September 18, 1977.

2.2. The device for finding the arrival directions of waves

The observations of arrival direction for elliptically polarized ELF and VLF electromagnetic waves, based on the method developed by TSURUDA and HAYASHI (1975), was carried out at Syowa Station from April 1974 to January 1975.

A diagram of the observation system is shown in Fig. 3 and the coordinate system used hereafter is shown in Fig. 4, where $\vec{N}$ is a unit vector in the direction of wave the normal. N_x and N_y can be written as $N_x = \sin\theta \sin\phi$ and $N_y = \sin\theta \sin\phi$ if θ is the incident angle measured from the zenith and ϕ is the azimuthal angle measured from the east, respectively. The vertical component of electric field (E_z) and the horizontal component of magnetic field (B_x, B_y) are detected by a vertical antenna and orthogonal loop antennas, respectively. The signals are fed to pre-amplifiers through the equalizer network. The signals after the pre-amplification of about 40 dB are transmitted through low impedance cables of 550 m in length to main amplifiers which were installed in an observation house. The signals then were amplified by 60 dB, and are fed to the band-pass filters with Q values of

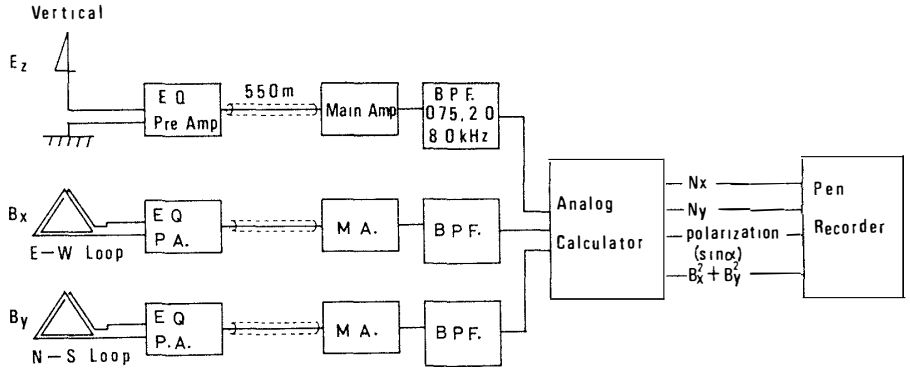

Fig. 3. Block diagram of the receiving system.

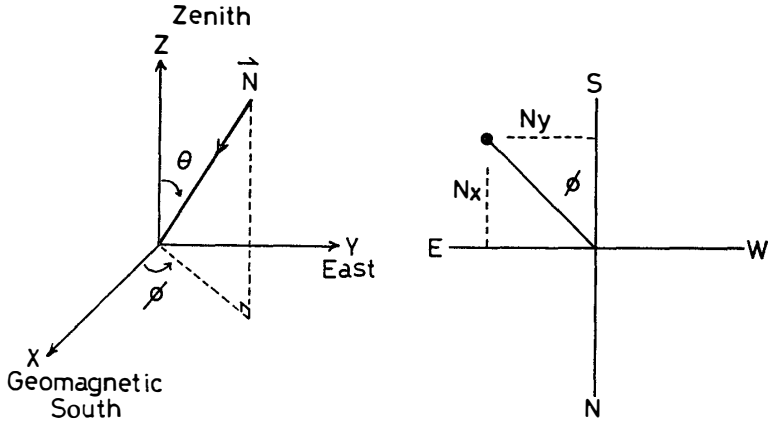

Fig. 4. Coordinate system for assigning the arrival direction of incident waves, wave normal vector ($\vec{N}$), incident angle (θ), azimuth angle (ϕ), north-south and east-west horizontal components of wave normal vector (N_x and N_y).

44, whose center frequencies are 0.75, 2.5 and 8.0 kHz. Then, the signals in the selected bands were fed to an analog calculator that calculates the horizontal components of wave normal vector (N_x, N_y) and the polarization angle ($\sin\alpha$). The calculated output signals were recorded on a strip chart. Furthermore, three components of the wide-band signals were recorded on magnetic tape using an FM data recorder.

2.2.1. Detection of the wide-band VLF signal

The antennas for detecting the arrival direction of the waves were set on a flat place 550 m away from the observatory house. The vertical antenna for receiving vertical electric field is a metal pipe 3 m long. In order to compensate for the effect of poor conductivity of the ground, a counterpoise was set out radially at the foot of the vertical antenna using 36 copper wires each 4 m long. The calculated value of capacitance of this vertical antenna was 39.9 pF. The crossed loops for receiving the magnetic field of the wave were oriented in the geomagnetic east-west (B_x) and north-south (B_y) directions. Each of the loop antennas was triangular in shape of two turns, 10 m in height and 20 m in length at the base. The effective area, inductance and DC resistance for these two loop elements were 200 m^2, 230 μH, and 0.3 Ω, respectively.

Usually, the E_z component is received by a vertical antenna which is equivalent to a series circuit of capacitance C_a fed from a voltage source $l \cdot E$, where l is the effective height of antenna and E is the intensity of electric field. The loop antenna is equivalent to the series circuit of inductance L_a, resistance r_a fed from a voltage source V_l. V_l can be estimated in terms of wave electric field E as;

$$V_l = -j\frac{S_a}{C} \cdot E,$$

where S_a is the effective area of the loop and C is the speed of light. Generally, antennas of these two types, vertical and loop antennas, respond differently to the

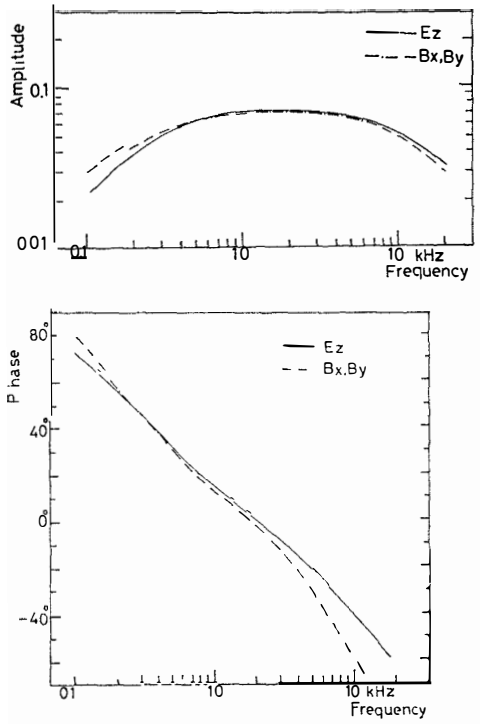

Fig. 5. Frequency-amplitude response (upper) and frequency-phase response (lower) of the equalization system (E_z, B_x and B_y) in the receiving circuit.

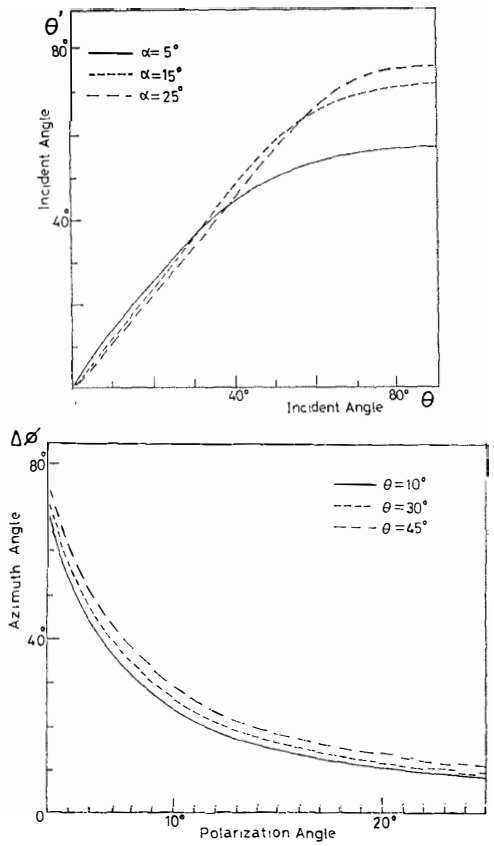

Fig. 6. Correction for the incident angle (θ) and azimuth angle (ϕ) due to the errors of the phase angle in the receiving system. In this calculation, the rate of TE to TM mode intensity and the phase difference between E_z and B_x, B_y are assumed to be unity and 3°, respectively.

incident wave fields, so that an additional CR network is required to equalize the response of the two antenna systems. Fig. 5 shows the changes for B_x, B_y and E_z in phase and amplitude with frequency of the original incident wave in the equalizing network. The phase differences are mostly caused by the phase shift of the signals in the input transformer of the loop system preamplifiers.

At 0.75 kHz, the phase of E_z was 3° in advance in comparison with B_x and B_y as shown in Fig. 5. Errors of the azimuth and incident angles were estimated for the case when the E_z phase precedes by 3° those of B_x and B_y (SATO and HAYASHI, 1976). The relationships between ϕ, θ, ϕ', θ', and sin α is shown in Fig. 6, where ϕ and θ are the calculated azimuth and incident angles when there is no phase difference between E_z and the magnetic components. ϕ' and θ' are calculated values of azimuth and incident angles with 3° of phase difference, and $\Delta\phi$ is the error between ϕ and ϕ'. In this estimation, the ratio of TE mode in-

tensity to TM mode intensity was assumed to be unity. From the curve in Fig. 6, we can conclude that the error in θ and ϕ are less than 10° and 20°, respectively, when the polarization angle α is greater than 15° and θ is smaller than 60°.

2.2.2. Direction analyzer

The block diagram of the direction analyzer is shown in Fig. 7. The center frequency of the narrow band-pass filter was chosen to be 750 Hz in this analysis. In the phase shifter netwark, E'_z, B'_x was lagged by 45° and B''_x, B''_y was lagged by 135°, with the phase difference of 90° between E'_z, B'_x and B''_x, B''_y. In order to calculate the horizontal component of wave normal vector N_x, N_y and polarization angle, E'_z, B'_x, B''_x and B''_y signals were multiplied by and divided by each other (details in TSURUDA and HAYASHI, 1975).

The integration time for output signal was selectable; 0.1, 1.0, 2.0 and 10 s. In this preliminary observation, 10 s was adopted for the integration time, because we were interested in the average arrival direction. As the dynamic range of the analog multiplier used in this calculator was about 30 dB, the division of $(E'_z \cdot B''_x)$ by $(B'_x \cdot B''_y)$ tended to enhance the error of the analog calculation, especially when the latter was small. Hence, the output of N_x and N_y were controlled to be zero when the calculated emission intensity $B_x^2 + B_y^2$ was small. From the examination of the statistical relation between calculated N_x, N_y and emission intensity $B_x^2 + B_y^2$ of natural emissions, we can conclude that i) errors due to the low dynamic range of the analog calculator increased more than 20% at the intensity level lower than 1.5×10^{-5} V/m$\cdot\sqrt{\text{Hz}}$, ii) the calculated incident angle is slightly smaller than the real incident angle but the calculated azimuth has reasonable accuracy when the intensity of the wave is in a range $1.5-3 \times 10^{-5}$ V/m$\cdot\sqrt{\text{Hz}}$, and iii) when emission intensity is greater than 3×10^{-5} V/m$\cdot\sqrt{\text{Hz}}$ the errors caused by the analog calculator are almost eliminated, within 10% for incident angle and 5% for azimuth. Thus, on the basis of this examination we analyzed the data only when the emission intensity was greater than 1.5×10^{-5} V/m$\cdot\sqrt{\text{Hz}}$. These results will be shown in Section 6.

The observation system for the direction of arrival operated from September 1976 to January 1977 was described by MAKITA (1978).

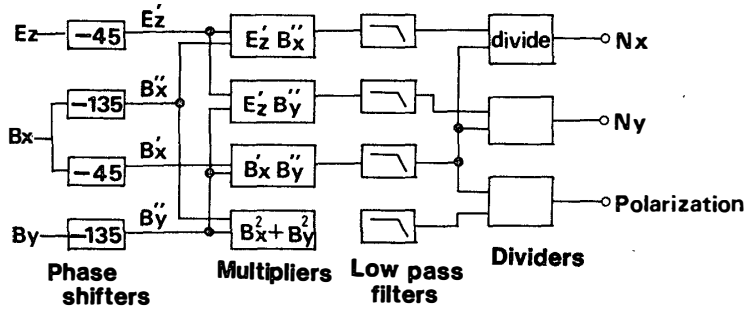

Fig. 7. Schematic illustration of the analog analyzer for the direction finder.

3. General Properties of QP Emissions

In this section we describe the statistical characteristics of QP emissions. ELF-VLF data used here are those obtained at Syowa Station in Antarctica. The intensity records of ELF-VLF emissions in narrow frequency bands recorded continuously for 2 year period from February 1970 to 1972 are examined.

QP emissions are classified into two types by a procedure similar to that of KITAMURA *et al.* (1969), according to whether or not the QP emissions are associated with magnetic pulsations. Fig. 8 shows amplitude records of VLF signal strength, magnetic pulsations and frequency-time spectra of emissions indicating typical examples of the QP emissions associated with magnetic pulsation. This type will be called Type 1 QP emissions in the following. It is noted that quasi-periodic modulations of VLF waves began almost simultaneously with the occurrences of magnetic pulsations at 1228 UT (Fig. 8a) and at 1256 UT (Fig. 8b). It is also seen in Fig. 8b that the cessation of QP modulation occurred in association with the disappearance of magnetic pulsations, indicating a close relation between the two phenomena. On the other hand, Fig. 9 shows typical examples of the frequency-time spectra of QPs and amplitude records of VLF signal strength and magnetic pulsations where QPs do not relate to magnetic pulsations. This will be called hereafter Type 2 QP emissions. As seen in Fig. 9a, well-defined QP emissions often occurred without any corresponding magnetic pulsation. In the example shown in Fig. 9b, QP emissions almost simultaneously appeared after magnetic pulsation activity decreased. Also, there are often QP emissions with the periods entirely different from that of the concurrent magnetic pulsations. QP emissions in these categories are classified as the same type (Type 2). It is noticeable from these figures that the recurrent periodicity of Type 2 QPs is much more regular than that of Type 1 QPs and the amplitude of magnetic pulsation corresponding to Type 2 QPs is much weaker than that of Type 1 QPs, so that we can easily distinguish the two types of QPs.

The two types of QPs have the following characteristics.

1) Type 1 QPs (QPs associated with concurrent magnetic pulsations):
   i) Intensities of magnetic pulsations are stronger than 0.05 γ/s.

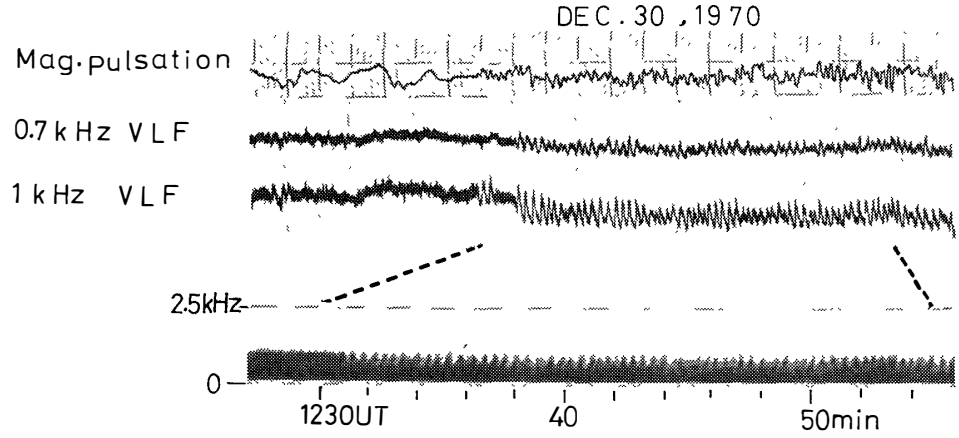

Fig. 8a. Examples of simultaneous onset and cessation of QP emissions and geomagnetic pulsations on December 30, 1970. It is seen that the modulation of preceding quasi-steady emissions occurred simultaneously with the onset of geomagnetic pulsations with periods of modulation of about 24 s.

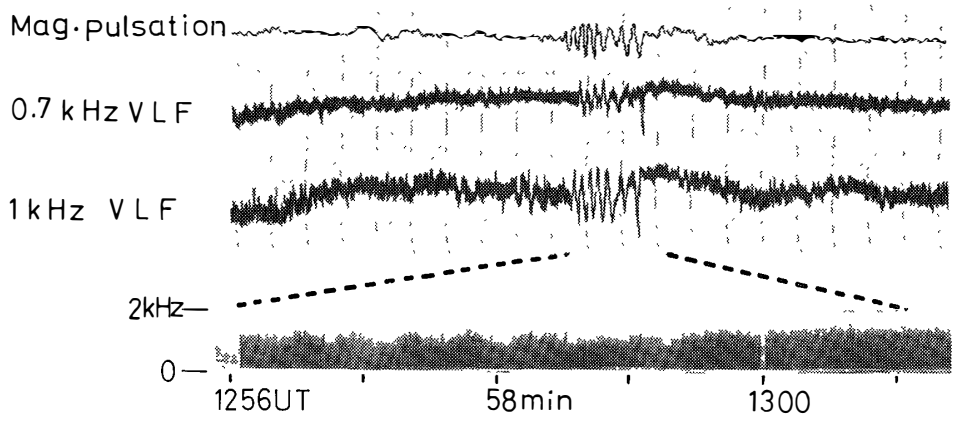

Fig. 8b. Same as for Fig. 8a, except for the data on November 26, 1970.

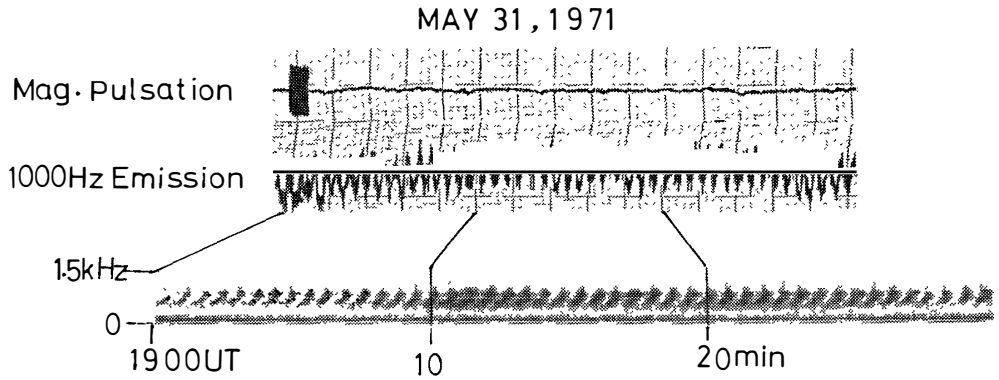

Fig. 9a. Example of a QP emission with a regular period of 40 s, and with no corresponding pulsation on May 31, 1971.

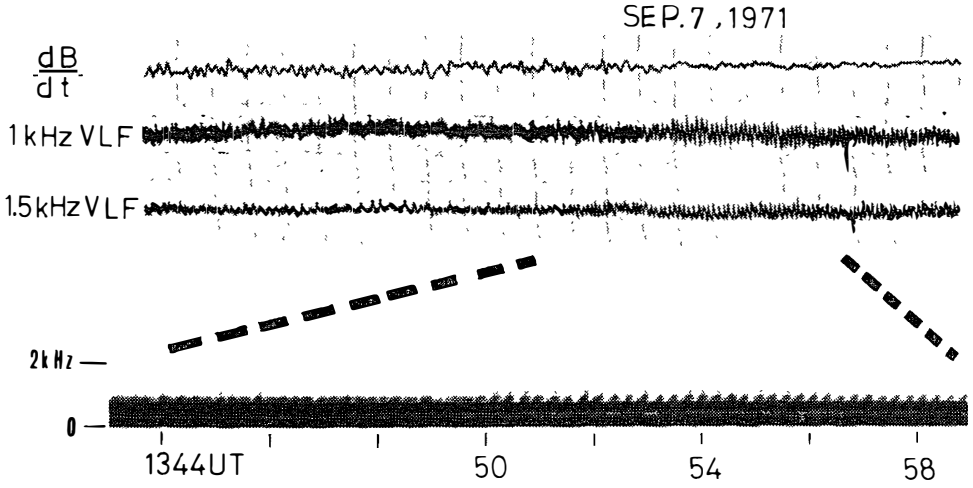

Fig. 9b. Example of a QP event in which the periods of QP emissions and pulsations are entirely different. In this case fairly regular QP emissions with a period of 16 s occurred following a decrease in pulsation activity.

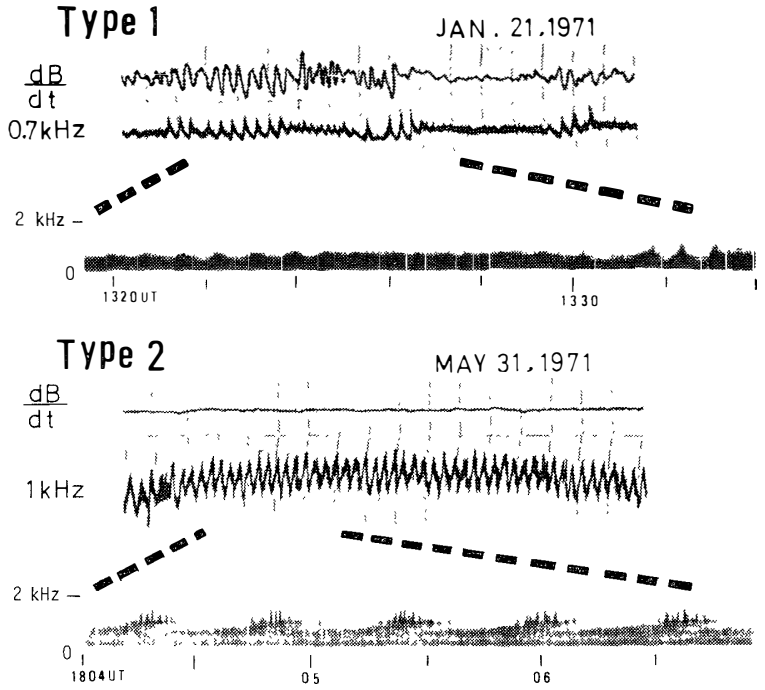

Fig. 10. Examples of QP emissions associated with geomagnetic pulsations with approximately the same period (Type 1), and without any corresponding pulsations (Type 2). It is noted that Type 2 emission is more regular than Type 1.

ii) Ten minute-average periods of QPs and magnetic pulsations are nearly the same (within the error of 10%).

2) Type 2 QPs (QPs not associated with magnetic pulsations):

i) Intensities of magnetic pulsations are weaker than 0.01 γ/s. The period of magnetic pulsations is difficult to determine from the chart record with the amplitude less than 0.01 γ/s.

ii) Ten minute-average periods of QPs and concurrent magnetic pulsations are entirely different.

iii) Recurrent periodicity is regular and their duration is longer than 10 min.

Fig. 10 shows typical Type 1 QP and Type 2 QP emissions. As will be described later, distinct differences of local time of occurrence, QP periods, emission frequency, Kp dependence and frequency-time spectra were observed between two types of QP emissions.

3.1. Diurnal variation of QP occurrences

Fig. 11 illustrates the diurnal variation of hourly occurrence of QP emissions at Syowa Station for a one year period from February 17, 1970 to February 16, 1971. Most of QP emissions were observed on the dayside with a maximum occurrence around noon, as was found by KITAMURA *et al.* (1969). This tendency is also corresponds to the diurnal variation of polar chorus occurrence (KOKUBUN *et al.*, 1969; HAYASHI and KOKUBUN, 1971). However, occurrences of two QP

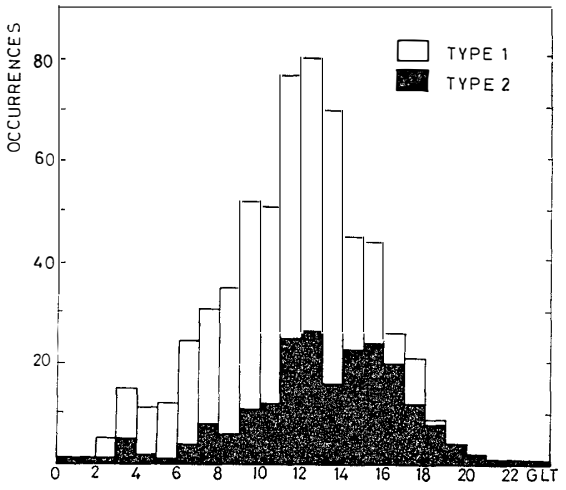

Fig. 11. Diurnal variations of QP emission occurrence. Hourly occurrences during one year period from 17 February 1970 are plotted for each of the two types.

types are significantly different. The occurrence of Type 1 had a maximum around noon while that of Type 2 had a maximum around noon and also a secondary maximum in the afternoon-evening period. It is worth noting that Type 2 was also observed between 19h and 02h MLT. The high occurrence of Type 2 in the afternoon-evening was very similar to QP emissions observed at Eights ($L\sim4$) (Ho, 1972).

3.2. Diurnal variation of QP periods

The diurnal variation of QP periods for each type is given in Fig. 12. In these statistics Type 1 QP emissions comprised one year's data from February 1970 to January 1971, and Type 2 QPs with duration longer than 10 min comprised two year's data from February 1970 to January 1972. The hourly

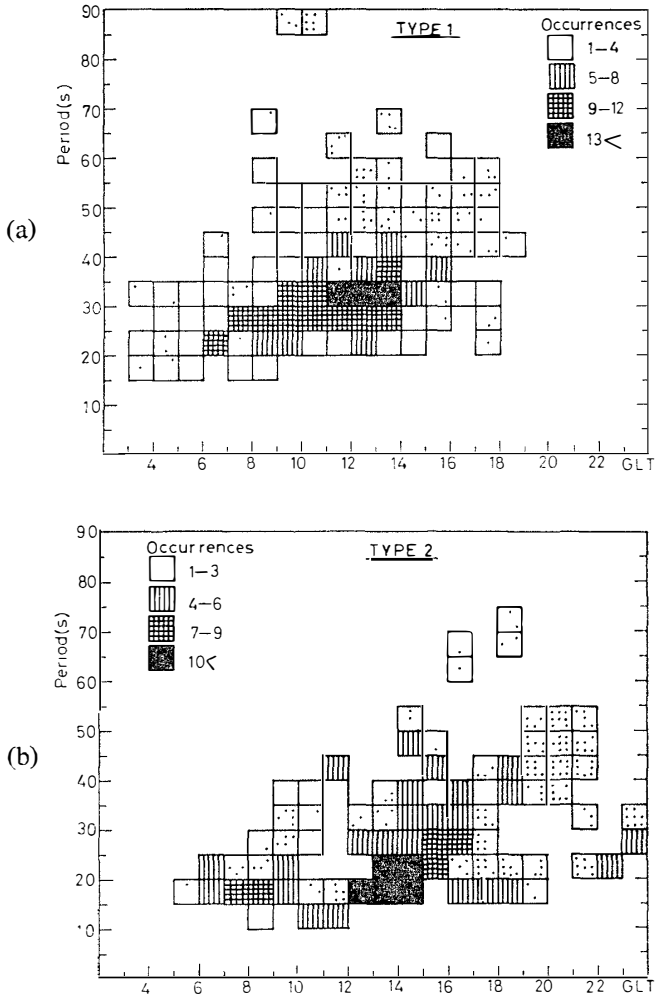

Fig. 12. Distributions of the QP period versus geomagnetic local time. (a) Type 1 and (b) Type 2.

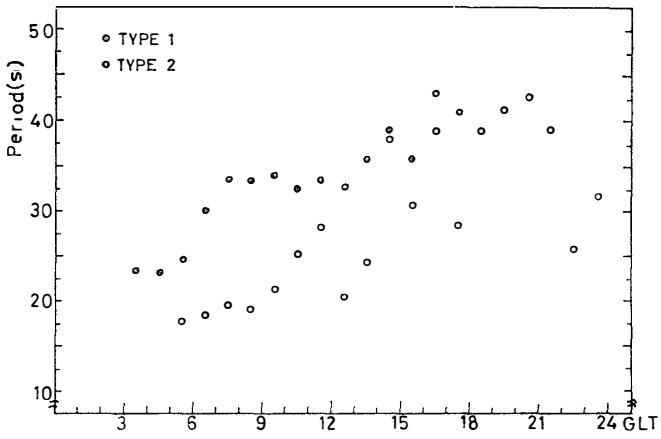

Fig. 13. Diurnal variations of hourly average periods. The black circles represent the average periods of the Type 1 QP emissions and the open circles show those of the Type 2.

occurrence distribution of QPs periods for Type 1 and Type 2 QP emissions, respectively, are plotted in Fig. 12a and Fig. 12b. In these statistics we neglected shorter period QPs (<10 s), since we could not determine such QP periods on a slow speed chart record (0.5 cm/min). QP periods longer than 90 s were also excluded from this figure. The period of Type 1 QP ranges from 15 to 60 s, mostly around 30 s, and that of Type 2 QP from 10 to 60 s, mostly around 20 s. Fig. 13 shows diurnal variation of the hourly average period for each type. It is evident that the period tends to increase gradually from morning to evening for each type, and that Type 1 QP period is longer than Type 2 QP, especially in the morning sector.

3.3. Diurnal variation of emission occurrences

The diurnal variations of emission occurrence for all QP events, both of Type 1 and Type 2 QP emissions, are given in Fig. 14. It is clear that 0.5, 0.7 and 1.0 kHz band QPs were more often observed than 1.5 and 2.0 kHz band QPs. Furthermore, all frequency bands have maximum occurrence around noon. These tendencies are in agreement with the average frequency spectra of polar chorus emissions observed at Syowa Station (HAYASHI *et al.*, 1968). Fig. 15 shows diurnal variations of the occurrence probability for a QP emission at each frequency band, 0.5, 0.7, 1.0 and 1.5 kHz for both Type 1 QPs (cross hatch) and Type 2 QPs (dots).

Concerning the emission frequency of the Type 1 QP, the 0.7 kHz band QP occurred most frequently at all local time. Type 1 QPs at the frequency band of 0.5 kHz had a maximum occurrence in the early morning and gradually decreased from morning to afternoon. On the other hand, the occurrence of higher emission frequencies of Type 1 QPs at the frequency bands of 1.0 and 1.5 kHz

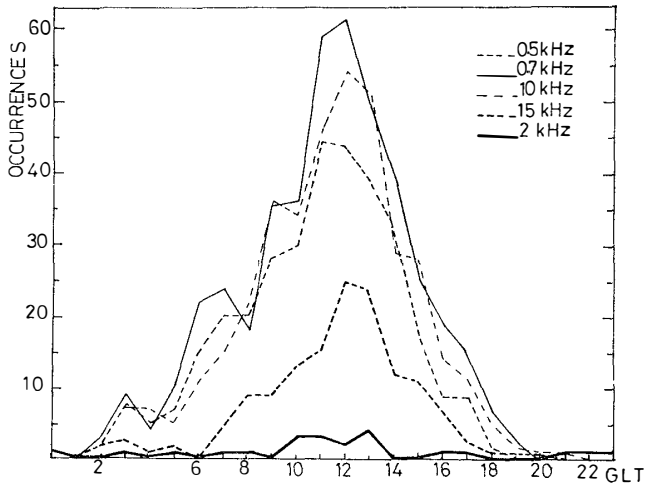

Fig. 14. Diurnal variation of QP occurrences for selected frequencies 0.5, 0.7, 1.0, 1.5 and 2.0 kHz.

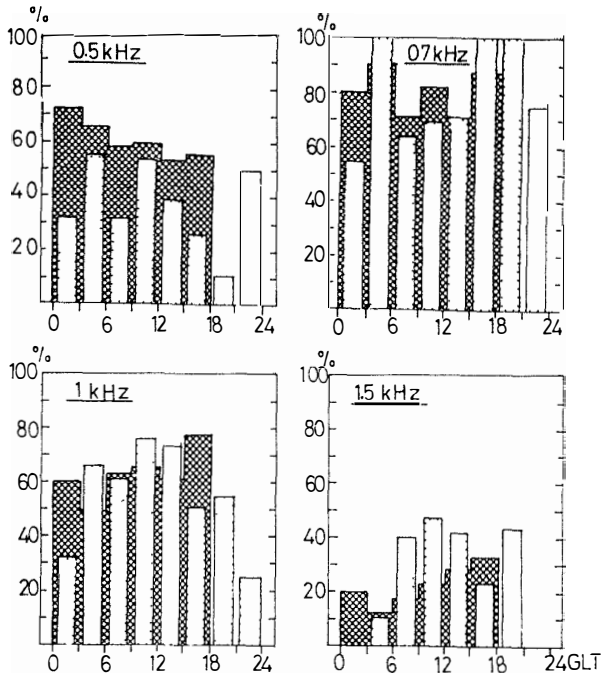

Fig. 15. Diurnal variation of the QPs occurrence probability for each frequency band, 0.5, 0.7, 1.0 and 1.5 kHz Type 1 QPs (cross hatch) and for Type 2 QPs (dots).

increased from morning to evening. That is, the emission frequency of Type 1 QP increased from morning to afternoon.

Concerning to Type 2 QP, 0.7 kHz band QP had high occurrence at almost all local times. Type 2 QPs did not show a clear diurnal variation at the all frequency band, in contrast to Type 1 QPs. It is worth mentioning that Type 1 QP were more often observed at the lower frequency band of 0.5 kHz than were the Type 2 QPs, however at the higher frequency band of 1.5 kHz Type 2 QPs were more often observed than were those of Type 1. That is, the emission frequency of Type 2 is slightly higher than that of Type 1. However, these tendencies are not so clear as those which KITAMURA *et al.* (1969) observed at Eights ($L\sim4$) and Byrd ($L\sim6.8$).

3.4. *Kp* dependence of QP occurrences

We examine here the relation between geomagnetic activity and QP occurrences. Fig. 16 shows *Kp* dependence of QP occurrence probability. It is seen that Type 1 QPs were observed during the period of moderate magnetic activity of $Kp\simeq2$–3 and Type 2 QPs tend to appear under the more quiet magnetic condition of $Kp\simeq1$.

KOKUBUN *et al.* (1969) reported that polar chorus activity correlates with worldwide magnetic activity with a time lag of about seven hours. TSURUTANI and SMITH (1977) also reported that the delay time between substorms and the

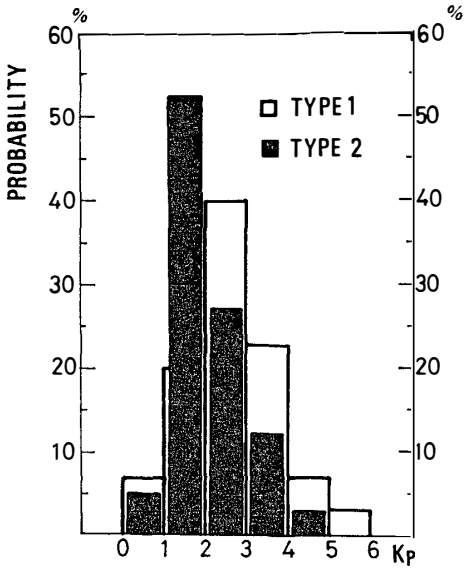

Fig. 16. Dependence of QP emission occurrences of geomagnetic activity.

onset of chorus observed near the equator in the outer magnetosphere by the Ogo 5 is consistent with a gradient drift of ~25 keV electrons. It is important to examine the relation between the onset of QP emission and the phase of the magnetic storm.

As mentioned above, we could find general properties for both the Type 1 QPs and Type 2 QPs. In the later section, we will examine the detailed characteristics.

4. Classification of QP Emissions Based on Frequency-Time (*f-t*) Spectra

A classification of VLF emissions, based on frequency-time spectra observed on the ground, have been made by GALLET (1959) and HELLIWELL (1965). According to HELLIWELL (1965), VLF emissions can be classified into six types, hiss, discrete emission, periodic emission, chorus, quasi-periodic (QP) emission and triggered emission. In the present section, an attempt is made to classify QP spectra further into subtypes, as an extention to that proposed by HELLIWELL (1965). The examination of *f-t* spectra of QPs in detail is one of the most important approaches to study the generation mechanism of QP emissions, because *f-t* spectra give us much information on the generation conditions of QPs.

The *f-t* spectra were prepared with the aid of a real time FFT spectrum analyzer by reproducing magnetic tapes. By using a few hundred QP events observed at Syowa and Mizuho Stations in Antarctica and Husafell in Iceland, QP spectra were classified into five types. Spectral characteristics and model spectral forms of five types of QPs are examined. Furthermore, statistical characteristics of each type of QPs are also examined by using *f-t* spectra of ELF-VLF emissions recorded continuously for 50 days in Iceland.

4.1. Classification of QP emissions

QP emissions are classified into five types as is shown in Fig. 17.

I. Non-dispersive type

i) The upper frequency of QP emissions changes synchronously with the emission intensity (Examples are shown in Fig. 18).

ii) The upper and lower frequencies of emissions change synchronously with emission intensity (Examples are given in Fig. 19).

II. Rising-tone type

i) Each QP emission element shows a rising-tone with hiss structure (Examples are given in Fig. 20).

ii) QP emission consists of dispersive or non-dispersive periodic emissions which form a rising-tone structure (*cf.* HELLIWELL, 1965) (Examples are given

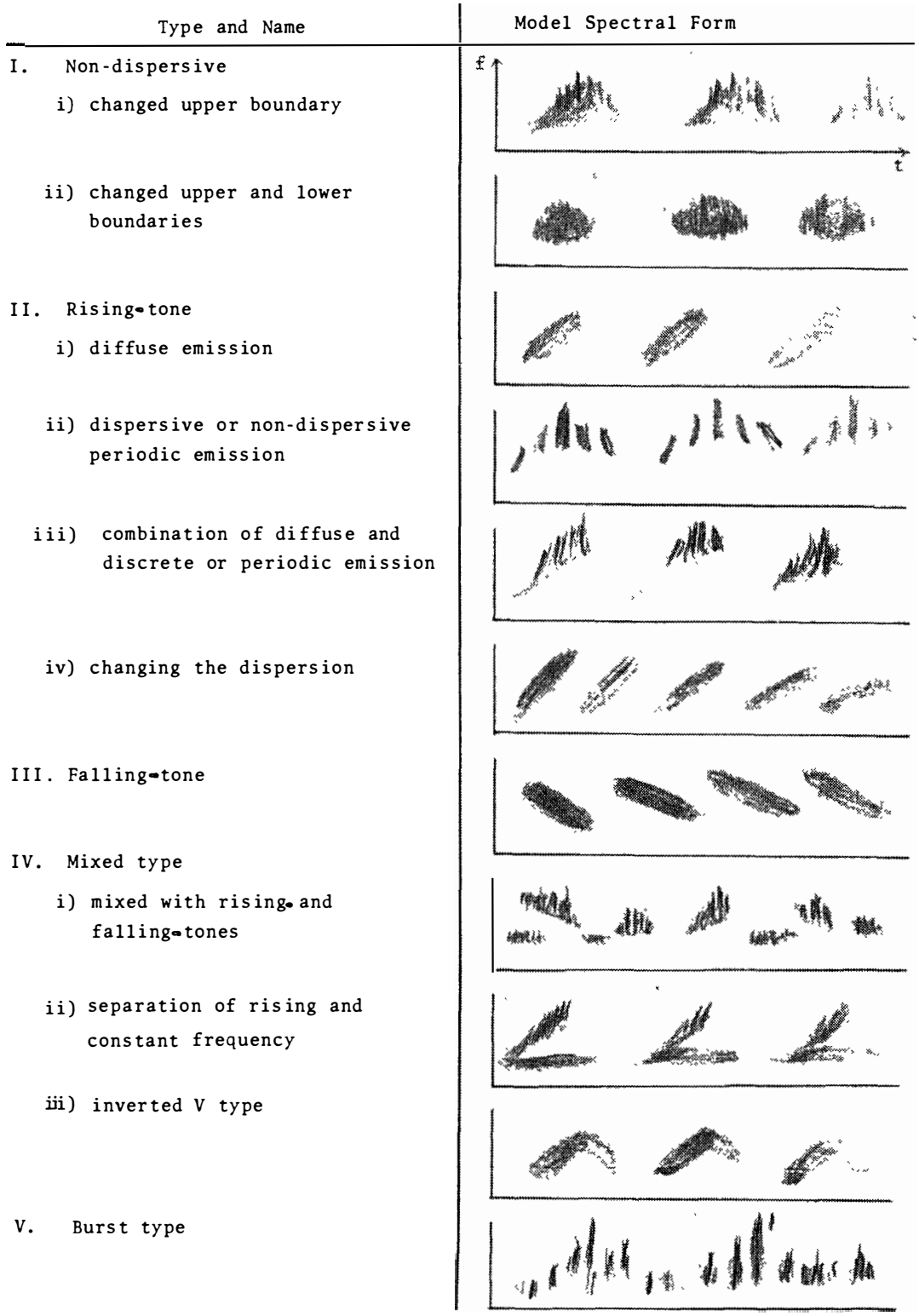

Fig. 17. Model spectral forms and classification of QP emissions into five types based on f-t spectra.

in Fig. 21).

iii) A rising-tone structure consists of a combination of diffuse emissions and discrete or periodic emissions (Examples are given in Fig. 22).

iv) The slope of rising-tone decreases with time (Examples are given in Fig. 23).

III. Falling-tone type

Each QP emission element shows a falling-tone structure (Examples are given in Fig. 24).

IV. Mixed type

i) QP elements with rising-tone and falling-tone structures are mixed (Examples are given in Fig. 25).

ii) Non-dispersive type and rising-tone type are excited synchronously (Examples are given in Fig. 26).

iii) Combination of rising- and falling-tone elements forms an inverted V structure (Examples are given in Fig. 27).

V. Burst type

QP elements consist of strong burst-like discrete emissions and weak diffuse emissions (Examples are given in Fig. 28).

4.2. Characteristics of each type of QP emissions

From *f-t* spectra of ELF-VLF emissions recorded continuously on magnetic tapes at Husafell in Iceland for 50 days from July 30 to September 17, 1977, 103 QP events were observed. These QP events were classified according to the model spectral forms shown in Fig. 17. Then, statistical characteristics as to duration, magnetic local time of occurrences and the relationship to magnetic pulsations were studied for each type of QP. Table 2 gives the statistical summary. Occurrence local time and period of QPs which were observed rarely at Husafell on this period are given by using the data observed at Syowa and Mizuho Stations, symbolized by star in Table 2. As shown by SATO *et al.* (1974) QP emissions are also classified into Type 1 and Type 2 depending upon whether the QP emissions are closely associated with magnetic pulsations or not. By the duration and the occurrence, QPs can be grouped into two classes. The first group, which is frequently observed, includes I-i), ii), II-i), ii), iii), IV-i) and V, and the other group, which is rarely observed, includes II-iv), III, IV-ii) and IV-iii).

4.2.1. Characteristics of 'non-dispersive' type

The non-dispersive type of QPs was observed mostly in the day time. As shown in the *f-t* spectra in Figs. 18 and 19, those QP emissions are polar chorus emissions whose intensities and frequencies are modulated quasi-periodically. It is found that most of these QP emissions are Type 1 QP emissions, and are usually associated with long period (T~40–150 s) magnetic pulsations.

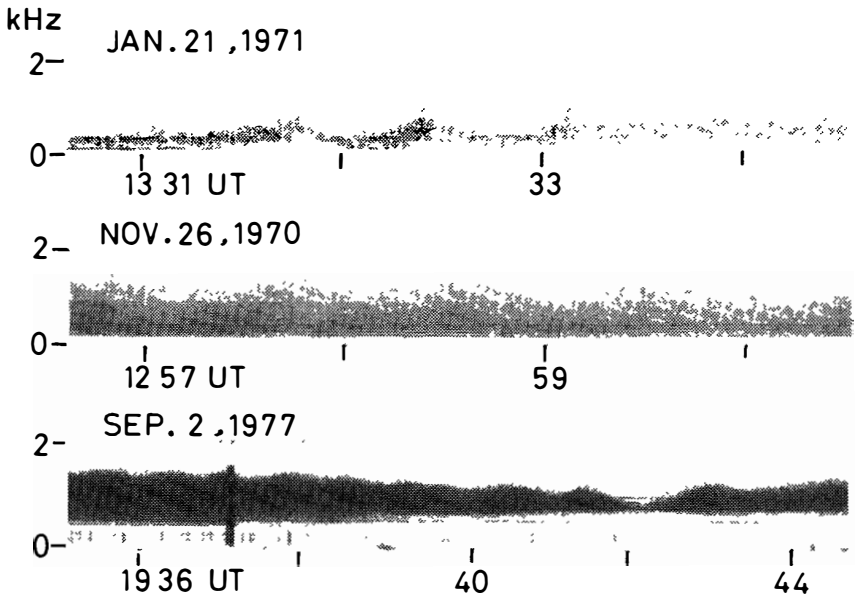

Fig. 18. Examples of QP events in which the upper boundary of emission frequency changes synchronously with the signal strength. The period of QPs is ~60 s in the January 21, 1971 event and in the November 26, 1970 event, and ~50 s in the September 2, 1977 event.

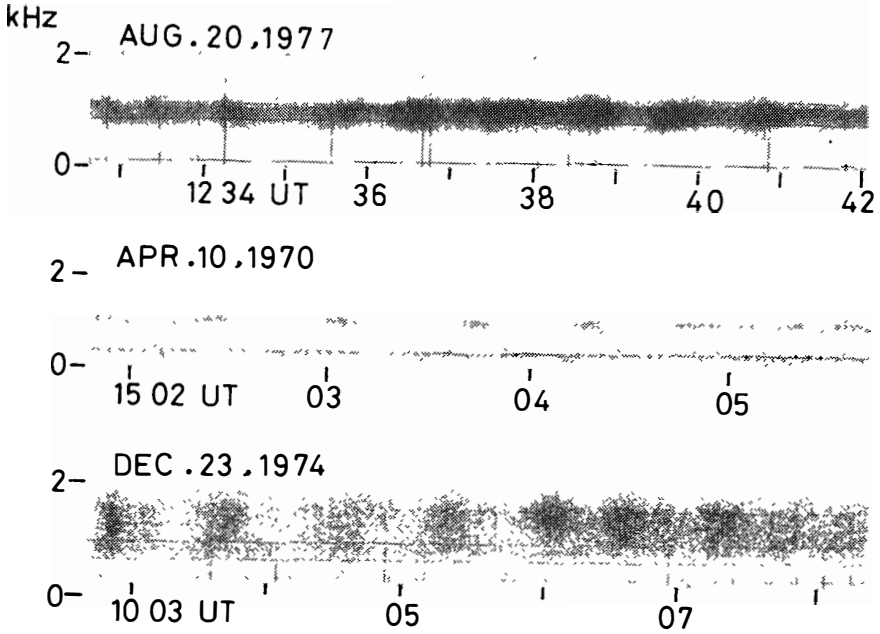

Fig. 19. Examples of QP events in which the upper and lower boundaries of emission frequency change synchronously with the signal strength. The period of QPs is ~60 s in the August 20, 1977 event, ~30 s in the April 10, 1970 event, and ~30 s in the December 23, 1974 event.

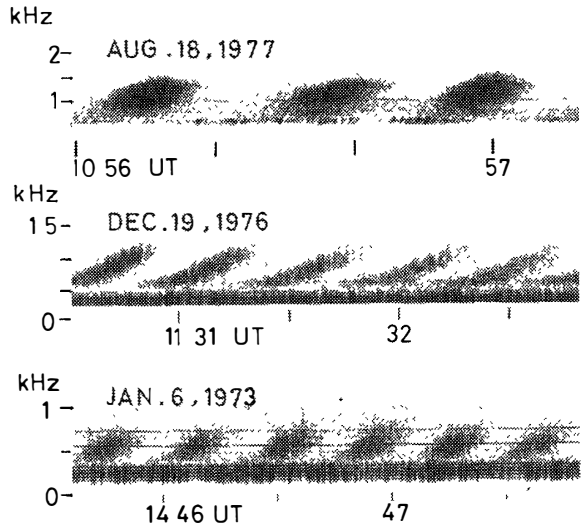

Fig. 20. Examples of QP emissions with a diffuse-type rising tone structure. The period of QPs is ~25 s in the August 18, 1977 event, ~30 s in the December 19, 1976 event and ~23 s in the January 6, 1973 event.

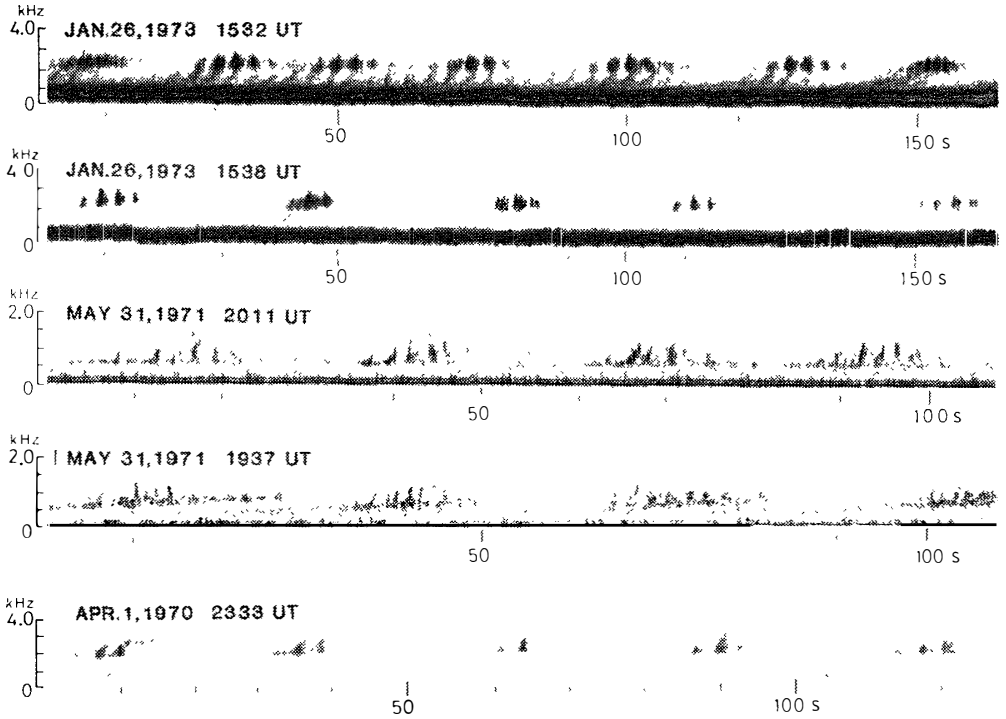

Fig. 21. Examples of periodic emissions which form QP emissions with a rising-tone structure. The spectral form of periodic emissions shows rising tone during the increasing stage of the QPs intensity and falling tone during the decreasing stage of the QPs intensity. The period of QPs is ~40 s in the January 26, 1973 event, ~30 s in the May 31, 1971 and April 1, 1970 events.

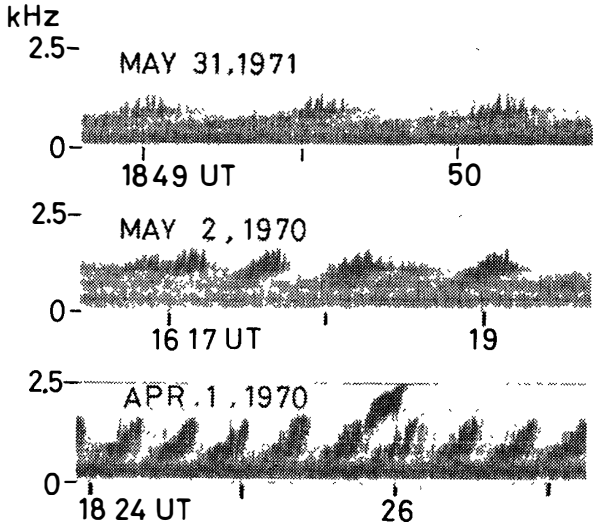

Fig. 22. Examples of QP emissions with a rising-tone structure which consist of a combination of diffuse and discrete or periodic emissions. The period of QPs is ~35 s in the May 31, 1971 event, ~40 s in the May 2, 1970 event and ~25 s in the April 1, 1970 event.

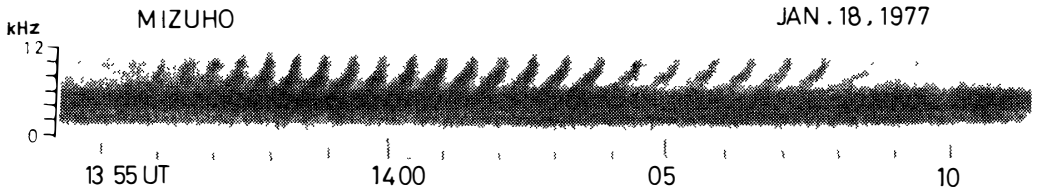

Fig. 23. An example of QP emissions in which the slope of rising tone changes with time. The period of QPs at 1 kHz changed from 30 s to 60 s.

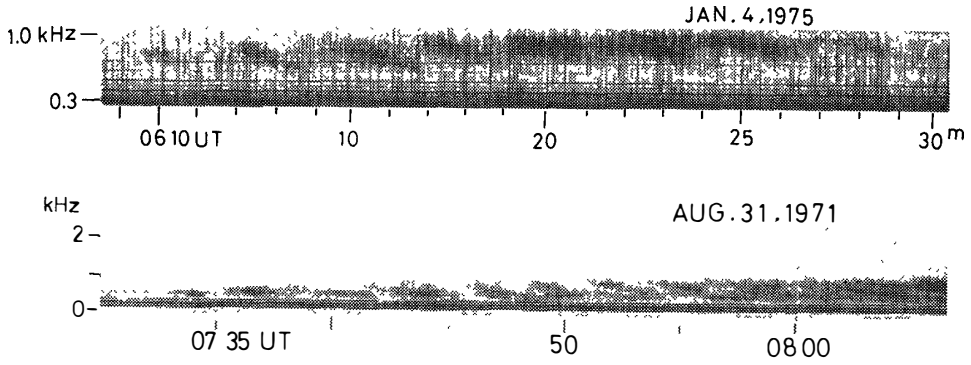

Fig. 24. Examples of QP emissions with a falling-tone structure. The period of QPs is ~180 s in the January 4, 1975 event and ~160 s in the August 31, 1971 event. It is found that the upper boundary of the emission frequency drifted to higher frequencies with time.

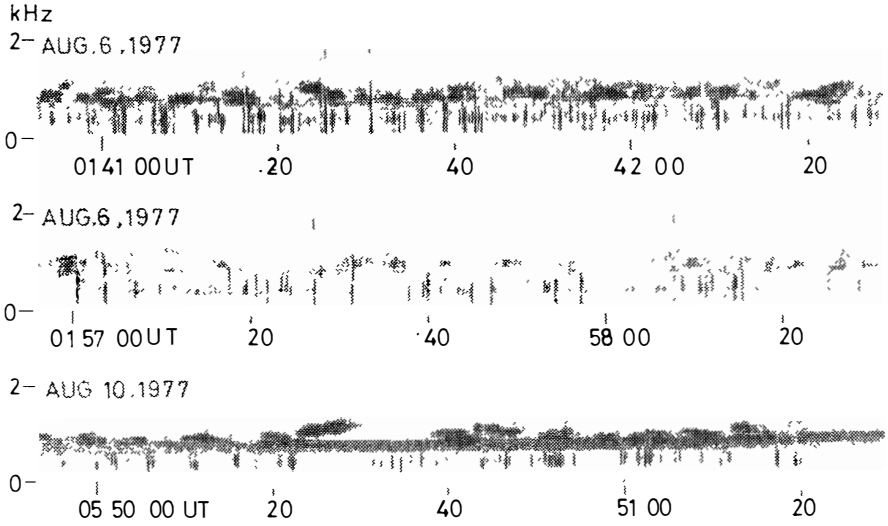

Fig. 25. Examples of QP emissions in which rising-tone and falling-tone elements and constant frequency bands are mixed. Fine structure in the f-t spectra of QPs shows the characteristics of auroral chorus. The period of QPs are ~5–10 s in the August 6, 1977 event, ~10–15 s in the August 10, 1977 event.

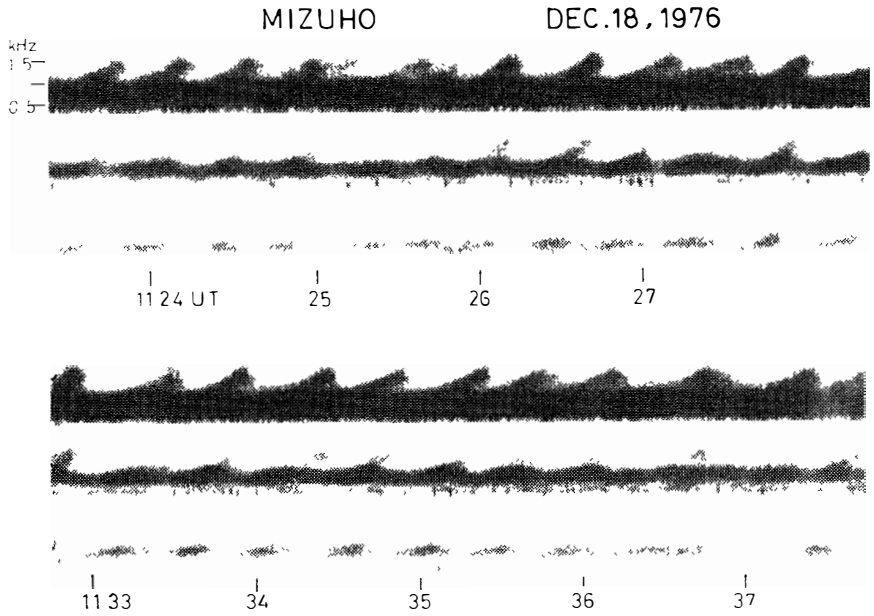

Fig. 26. Examples of QP emissions in which a rising-tone element separates from a constant frequency band during one quasi-period. The f-t spectra are displayed at three different intensity levels.

Table 2. Statistical characteristics of QP emissions.

Type and name	Number of events		Duration (min)	Local time	Period(s)
	Type 1	Type 2			
I. Non-dispersion					
i) Changed upper boundary	9	1	560	10–13	40–150
ii) Changed upper and lower boundaries	15	1	1045	09–15	40–150
II. Rising-tone					
i) Diffuse emission	8	3	515	11–15	20–40
ii) Periodic emission	3	7	735	07–18	20–50
iii) Combination of diffuse and discrete or periodic emission	10	8	1240	09–15	10–40
iv) Changing the dispersion	0	1	10	*13–14	20–50
III. Falling-tone	0	0	0	*04–09	100–200
IV. Mixed type					
i) Mixed with rising- and falling-tone	17	0	1095	00–05	5–15
ii) Separation of rising and constant frequency	0	0	0	*09–12	20–40
iii) Inverted V shape	1	1	35	*08–11	20–30
V. Burst type	12	7	1405	05–10	5–20

4.2.2. Characteristics of 'rising-tone' types

1) The rising-tone type QPs with diffuse structure are most frequently observed between 20 and 40 s. In the 50 days period, 75 percent of the events of this type were associated with magnetic pulsations (Type 1), while 25 percent of the events were not associated with magnetic pulsations (Type 2). The periodicity of the Type 1 QP emission is generally not very regular, while that of Type 2 QP is quite regular.

2) The rising-tone type in which each QP element consists of periodic emissions occurring at a wide range local times from morning to evening, and sometimes even at midnight as is shown in the April 1, 1970 event in Fig. 21. The local time of maximum occurrence is 15–17 MLT. This type of QP emission was observed during low magnetic activity, and 70 percent of the events were classified into Type 2 QPs. This type of QP is also often observed in sub-auroral zone (CARSON *et al.*, 1965; HO, 1973). The period of the QP ranges between 20–40 s, while the period of periodic emissions that form each QP element is 3–4 s. The periodic emissions in QP emissions are sometimes associated with Pc 1 magnetic pulsations (see, after Section 8). From *f-t* spectra in the time interval of 1532:20–1534:20 UT on January 26, 1973 and in the time interval of 2011:45–2012:50 UT on May 31, 1971 in Fig. 21, it is seen that the spectral

form of periodic emissions is a rising-tone during the first half of the QP emission, then a falling-tone in the latter half stage of the QP emission.

3) QP emissions which consist of a combination of diffuse and periodic emissions were usually seen between morning and late afternoon. About half the QPs of this type were not associated with magnetic pulsations (Type 2). The repetition of *f-t* spectral pattern in Type 2 QPs is quite regular in contrast with that of Type 1. The period of QP emissions is 10–40 s. There is a tendency for QPs with shorter periods (T~30–40 s) to be observed in the afternoon. It seems that this type is the same as typical examples of QP emissions in the sub-auroral zone observed by HELLIWELL (1965), CARSON *et al.* (1965) and KITAMURA *et al.* (1969).

4) QP emissions with a rising-tone structure whose slope decreases or increased with time were rarely observed during the 50 days observation period at Husafell (*cf.* Table 2). Six events of this type were found in *f-t* spectra of QP events observed at Syowa Station in the period of February 1970–February 1972. Half of these QPs were associated with worldwide geomagnetic changes as shown by SATO *et al.* (1974). The slope of rising-tone steepens during the period of positive geomagnetic changes, whereas the effect is reversed during negative geomagnetic changes.

4.2.3. Characteristics of the 'falling-tone' type of QP emissions

QP emissions with falling-tone structure are rare events. This type of QP event was not observed during the observation period of 50 days at Husafell (*cf.* Table 2). Three events were found in Syowa Station data for the period of February 1970–February 1972. It is found that they occurred only in the early morning, and were associated with long period magnetic pulsations (T~150–200 s).

4.2.4. Characteristics of the 'mixed type' of QP emissions

1) The spectral form of the mixed type, with rising- and falling-tone structures, was quite similar to the spectral form of the auroral chorus (HAYASHI and KOKUBUN, 1971). The occurrence of this type is limited to the dawn sector. This type of QP emissions is also associated with pulsating auroras and Pi C magnetic pulsations (OGUTI and WATANABE, 1976), and the period of QPs are scattered around 10 s. All QPs of this type seem to be Type 1 QP emissions, because of their close association with Pi C magnetic pulsations.

2) This type is characterized by a separation of rising-tone elements from QP emissions occurring at the same time with a constant frequency. This type of QP emission was a rare phenomenon, and was not observed in the 50 days data at Husafell (*cf.* Table 2). Only 4 events were found in Syowa and Mizuho Stations VLF data in 1970–1972 and 1976. The occurrence was limited to the morning sector. From the *f-t* spectra displayed at three different intensity levels

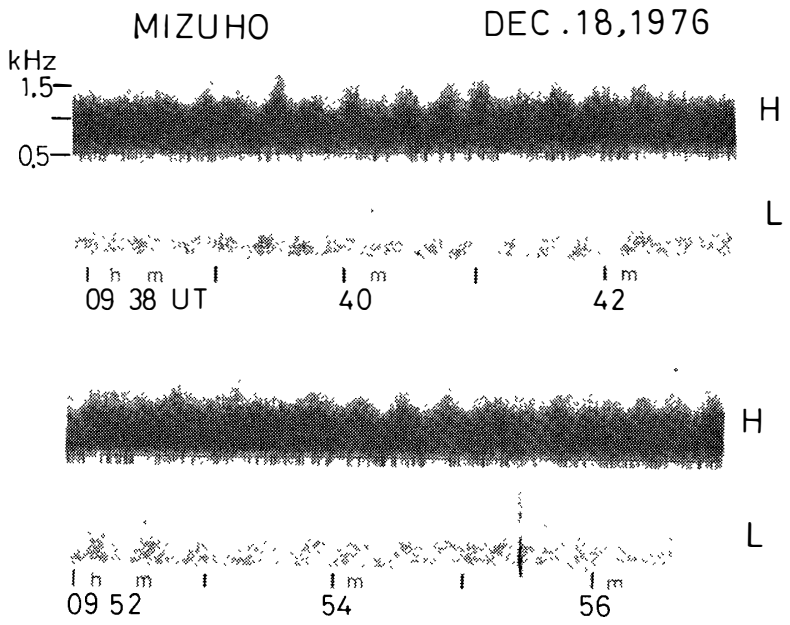

Fig. 27. Examples of 'inverted V' shape QPs in the f-t spectra displayed at two intensity levels. From the lower intensity level display, it is found that the emission intensity of the rising tone is stronger than that of the falling tone.

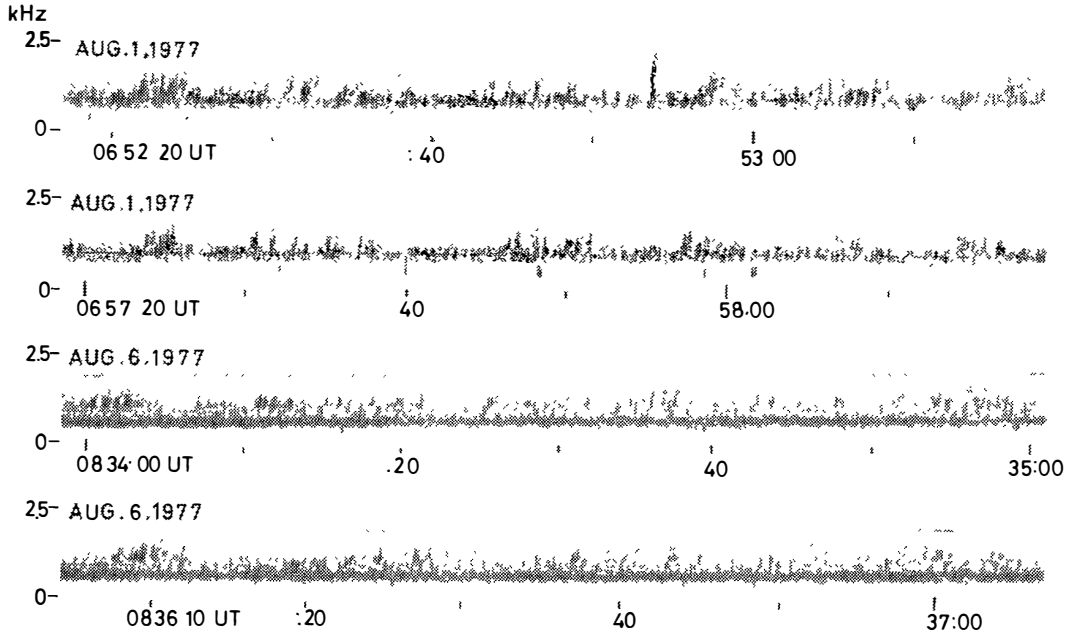

Fig. 28. Examples of QP emissions which consist of strong burst-like discrete emissions and weak diffuse emissions. The period of QPs and the spectral form both change with time.

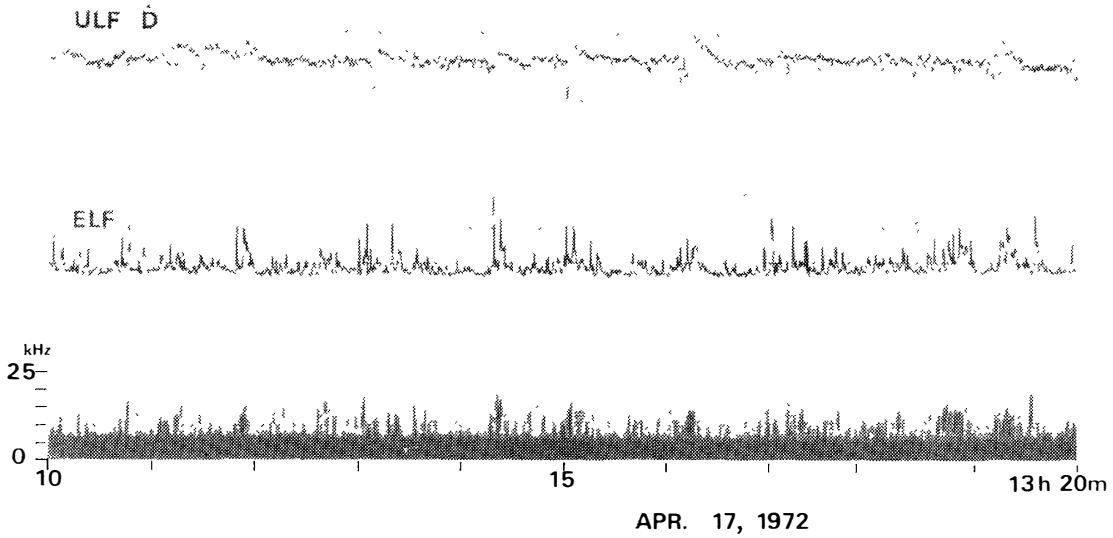

Fig. 29. Intensity records of the Ḋ component of magnetic pulsations (top), ELF emissions at 1–2 kHz band (middle), and f-t spectra of ELF emissions observed at Syowa Station on April 17, 1972. It is found that discrete elements in ELF bursts are sometimes associated with Pi magnetic pulsations.

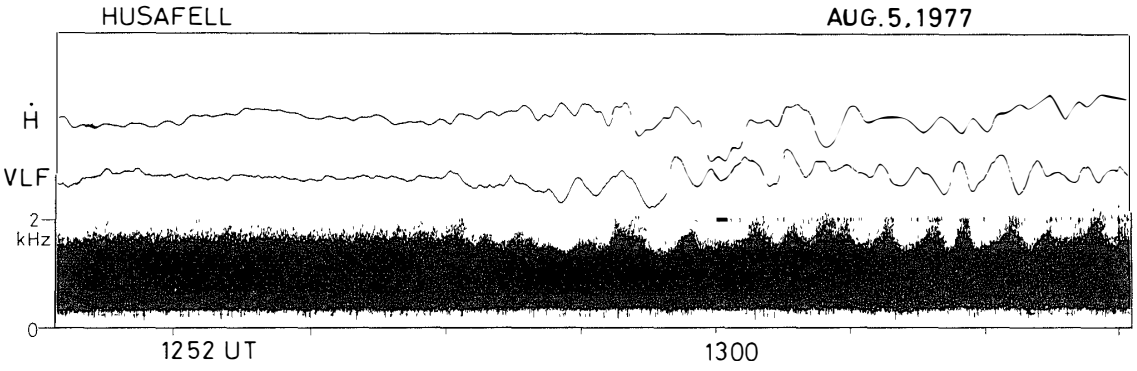

Fig. 30. The Ḣ component of magnetic pulsations and the VLF intensity at the selected 0.8–1.8 kHz band and f-t spectra of QP emissions observed at Husafell on August 5, 1977.

in Fig. 26, it is apparent that QP elements with a rising-tone structure separate from the constant frequency band as the intensity of the constant band increases.

3) An example of QPs with 'inverted V' shape is presented in the *f-t* spectra displayed at two different intensity levels in Fig. 27. It is apparent in the *f-t* spectra with the lower intensity level in Fig. 27 that the frequency of QP emissions first increases and then decreases. The emission intensity of the rising-tone is usually stronger than that of the falling-tone. This type was observed in the morning sector associated with magnetic pulsations. However, this type is a rare phenomenon, only one event being observed at Husafell (*cf.* Table 2) and two events at Syowa and Mizuho Stations in 1976.

4.2.5. Characteristics of the 'burst type' of QP emissions

Burst type QP emissions were mostly observed in the early morning. The periods were 10–20 s, which are shorter than the periods of other types of QP emissions. Burst type QPs associated with magnetic pulsations (Type 1) occurred during moderate and high magnetic activity and their spectral forms were quite variable as shown in Fig. 28, whereas burst type QPs which were not associated with magnetic pulsations occurred during magnetic quiet times. Sometimes each discrete element in burst-type QPs was associated with a Pi magnetic pulsation. An example is shown in Fig. 29.

4.3. Spectral structure at the onset time of a QP

It is useful for the study of generation mechanisms of QPs to examine the change in the spectral structure before and after the onset of QPs. Fig. 30 shows the $\dot{H}$ component of magnetic pulsations, the VLF emission intensity at a selected 0.8–1.8 kHz band and *f-t* spectra observed at Husafell on August 5, 1977. It is clearly shown that the amplitude of VLF emissions was modulated quasi-periodically and was associated with an enhancement of Pc 3–4 magnetic pulsations (T~25–50 s) during the time interval of ~1256–1306 UT. The frequency-time spectra of the QP emissions are classified as the 'rising-tone' type, and the upper and lower cut-off frequencies remained the same before and after the onset of QPs. It is worth noting that the maximum intensity of the QP, when it occurred, became stronger than the intensity level of pre-existing emissions while the minimum intensity level of the QP became lower than the pre-existing emission level. An other example showing such a relation was given in Fig. 23 of SATO *et al.* (1974). These results strongly suggest that QP emissions are not special types of emissions, and that they are reasonably understood as a modulation of ELF-VLF emissions (polar chorus, auroral chorus and periodic emissions) which occur before the onset of the QPs.

Fig. 31 shows the *f-t* spectra of QP emissions and pulsation wave forms observed at Husafell in Iceland at 1027–1115 UT on August 18, 1977. The frequency-time spectra of the QP emissions are the 'rising-tone' type. It is seen that the sudden enhancement of VLF emissions occurring in the time interval 1103–1106 UT was accompanied by a positive impulse of the magnetic field. The frequency band of this event is same as that of the rising-tone QP emissions which were observed just before the sudden impulse. Therefore, Type 1 QP emissions are probably explained by the modulation of pre-existing ELF-VLF emissions by compressional mode magnetic field variations in the magnetosphere as reported by HAYASHI *et al.* (1968).

Fig. 32 shows the record of magnetic pulsations in the $\dot{H}$ component, the emission intensity in the 0.75 kHz frequency band and *f-t* spectra for the No-

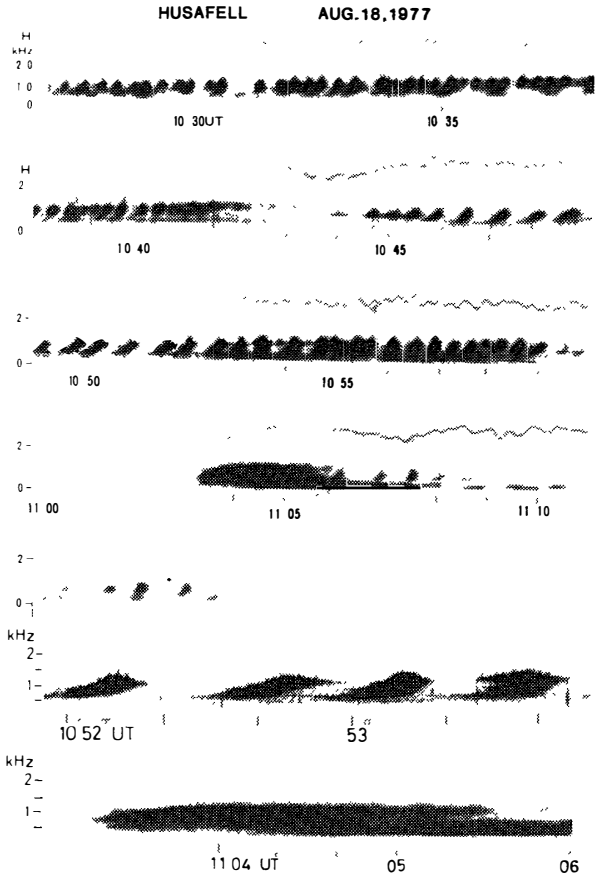

Fig. 31. The $\dot{H}$ component record of magnetic pulsations and concurrent f-t spectra of QP emissions observed at Husafell on August 18, 1977, and enlarged display of f-t spectra in the time intervals of ~1052–1054 and ~1103–1106 UT.

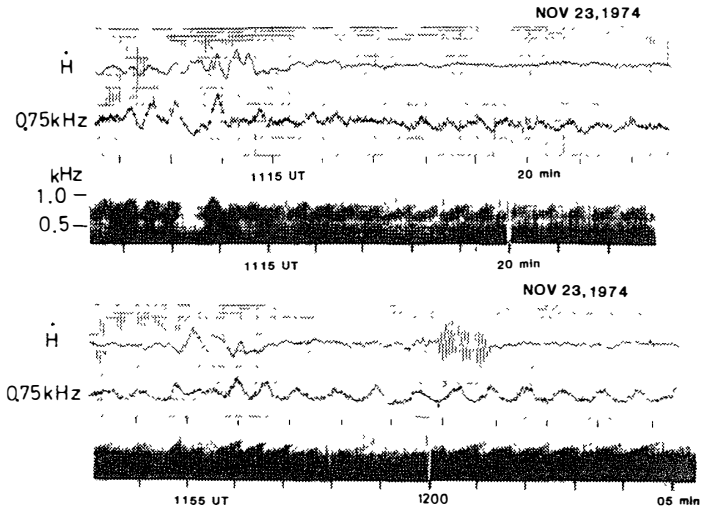

Fig. 32. $\dot{H}$ component of magnetic pulsations, VLF emission intensity at 0.75 kHz and f-t spectra of QP emissions on November 23, 1974 at Syowa Station.

vember 23, 1974 event. It is obvious that the ELF emissions in Fig. 32 are modulated quasi-periodically by associated magnetic pulsations during the intervals of 1112–1116 UT and 1154–1157 UT. The *f-t* spectra of QP emissions during these time intervals are the non-dispersive type. However, when the amplitude of magnetic pulsations was damped, at 1115 and 1157 UT, the *f-t* structure changed into a rising-tone type. That is, Type 1 QP emissions changed continuously into Type 2 QP emissions when magnetic pulsation activity decreased. It is also found that not only the emission frequency range but also the fine structure in QP emission elements of Type 1 and Type 2 QPs in this event are quite similar. These facts suggest that the background condition which is responsible for the generation of QP emissions in the magnetosphere is the same for both of Type 1 and Type 2 QPs, but the modulation mechanism is different.

As described above we were able to find interesting and important characteristics of QPs based on the *f-t* spectram, *e.g.*, the differences between Type 1 and Type 2 QPs, the most frequently observed types of QPs, their local time of occurrence, periodicity, and spectral fine structure forms. These characteristics are very important when discussing the generation mechanism of QP emissions. Details will be discussed in later section.

5. Occurrence of QP Emissions Associated with Worldwide Geomagnetic Variations

Daytime ELF-VLF emissions at auroral zone stations are strongly affected by magnetospheric conditions associated with changes in solar wind momentum (MOROZUMI, 1965; HAYASHI *et al.*, 1968). HAYASHI *et al.* (1968) have shown that a positive sudden impulse in geomagnetic field is accompanied by a sudden enhancement of polar chorus, whereas a negative impulse is associated with a sudden decrease in intensity of emission and even fading of the pre-existing emission for some time. These facts indicate that the acceleration of electrons during the period of magnetospheric compression plays an essential role in the wave-particle interactions which cause ELF-VLF emissions, as suggested by HAYASHI *et al.* (1968). In this section an attempt is made to examine the effects of worldwide magnetic changes on QP emissions.

5.1. Relationship between Type 1 QPs and worldwide geomagnetic variations

When the amplitude of magnetic pulsations accompanying a QP emission is larger than a few gammas at Syowa Station, corresponding pulsations are often observed at middle and low latitudes. Fig. 33a shows frequency-time spectra of QP emissions at Syowa Station compared with the *H* component of geomagnetic variations at San Juan (29.9°, 3.2° in geomagnetic coordinates). This is a typical example showing a good correlation between QP emissions at Syowa Station and magnetic pulsations at San Juan, which is separated from Syowa Station by 75° in longitude. As seen in the figure, the association of QP emissions with magnetic pulsations is evident during the time intervals 1134–1143, 1210–1227 and 1243–1253 UT, while during other periods the concurrence is not seen. Fig. 33b shows another example of the relation between Type 1 QP emissions at Syowa Station, and the *H* component of magnetic pulsations at Great Whale River (65.6°, 358.5°) in the northern auroral zone, and at San Juan. It is evident that QP emissions at Syowa Station are closely related to magnetic pulsations that occurred between the 1255 and 1300 UT at all the three stations.

In addition to the modulation of emissions related to magnetic pulsations

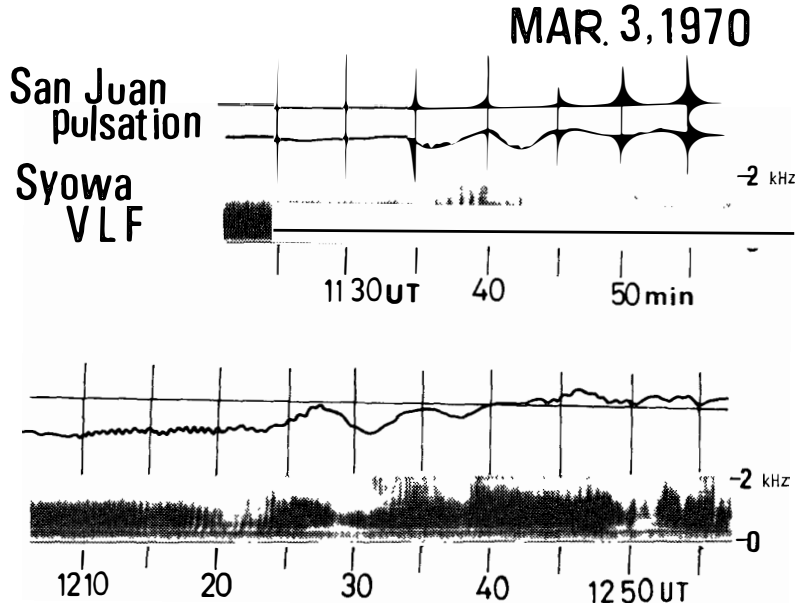

(*a*) *March 3, 1970.*

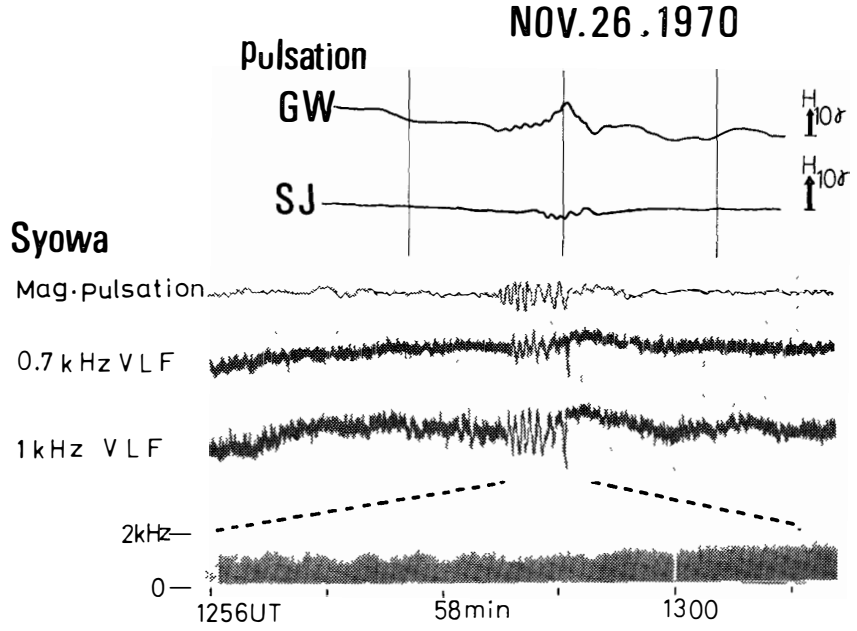

(*b*) *November 26, 1970.*

Fig. 33. Correlations between QP emissions at Syowa Station and geomagnetic changes at low latitude and northern auroral zone stations.

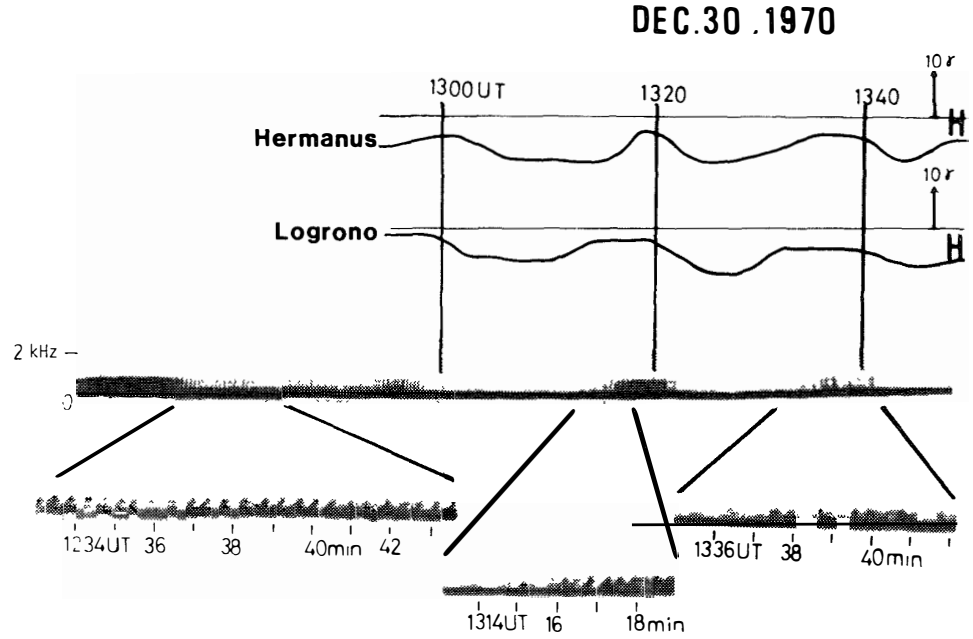

Fig. 34. Changes of Type 1 QP emissions associated at times of worldwide magnetic variations on December 30, 1970.

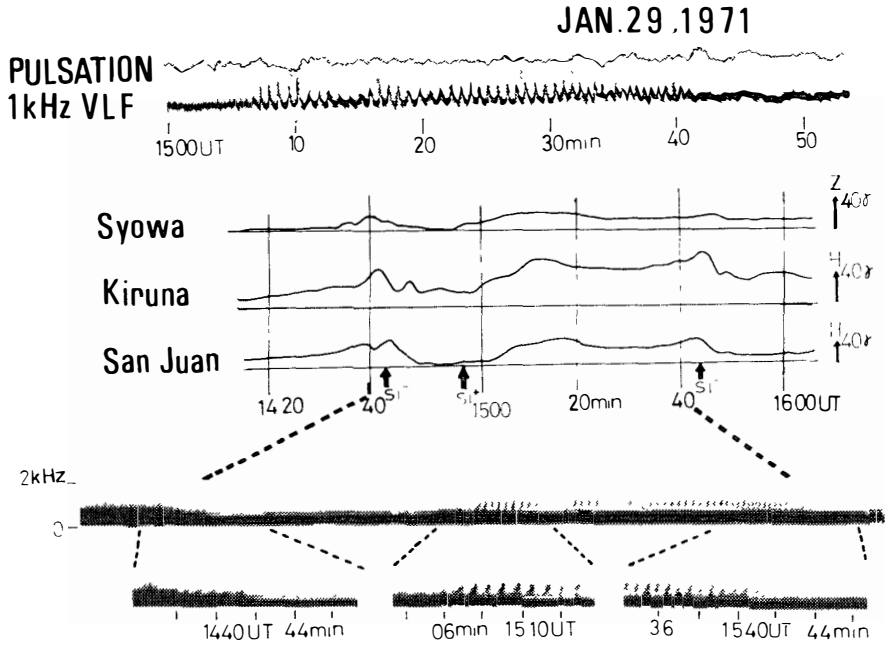

Fig. 35. Emission intensity changes of Type 2 QP emissions at times of worldwide geomagnetic variations. QP emissions disappeared at 1442 and 1542 following negative variations. A slow increase from 42 to 38 s in QP period was observed for the 35 min interval from 1507.

with periods of 20–60 s mentioned above, the slower fluctuations in signal strength of the emissions in Fig. 33a are seen to be almostly synchronously associated with the slowly varing geomagnetic H component. When the H component of geomagnetic field increases the emission intensity increases and a negative change in H is related to decreases in intensity during the time intervals 1135–1145 and 1220–1255 UT. A typical example indicating the concurrent slow variations in emissions and geomagnetic fields is given in Fig. 34. Fig. 34 illustrates frequency-time spectra of ELF-VLF emissions at Syowa Station (lower panel) and the H component of geomagnetic field at Hermanus (−33.5°, 81.2°) and Logrono (45.9°, 77.9°) on December 30, 1970 (see Fig. 8a). The occurrences of ELF-VLF emission in the frequency band below 1.0 kHz were likely controlled by geomagnetic variations at middle and low latitudes. The QP emissions in this figure were known to be almost synchronously related with magnetic pulsations at Syowa Station when the wideband intensity of emissions attained a certain level, but no rapid variations of geomagnetic field corresponding to the QPs were found at Hermanus and Logrono. It is interesting to note that during this event magnetic pulsations with periods similar to the QP emissions were observed by using high sensitivity magnetometers at Siple in Antarctica and at its conjugate point Girardville in Canada ($L\sim4$), both being separated from Syowa Station by about 6° in latitude and 85° in longitude (LANZEROTTI, private communication, 1973).

It was found from the examination of magnetic records from several stations in low latitudes that the slow magnetic changes at this time occurred on a worldwide scale. When the horizontal component of geomagnetic field increases, the emission intensity increases. A negative variation is related to decrease in intensity or a fade-out of emissions as reported by HAYASHI *et al.* (1968) and KOKUBUN (1971). These tendencies suggest that the compression and expansion of the magnetosphere cause the increase and decrease in intensity of ELF-VLF emission in the magnetosphere.

5.2. Relationship between Type 2 QPs and worldwide geomagnetic variations

When worldwide geomagnetic changes take place during the occurrence of Type 2 QP emissions, the effect of geomagnetic changes also appears in the emissions as with the case of Type 1 QPs. Examples are shown in Figs. 35 and 36. Fig. 35 shows amplitude records of the $\dot{H}_h$ component of magnetic pulsations, VLF signal strength at 1 kHz band (upper panel) and the frequency-time spectrum of QP emissions (lower panel) at Syowa Station, and the H component of geomagnetic field variation at Syowa Station, Kiruna (65.3, 115.6) and San Juan (middle panel) on January 29, 1971. From amplitude records of magnetic pulsation and VLF emission at Syowa Station, it is evident that the average periods of QPs and concurrent magnetic pulsations were entirely different. The

period of magnetic pulsations was much longer than that of QPs, so that we have identified the QP emissions as Type 2 QPs. The effect of geomagnetic variation on emission intensity is the same as in the case of Type 1 QPs. This figure shows that the enhancement of QP intensity occurred at ~1506 UT associated with a positive magnetic variation, whereas the emission faded at 1442 and 1542 UT in association with negative magnetic changes.

In Fig. 35 it may be interesting to note that the rate of middle frequency rise in the quasi-periodic component decreases as emission intensity decreases at times of negative geomagnetic changes, and it increases when positive magnetic changes occur. Fig. 36a shows the other example which indicates the interesting relation between Type 2 QP emission and worldwide geomagnetic variations. The upper panel of this figure shows the *H* component of geomagnetic field variation at Bangui (4.8, 88.5), Tbilisi (36.7, 122.1), Odessa (43.7, 111.1) and Guam (4.0, 212.9) and frequency-time spectra of QP emission at Syowa Station on April 1, 1970. It is evident from the geomagnetic field data that a weak positive sudden impulse (several gammas) occurred at 0853 UT and a weak negative impulse (~few gammas) occurred at near 0915 UT. As is evident in the figure, a positive sudden impulse occurring at 0853 gave rise to an increase in emission intensity and a small negative change at 0915 caused a decrease in intensity, and QP component disappeared until about 0920 UT. Furthermore, it is interesting from the lower panel of Fig. 36a that the period of the Type 2 QP changed from 25 s to 11 s. It was also observed that the slope of the middle frequency rise in the QP elements become steeper as the intensity increased. Fig. 36b shows the temporal variation in the 10 min averages of QP periods on April 1, 1970. There is a general increase of the QP period from 07h to 11h UT. This increase is vary similar to the diurnal variation of QP period mentioned in Section 3 (Fig. 13). Overlapping to this tendency, a sudden decrease and a sudden increase in QP period are seen associated with positive and negative sudden impulses, *i.e.*, the QP period became shorter when associated with a positive impulse and longer with a negative impulse. Fig. 37 also illustrates an example of Type 2 QP periods related to low-latitude geomagnetic field variations. The upper two panels show amplitude records of VLF emissions at 1.0 kHz and 1.5 kHz bands at Syowa Station, and the middle panel indicates the *H* component of geomagnetic field variations at Guam. It is evident that the QP period become shorter and the emission intensity increased, associated with positive magnetic changes, and the opposite effect was noted at times of negative changes.

5.3. SSC or SI triggered ELF-VLF emissions

HAYASHI *et al.* (1968) have shown that a SSC or positive SI in geomagnetic field is accompanied by a sudden enhancement of the polar chorus and that a modulation effect on polar chorus precedes the commencement of magnetic

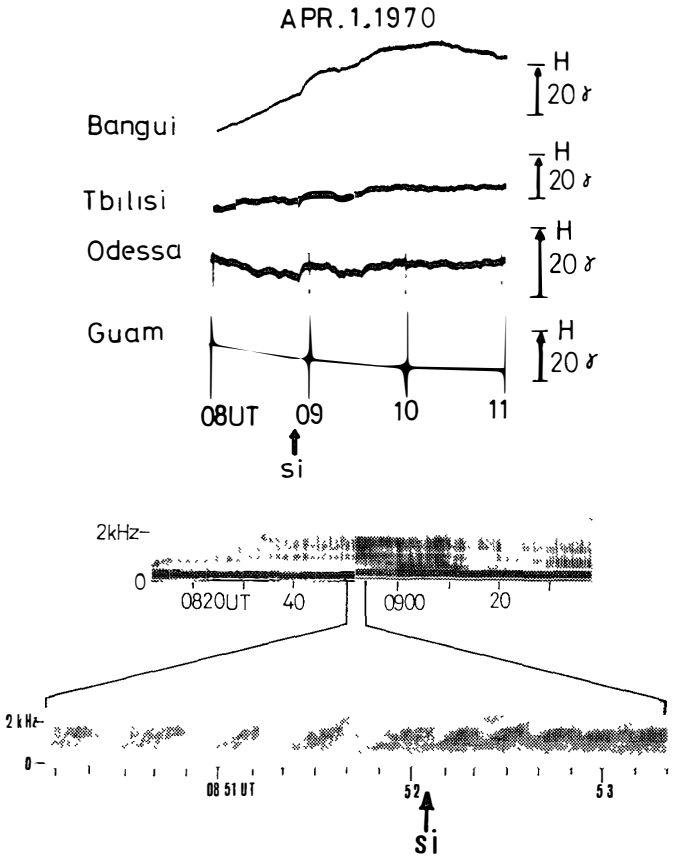

Fig. 36a. A typical example of a period decrease at Syowa Station associated with a sudden impulse. No detectable geomagnetic pulsation was observed at Syowa Station during this event. A period changed from 25 to 11 s.

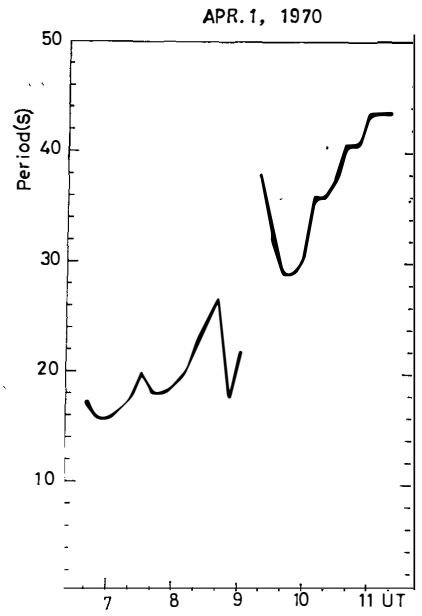

Fig. 36b. Variation of 10 min averages of QP periods on April 1, 1970. A positive sudden impulse was observed at 0853 and a small negative one at 0915.

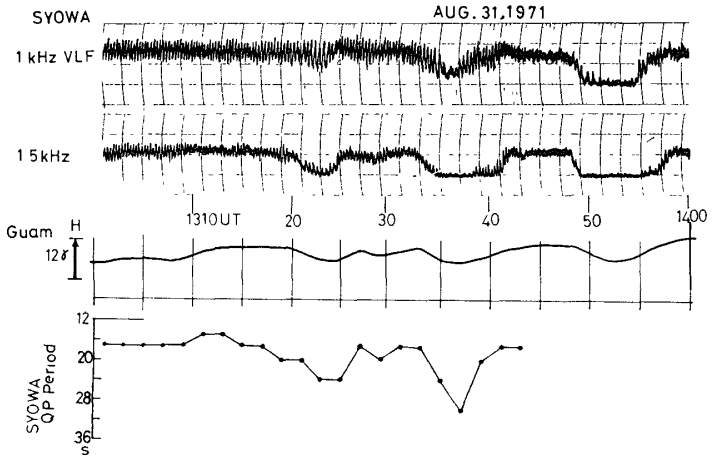

Fig. 37. A typical example of changes in Type 2 QP period and emission intensity associated with slowly varying magnetic changes at low latitude.

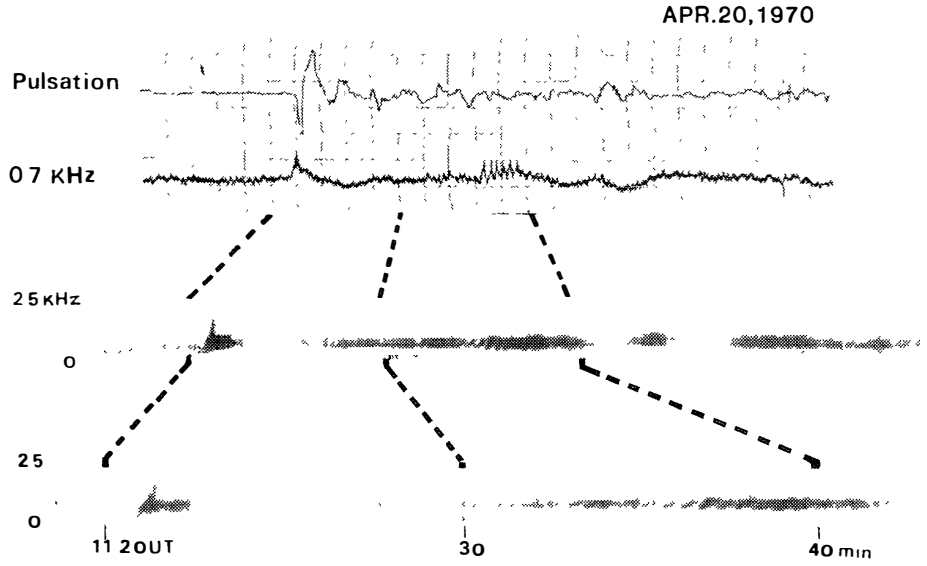

(*a*) *Syowa Station on April 20, 1970.*

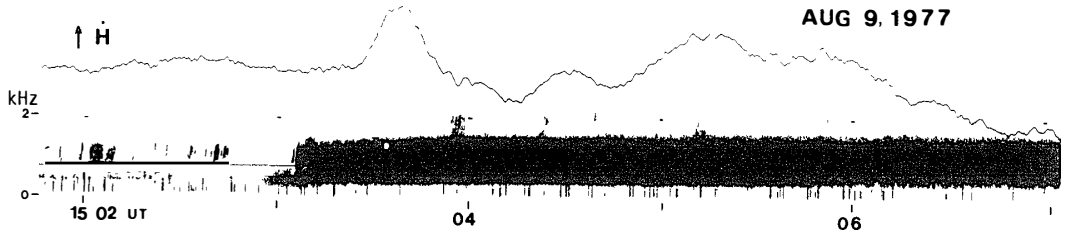

(*b*) *Husafell on August 9, 1977.*

Fig. 38. Examples of SSC- and SI-triggered polar chorus and magnetic field variation.

variation on the ground by tens seconds or more. We also examine here the difference of commencement time between SSC or SI magnetic field variations and triggered ELF-VLF emissions. Fig. 38a shows an amplitude record of the $\dot{H}$ component of the magnetic pulsation and of the ELF emission intensity at 0.7 kHz band (top panel), a frequency-time spectrum of ELF-VLF emission (middle panel) and an expanded *f-t* spectrum (bottom panel), at Syowa Station on April 20, 1970. It is evident that ELF-VLF emissions were triggered by the SSC and the mean frequency of emission shifted upward in the time interval ~1120–1121 UT. It is clearly seen on simultaneous records of magnetic pulsation and ELF-VLF emission that commencement times differ between a sudden enhancement of ELF-VLF emission and SSC *i.e.*, the enhancement of ELF-VLF emission was recorded at about 30 s prior to the commencement of magnetic field variation. Fig. 38b illustrates an example of SI-triggered polar chorus observed in Iceland on August 9, 1977. This figure was obtained by a real time spectral analyzer reproducting the FM data tapes which recorded simultaneously the magnetic pulsations and wide-band VLF emissions. It is evident that the

polar chorus suddenly enhanced at ~1503:05 UT and that the associated variation in the H component of geomagnetic field began at ~1503:25 UT. The fact that the start of SSC effect on the polar chorus precedes the SSC or SI by 20–30 s strongly suggests that the polar chorus is generated near the equatorial plane in the outer magnetosphere, because the observed difference in travel time from the interaction region, between the emission and the SSC or SI is found to be reasonable taking into account the difference between velocities of the whistler mode waves (ELF-VLF emissions) and the Alfvén waves (magnetic pulsations).

It is also suggested that the interaction region of QP emission is near the equatorial plan in the outer magnetosphere, because fluctuations in background emission signal strength of both Type 1 and Type 2 QP emissions are almost always associated with SSC, SI or slowly varing changes in the worldwide geomagnetic H component, as mentioned in previous section. A detailed discussion will be given in Section 8.

6. Arrival Direction of ELF-VLF Chorus and QP Emissions

Recently, TSURUDA and HAYASHI (1975) have developed a new method for finding the arrival direction. The transverse-electric-field (TE) mode is eliminated by taking the simple algebraic combinations among three components of wave field, the vertical electric field and two horizontal magnetic fields, where the whole information in the amplitude ratio and the phase differences of these components is effectively used. This method has the following advantages: (i) both azimuth and elevation angles can be determined with an accuracy of within a few percents even for nonmonochromatic waves, (ii) it is easy to design a device for a real time measurement, (iii) if the ground is flat with the electric conductivity dependent only on the depth, it can be shown that this method is not affected by the magnitude of the ground conductivity, (iv) and that the error in azimuth and elevation angles caused by multiple reflection is less than 10° (TSURUDA and HAYASHI, 1975). Details of this method and the design of a real-time system have been described by TSURUDA and HAYASHI (1975).

The arrival directions of ELF and VLF emission were measured at Syowa Station from March 1974 to January 1975, based on the above method, and an improved system was operated from March 1976 to January 1977. This section presents the statistical characteristics of the arrival directions along with some individual examples of daytime ELF emissions and QP emissions in the frequency band 0.75 kHz during summer season from December 24, 1974 to January 31, 1975. Details of the real time direction finding system used at Syowa Station were described in Section 2 and SATO and HAYASHI (1976).

6.1. Arrival direction of ELF-VLF waves in individual examples

In our observation system, analog output of calculated intensity, north-south and east-west components of the wave normal vectors (N_x and N_y), and the polarization angle α of the 0.75 kHz band were continuously recorded on a strip chart with a speed of 0.25 cm/min. In this section temporal changes of the arrival direction in individual cases are described. ELF emissions were frequently found to be incedent from nearly the same direction during several hours, for

example on December 31, 1974 seen in Fig. 39, but we also found the other examples, that show a gradual change in the arrival direction within an hour, such as those on December 29, 1974, January 23, 1975 and January 28, 1975 seen in Figs. 40–42.

6.1.1. An example on December 31, 1974

Fig. 39 shows an example of the measurement of arrival directions obtained on December 31, 1974. The top panel represents the temporal variation of ten-minute averages of the arrival direction vector of the wave for the 0.75 kHz band. The middle and bottom panels show the variations in emission intensity and in polarization, respectively. A broken line in the middle panel indicates the intensity value of 3×10^{-5} V/m·$\sqrt{\text{Hz}}$. The errors caused by analog calculators are negligibly small for signals larger than this value. In the bottom panel of Fig. 39, R and L mean right-handed and left-handed polarizations, respectively, and sin $\alpha=1$ and sin $\alpha=0$ correspond to circular and linear polarizations, respectively. In this example, ELF emissions, called daytime chorus or polar chorus, were received during the 8.5 hours from 05h50m UT and 14h20m UT. The emissions were incident from the north near the zenith for 06h–07h UT and the arrival direction changed to the south-east after passing through the zenith at about 07h10m UT. The angle of incidence of the emissions increased between 07h10m–08h00m UT, but the azimuth angle remained almost unchanged. The arrival direction was almost constant for about 5 hours from 08h UT. During

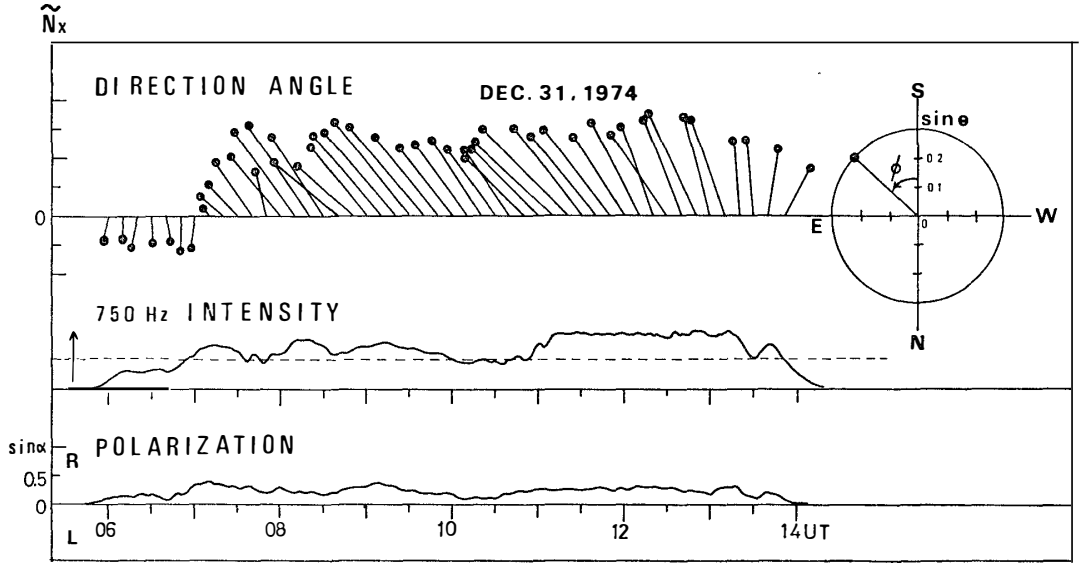

Fig. 39. The top panel shows 10 min average values of arrival direction of 0.75 kHz ELF emissions. The middle panel shows the emission intensity and the bottom panel shows the polarization angle. R and L mean right-handed and left-handed polarizations where sin $\alpha=1$ and sin $\alpha=0$ correspond to circular polarization, and linear polarization, respectively. Arrival directions between 08 h UT–11 h UT on December 31, 1974 remained almost unchanged.

the interval 13h–14h UT, the arrival direction gradually changed from the south-east to the south-west as the emission intensity decreased. Similar examples where the arrival direction remained almost constant for several hours were frequently found. This suggests that the emission source often corotates with the earth for a long time. The polarization of the emission was generally right-handed and was highly elliptical as is seen in the lower panel of Fig. 39.

6.1.2. An example on December 29, 1974

The four-minute average values of the arrival direction are plotted in Fig. 40. Note the variation in arrival direction during the two hours, 08h–10h UT. Between 08h and 09h UT, the emission source moved from the south to the west, and during the next one hour, 09h–10h UT, the arrival direction moved from the south-east to the south-west. These systematic westward changes of arrival direction seem to indicate the motion of the source region with respect to the observation site, however the motion is likely due to the rotation of the earth with respect to the magnetospheric coordinates, and not due to the motion of the sources.

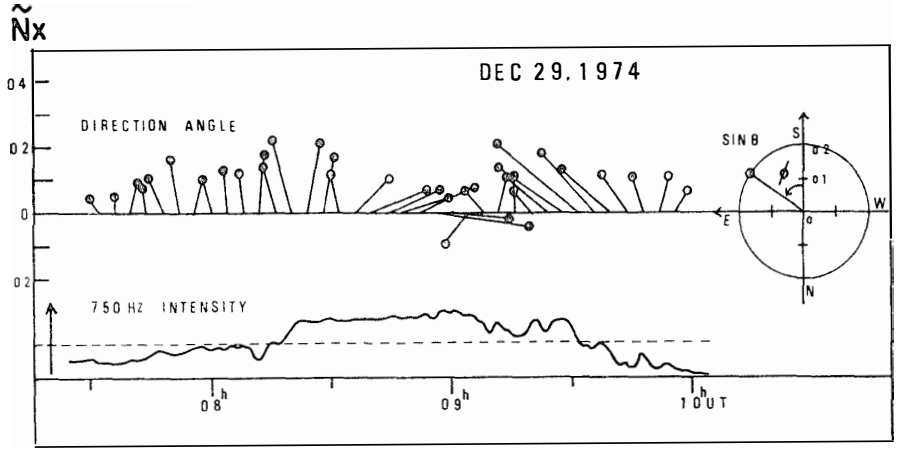

Fig. 40. Same as for Fig. 39, except that it is for the data on December 29, 1974.

6.1.3. An example on January 23, 1975

Fig. 41 show the plots of ten-minute average values in arrival direction, emission intensity and polarization. The arrival direction between 10h30m and 14h UT is worth noting. The arrival direction gradually changes from the south-east, passing through the zenith to the north-east and finally to the south-west. The change in the arrival direction in this example suggests that the source region shifted gradually in the magnetosphere, in contrast to the previous example. On the other hand, the arrival direction between 05h30m and 07h UT shifts irregularly in comparison with the interval 10h30m–14h UT. The polarization of the emission was right-handed and was highly elliptical.

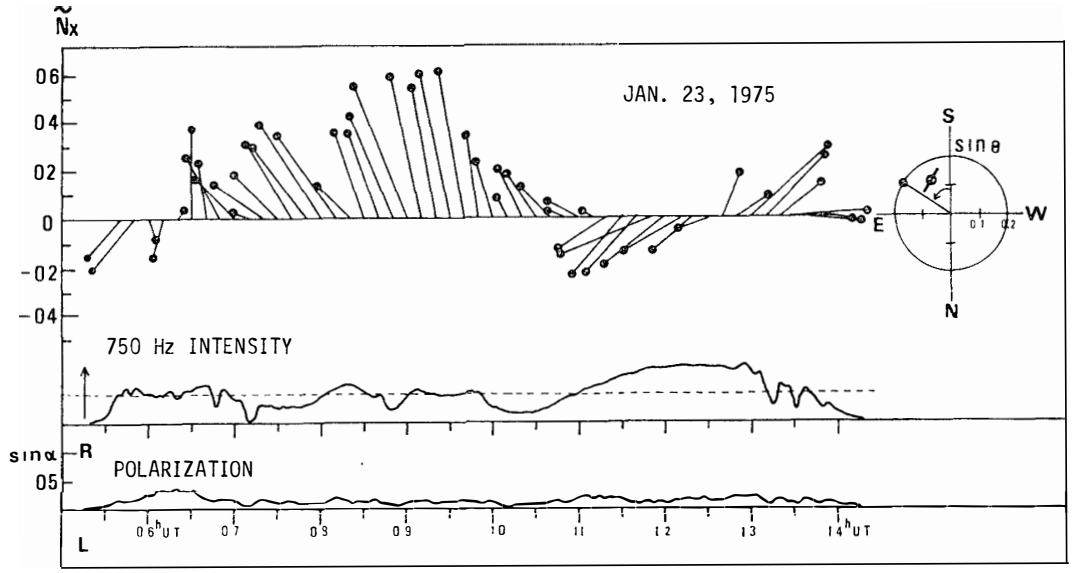

Fig. 41. Same as for Fig. 39, except that it is for the data on January 23, 1975. In this event, it is clear that the arrival direction rotates slowly during 09h UT–14h UT.

6.1.4. An example on January 28, 1975

Fig. 42 show the locus of ten-minute average values of arrival direction and emission intensity during the period 10h–15h UT on January 28, 1975. This

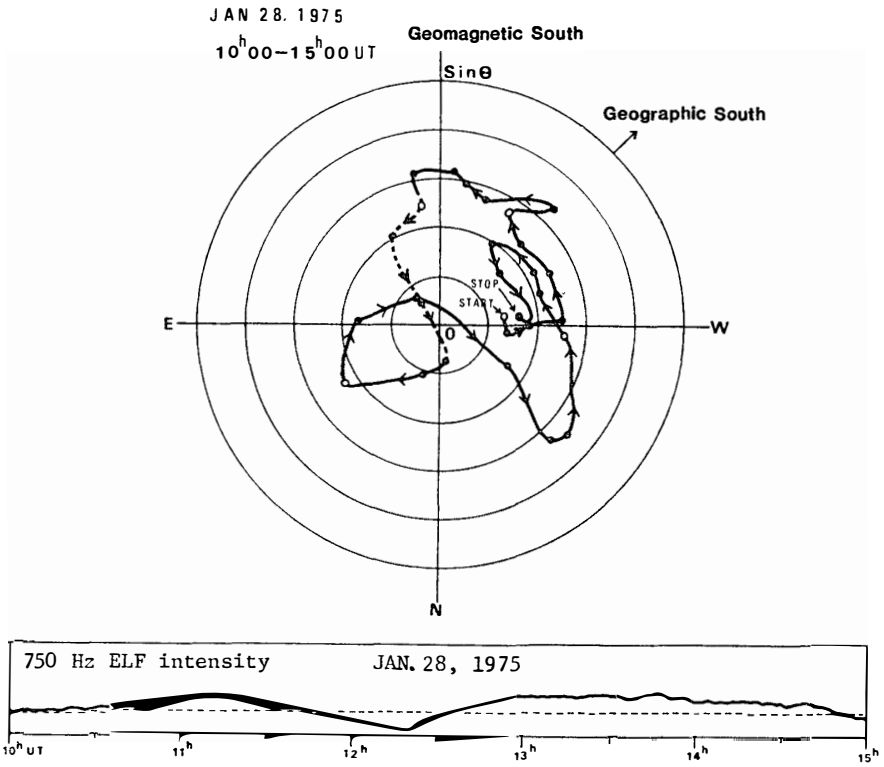

Fig. 42. The locus of 4 min average values of arrival direction, and 0.75 kHz ELF intensity, between 10h00m UT–15h00m UT on January 28, 1975.

event is a typical example in which the emission source shifts gradually.

As mentioned above, two types of ELF chorus are often found, one shows almost a constant direction of arrival during several hours, and the other shows a gradual shift in direction of arrival within one hour. The latter would represent the movement of the generation region and the wave duct from magnetosphere to the ionosphere. These properties of temporal variation for ELF chorus give important information for the study of the physical condition in the magnetosphere and in the ionosphere. This is a future research problem.

6.2. Statistical distribution of arrival direction

In this section we examine statistically the diurnal variation of arrival direction of ELF chorus, in order to study the general pattern of movement of the generation region. The statistical distribution of ELF emissions in the 0.75 kHz band was examined by using the data observed at Syowa Station for 40 days from December 23, 1974 to January 31, 1975. In this analysis, the data for which the emission intensity was weaker than 1.5×10^{-5} V/m$\cdot\sqrt{\text{Hz}}$ were excluded, as the calculated arrival direction is not accurate for such emissions, as mentioned in Section 2.

Fig. 43 shows the diurnal variation of the probability of occurrence of emissions in the 0.75 kHz band for 40 days. Most of the ELF emissions in this frequency band were observed on the dayside and in the summer period. This tendency is the same as previous results for the polar chorus (HAYASHI and KOKUBUN, 1971). Fig. 44 shows the diurnal variation of the duration of events for 40 days when the east-west component of the arrival direction is from the east (upper panel), or from the west (lower panel). In the morning sector, emissions come from both the east and west with nearly the same probability, while in the afternoon sector the tendency changes drastically, *i.e.*, emissions are dominantly incident from west. Fig. 45 shows the diurnal variation of the percentage of occurrence of the north-south component, where S_1 or N_1 incident emissions coming from the south (poleward) or the north (equatorward), respectively, with the incident angles greater than 20 degrees and S_2 or N_2 incident emissions coming from the south or the north with incident angles smaller than 20 degrees. In the early morning (04–07 UT), emissions come mostly from the north, the arrival direction shifting gradually from the north to the south toward noon. Then it gradually backs up from the south to the north during the afternoon (13–20 UT). The local time dependence is important in order to examine the physical behavior of the magnetosphere in which ELF and VLF emissions are expected to be generated.

The occurrence frequency of ELF and VLF emissions versus local time and latitude has been studied by using ground data (UNGSTRUP, 1967), by using ionospheric altitude satellite data (TAYLOR and GURNETT, 1968; BARRINGTON

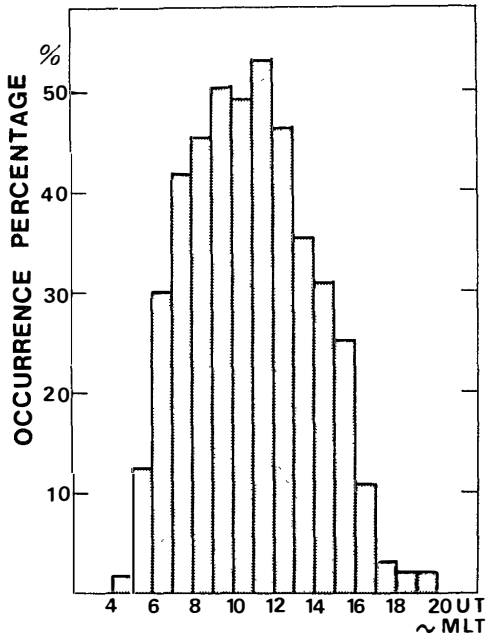

Fig. 43. Diurnal distribution of percentage occurrence 0.75 kHz ELF emissions for 40 days from December 23, 1974.

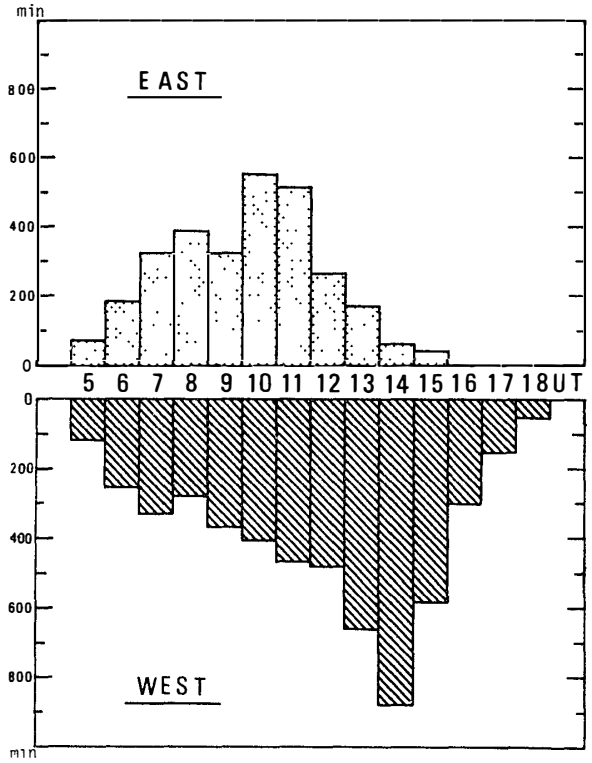

Fig. 44. Local time distribution of the durations of the arrival direction of ELF emissions in the east-west component for 40 days from December 23, 1974.

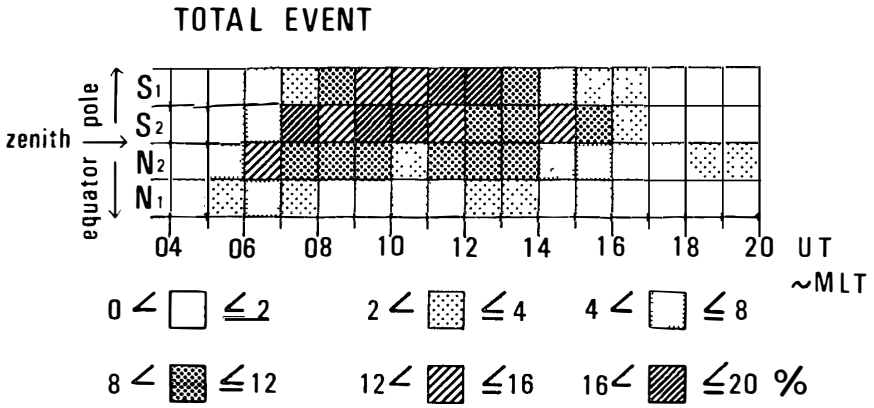

Fig. 45. Local time distribution of the arrival direction of ELF emissions in the north-south component for 40 days. S_1 or N_1 shows that waves are received from the south or the north with the incident angle greater than 20 degrees and S_2 or N_2 shows that waves are received with the incident angle smaller than 20 degrees.

et al., 1971; KELLEY *et al.*, 1975), and by using the data obtained in the magnetospheric region where chorus is believed to be generated (RUSSELL *et al.*, 1969; DUNKEL and HELLIWELL, 1969; TSURUTANI and SMITH, 1977). TSURUTANI and SMITH (1977) have shown that ELF hiss and chorus are present throughout

whole day but predominantly in the dayside magnetosphere. They are seen at lower L values in the post midnight and the early morning, gradually shifting to higher L values from morning to noon, and then in the late afternoon the region moving lower L values. These results are roughly consistent with our results of diurnal variation of north-south component observed at 66.7° invariant latitude, shown in Fig. 45. That is, emissions are incident from the equatorward side in the early morning, from the poleward side between the late morning and the early afternoon, and from the equatorward side in the late afternoon. Furthermore, the local time variation of the occurrence region of ELF and VLF emissions corresponds to the diurnal variation of the trapping boundary and of precipitating electrons (E~40 keV) detected by a low altitude satellite (FRANK *et al.*, 1964; FRITZ, 1968; MCDIARMID, 1968).

As discussed above the arrival directions of ELF-VLF waves observed at Syowa Station, especially the diurnal variation, are consistent with the results of previous workers.

6.3. Arrival direction of QP emissions

General characteristics of the arrival direction of emissions in 0.75 kHz band observed at Syowa Station were discussed in the previous section. In this section we will examine the arrival direction of QP emissions. If we can locate the generation region of QP emissions by examining the arrival directions, we can study the generation mechanism of QP emissions. Furthermore, if we can detect the change of direction of each recurrent QP element with fine time resolution, whether latitudinal direction or longitudinal, it would suggest some interaction processes between ELF emissions and ULF waves. We will show first statistical results of arrival direction for Type 1 QPs and also show the arrival direction for the QP elements.

6.3.1. The statistical arrival direction of Type 1 QP emissions

Occurrences of QP emissions observed for 40 days from December 23, 1974 to January 31, 1975 are nearly the same as those shown in Fig. 11 (Section 3). Type 1 QP emissions were more often observed than Type 2 QP. We have analyzed only Type 1 QPs. Fig. 46 shows the diurnal variation of Type 1 QP occurrence in this 40 days observation period. Most of QPs were observed between 08 and 13 UT. Fig. 47 (lower) illustrates the total duration of ELF emissions in the 0.75 kHz band versus incident angles defined as in Fig. 45. Most of ELF emissions came from the S_2 and N_2 regions and predominantly from the S_2 region. Fig. 47 (upper) shows the percentage occurrence ratio of Type 1 QPs to total events of ELF emissions for each region. This figure indicates that Type 1 QPs dominantly came from the region poleward of the station, indicating that Type 1 QPs are more apt to occur in high latitudes. Table 3 summarizes the

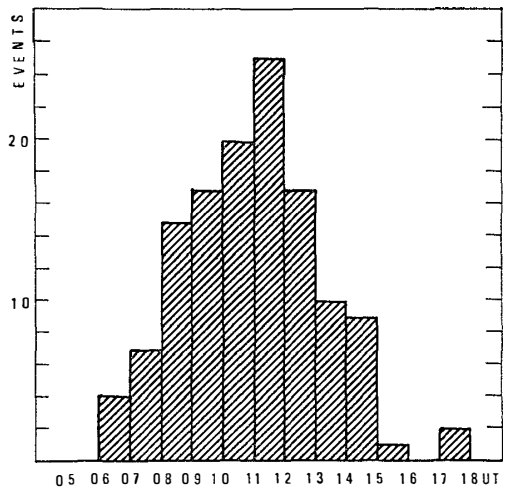

Fig. 46. Diurnal distribution of occurrences of Type 1 QPs for 40 days from December 23, 1974.

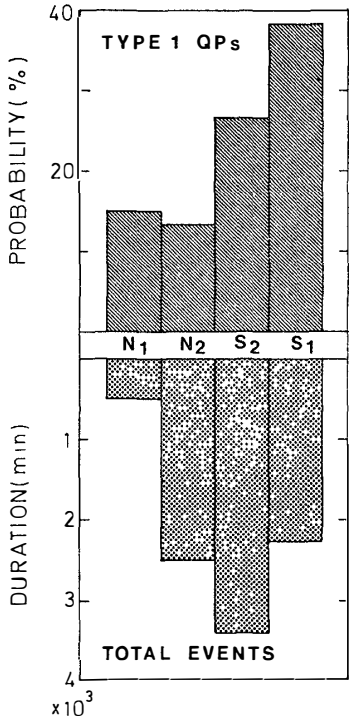

Fig. 47. Upper panel indicates occurrence rate of Type 1 QPs to total event of lower panel. Lower panel shows total duration of 0.75 kHz ELF emissions versus arrival direction for 40 days derived from Fig. 45.

Table 3. Local time distribution of percentage occurrence of Type 1 QPs to total emissions (%).

Time (UT)		6–8	8–10	10–12	12–14	14–16
Arrival direction	S_1	20.6	57.7	43.8	23.3	0
	S_2	7.2	37.6	37.5	28.7	7.4
	N_2	4.3	8.2	16.7	30.5	10.5
	N_1	7.0	—	—	15.6	—

diurnal variation of the arrival direction of ELF emissions in the 0.75 kHz band and percentage occurrence of QPs from the morning sector to the afternoon sector. In the morning sector, most of QPs come from poleward region, while the arrival direction of QPs is widely scattered, coming from both north and south directions in the afternoon sector between 12–14 UT. This local time dependence of arrival direction is also related to the generation mechanism of QP emissions as will be discussed in detail later.

Fig. 48 shows a typical example of the change in emission type from Type 1

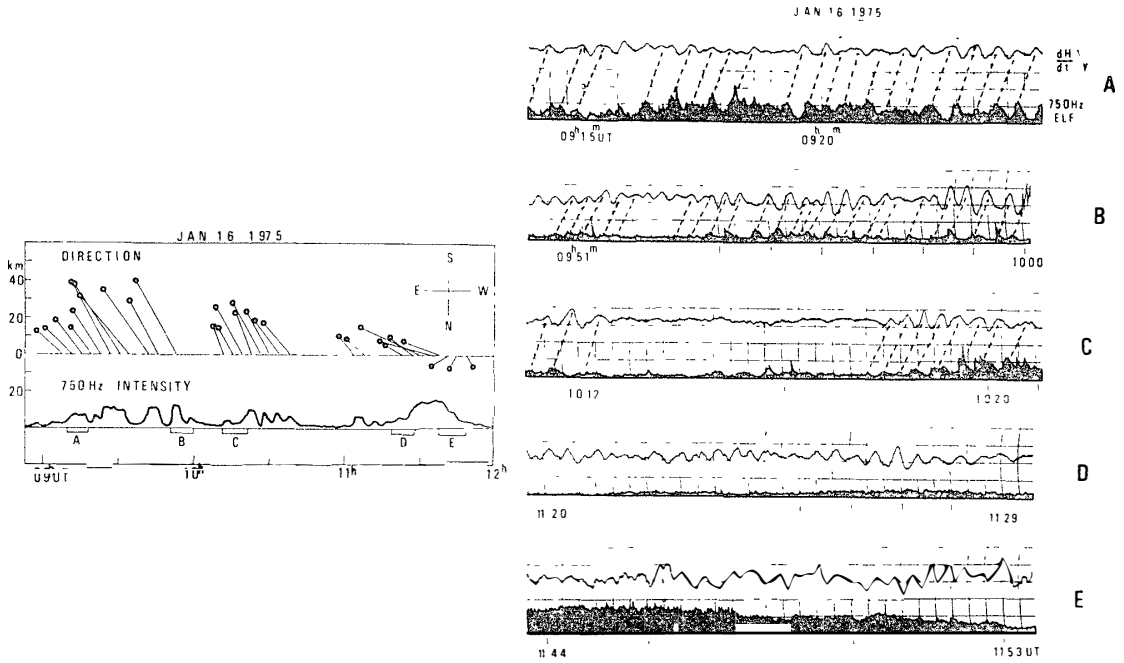

Fig. 48. The left side shows 4 min average values of arrival direction of 0.75 kHz emissions (upper panel) and 0.75 kHz emission intensity (lower panel) on January 16, 1975. The right side shows the east-west (Y) component of geomagnetic pulsations and 0.75 kHz emission intensity for the intervals A, B, C, D and E, of the lower left panal.

QP to unmodulated ELF emissions during a period of active magnetic pulsations that occur on January 16, 1975. The left panel of Fig. 48 indicates four-minute average values of the arrival direction of the emission at 0.75 kHz (upper panel), and its intensity (lower panel). The exist points from the ionosphere, estimated from the arrival directions, are shown, assuming that the exist altitude is 100 km. The right panel indicates the east-west component of magnetic pulsations and the intensity of the ELF emission in the 0.75 kHz band during the intervals A, B, C, D and E shown in the left panel. Judging from the correlation between magnetic pulsation and ELF emission intensity, the emissions are classified as Type 1 QPs during the periods A, B and C, and then, the modulation by magnetic pulsations disappeared during the periods D and E. It is evident that Type 1 QPs were incident from the SES (pole side) at large incident angles during the intervals A, B and C. On the other hand, the emission during the interval D has a small incident angle from the north-east and the north-west. This is a typical example which indicates qualitatively that the Type 1 QP is incident from high latitudes and emissions unmodulated by active magnetic pulsations are incident from lower latitudes.

6.3.2. Direction of arrival of QP elements

A new system for finding the arrival direction with higher accuracy and resolution has been operated at Syowa Station since March 1976 and simultaneous

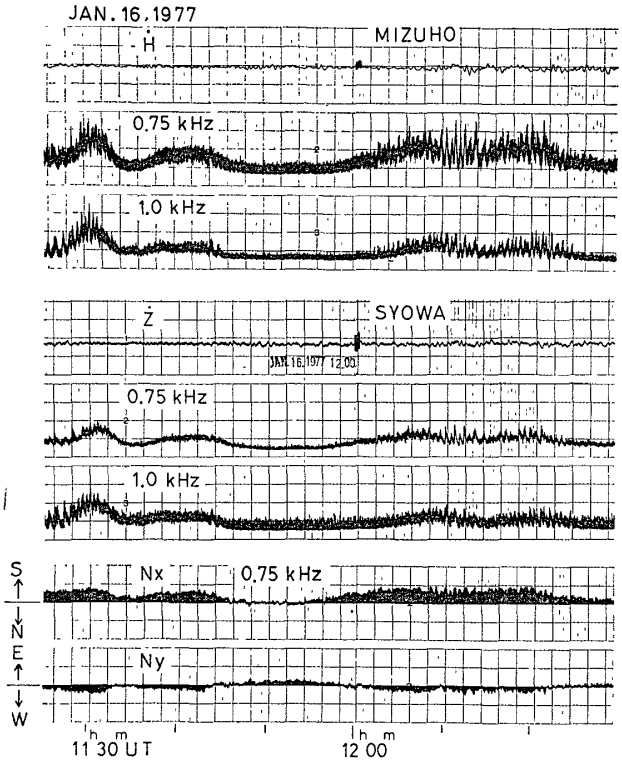

Fig. 49. Upper two panels show intensity records of ELF chorus emissions and magnetic pulsations observed at Mizuho and Syowa Stations. Lower panel shows the arrival directions of 0.75 kHz emissions observed at Syowa Station. N_x and N_y denote north-south and east-west components, respectively. It is found that 0.75 kHz band emissions were incident from the south of Syowa Station.

observations of ELF-VLF emissions, and magnetic variations have been carried out at Syowa and Mizuho Stations since June 1976. Details of the observation system were described by MAKITA (1978). In this section we will discuss the changes in arrival direction of QP elements using the data from this new observation system.

Fig. 49 shows simultaneous records of magnetic pulsations and intensity of ELF emissions at two selected narrow bands, 0.75 kHz and 1.0 kHz, obtained at Mizuho and Syowa Stations, along with the north-south (N_x) and the east-west (N_y) of arrival direction of the wave in the 0.75 kHz band at Syowa Station on January 16, 1977. Time variations of the intensity at both the stations were vary similar, while the intensity of the 0.75 kHz band at Mizuho Station was larger than that at Syowa Station throughout the period shown in this figure. The arrival direction of the 0.75 kHz band emission showed that the emissions came from the south (pole side). This tendency is consistent with the fact that the intensity of the emission at Mizuho Station was stronger than that at Syowa Station. The exist point of the emission would be nearer to Mizuho Station. The upper panel of Fig. 50 indicates the intensity of E_z component of the wave, and the north-south (N_x) and east-west (N_y) components of arrival direction for the 1.3 kHz frequency band, on December 18, 1976. The frequency-time spectra of this event are also shown in the lower panel in an expanded time scale. It is

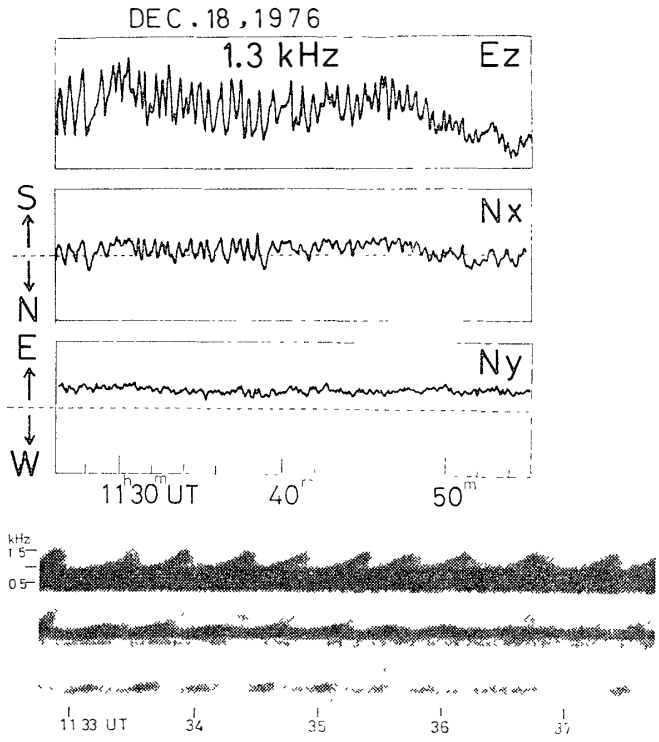

Fig. 50. Emission intensity of the E_z component, and the north-south (N_x) and east-west (N_y) components of arrival direction at the center frequency of 1.3 kHz, on December 18, 1976. Only the north-south component of arrival direction fluctuated was associated with the QP fluctuations. The frequency-time spectra of this event is shown in the lower panel.

worth noting that the north-south component of the arrival direction fluctuated concurrently with each QP element. The east-west component, on the other hand, did not fluctuate remaining nearly constant from the east. This fact suggests that the generation region oscillates radially with the fluctuations in intensity of the QPs as if emissions were generated in the equatorial region and ducted to the observation site along field lines. The frequency-time spectrum indicates that this QP emission belong to the rising tone type. Fig. 51 shows some other examples indicating similar fluctuations in the arrival direction associated with the appearance of QP elements. Significant fluctuations are seen in the north-south component only for events on November 19, 1976, January 12, 1977 and January 21, 1977 as in the previous example of December 18, 1976 (Fig. 50). On the other hand, fluctuations in both of the north-south and east-west components are seen in the example of January 16, 1977. No example was found with fluctuations of only the east-west components associated with QP elements.

Frequency-time spectrum of QP elements is related to fluctuations of the arrival direction. The rising tone spectrum mostly occurs associated with fluctuations in north-south component only, and 'non-dispersive' type of QP is associated

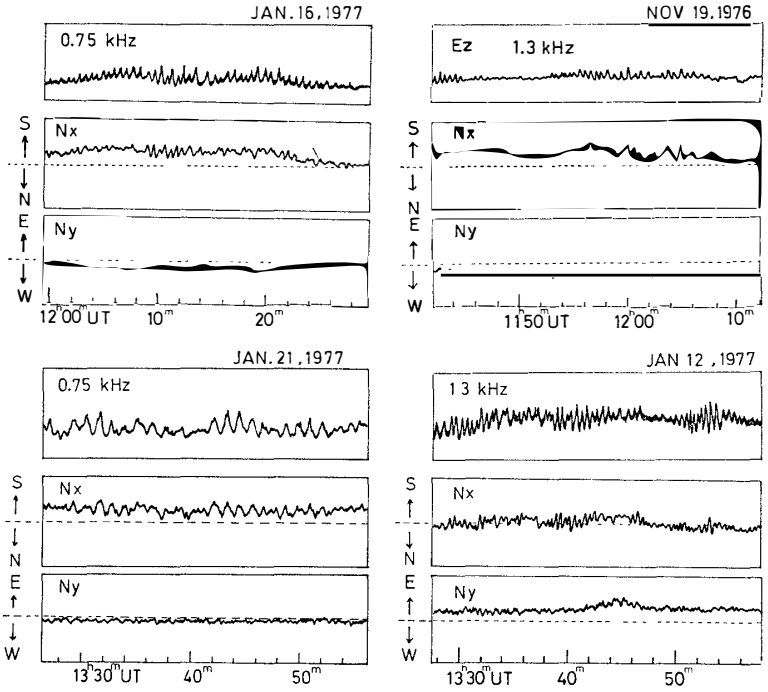

Fig. 51. Shows some examples where arrival direction fluctuated were associated with QP fluctuations.

with the fluctuations of both north-south and east-west component or with no fluctuations at all. From these results it is very likely that the source region of a QP emissions sometimes moves quasi-periodically in a radial direction concurrent with the appearance of the QP elements of the emissions.

7. Coordinated Observations of ELF-VLF Emissions at Two Separated Stations and at the Geomagnetic Conjugate-Pair Stations

7.1. Distribution in intensity of ELF-VLF emissions simultaneously observed at Syowa and Mizuho Stations

Simultaneous observations of ELF-VLF emissions, magnetic variations, cosmic noise absorptions and auroras have been carried out at Syowa and Mizuho Stations since June 1976. Mizuho Station is about 270 km distance poleward from Syowa Station on the same geomagnetic meridian. Fig. 52 shows the location of both stations. In this section, we will examine the characteristics of the polar chorus (daytime ELF-VLF chorus) emissions and QP emissions observed simultaneously at both stations. The observation systems at Mizuho and Syowa Stations were described in Section 2 and in detail by MAKITA (1978).

The spatial distribution of individual chorus emission observed at the ground was reviewed by HELLIWELL (1965). Discrete emissions are often observed

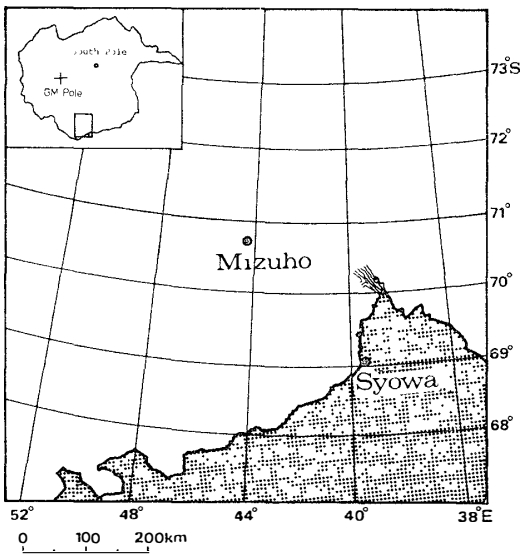

Fig. 52. Location of Syowa and Mizuho Stations.

simultaneously at stations a few hundred kilometers apart or less. Occasionally the same emissions can be observed at widely separated stations. Spatial distributions of ELF-VLF chorus emissions observed at a large distance from the earth were examined by TSURUTANI and SMITH (1974, 1977). The satellite data of ELF chorus in the outer magnetosphere indicated that the spatial distribution of frequency of the peak in power spectrum is proportional to 0.25–0.30 Ω^- where Ω^- is the local electron gyrofrequency. These results suggest that ELF-VLF chorus is a localized phenomenon in the outer magnetosphere. If ELF chorus is generated locally in the outer magnetosphere and propagates along the magnetic field line of force, it is important to examine the spatial distribution of individual ELF-VLF chorus and QP emissions observed on the ground in order to study the propagation characteristics of them.

7.1.1. October 21, 1977 event

The October 21, 1977 event is one of the typical examples of ELF-VLF chorus with a long duration of more than eight hours, including fluctuations of intensity with periods longer than a few minutes, QP emissions, periodic emissions and discrete emissions. Fig. 53 shows the intensity record of ELF chorus emissions

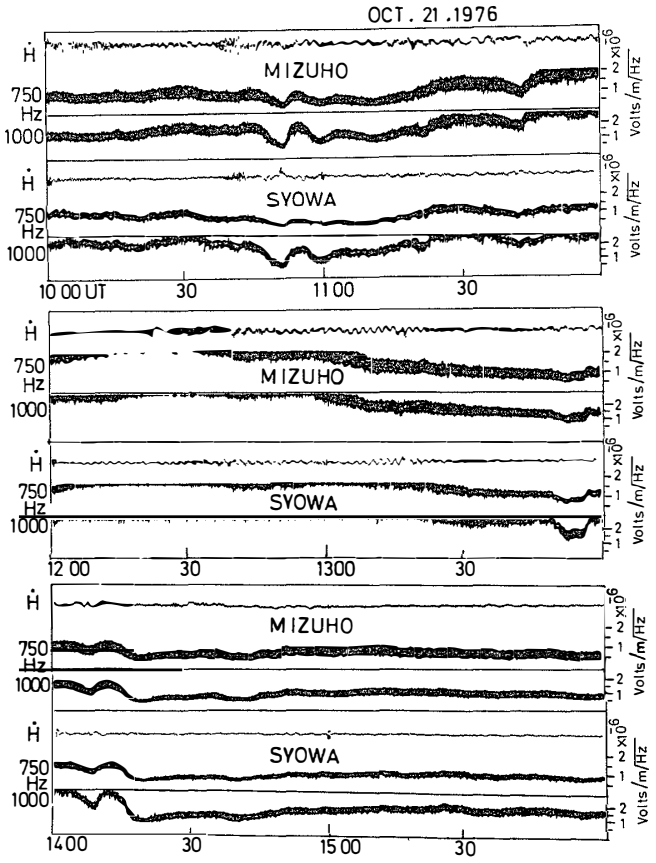

Fig. 53. Intensity records of ELF chorus emissions and the $\dot{H}$ components of magnetic pulsations observed at Mizuho and Syowa Stations.

in the frequency bands 0.75 kHz and 1.0 kHz, and the H component of the induction magnetogram obtained at Mizuho and Syowa Stations. Slow fluctuations in intensity of ELF chorus were simultaneously observed during the time intervals of 1030–1105, 1115–1145 and 1345–1420 UT. Fig. 54 shows the frequency-time (f-t) spectra of ELF chorus emissions, presented in Fig. 53. It is found that fluctuations in emission intensity and band width were nearly the same at both the stations. The narrow intense frequency band 1.0 kHz at Syowa Station is the contamination from instrumental noise.

Fig. 55a shows the time expanded f-t spectra of discrete and diffuse emissions for the time intervals of 1201:25–1202:15 UT and of 1202:54–1203:50 UT on October 21, 1976 (*cf.* Fig. 54). It is found that the intensity of discrete emissions was greater at Syowa Station than at Mizuho Station, while the intensity of diffuse emissions was smaller at Syowa Station. Fig. 55b shows the f-t spectra of periodic emissions for the interval 1551–1558 UT. The periodic emissions were modulated quasi-periodically with a period of about 30 s. The periods of the periodic emissions and of the QP modulations were almost the same at both the stations.

As mentioned above, the frequency-time spectrum and the fluctuations in intensity of the ELF chorus were very similar at both stations, whereas the emission intensities were different. Details are described in a later section.

7.1.2. *Relationship between relative intensity at the two stations and arrival directions*

Fig. 49 shows the intensity records of ELF chorus emissions in 0.75 and 1.0 kHz bands and the H component (Mizuho Station) and the Z component (Syowa Station) for magnetic pulsations observed at both stations (two upper panels). Type 1 QP emissions with periods of 30–40 s were observed at both stations in the time intervals 1120–1132 and 1202–1225 UT. The bottom panel of Fig. 49 shows the arrival direction of the wave at 0.75 kHz observed at Syowa Station. N_x and N_y denote the north-south and the east-west components of the angles of incidence, respectively. It is found from the intensity record and arrival direction that the intensity of the 0.75 kHz band at Mizuho Station was about twice of that at Syowa Station, and the 0.75 kHz and band emissions were incident from the south (poleward side) of Syowa Station. The fact that the emission intensity is greater at Mizuho Station than at Syowa Station is consistent with the finding that the arrival direction is the south of Syowa Station.

Furthermore, the emission intensity in the 1.0 kHz band at Mizuho Station is about 1.5 times that at Syowa Station. It is evident that the intensities in the low frequency range were greater at higher latitudes. These results observed at two separated stations are consistent with the spatial distribution, with respect to L in the outer magnetosphere, of the chorus emissions examined by TSURUTANI and SMITH (1974, 1977).

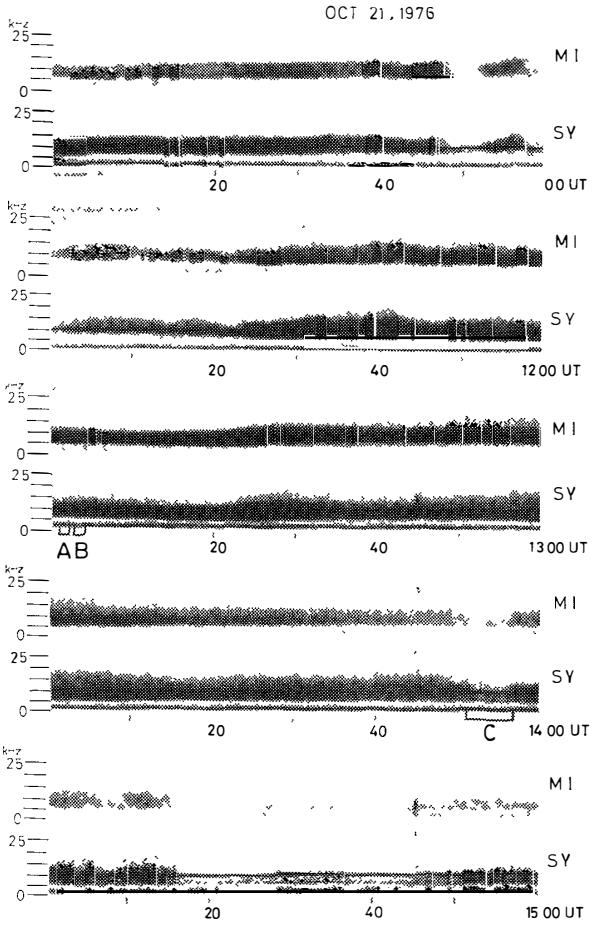

Fig. 54. Frequency-time spectra of the ELF chorus emissions which are presented in Fig. 53.

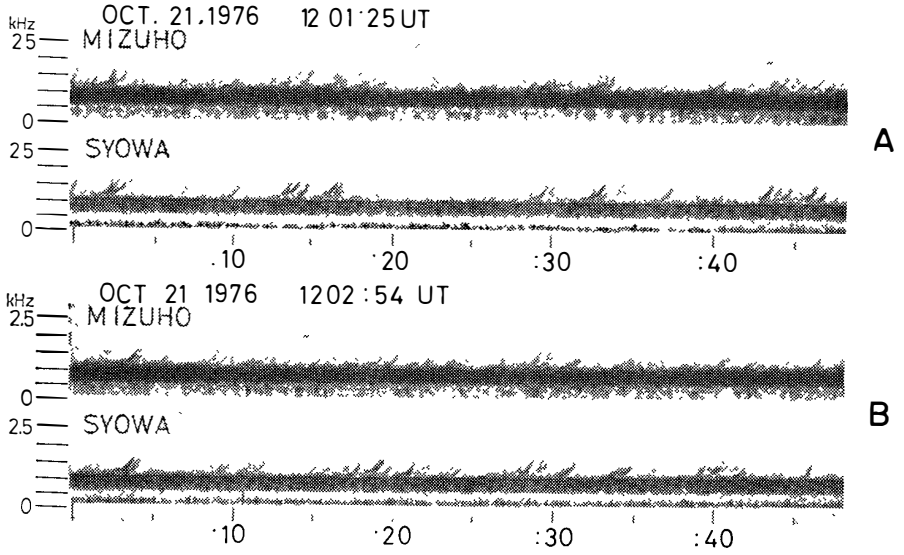

Fig. 55a. Frequency-time spectra of discrete emissions for the time intervals 1201:25–1202:15 UT and 1202:54–1203:50 UT on October 21, 1976 (cf. Fig. 54).

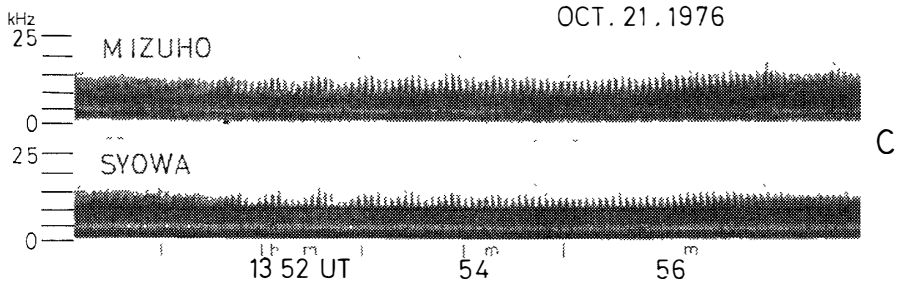

Fig. 55b. Frequency-time spectra of periodic emissions for the time interval 1350–1358 UT on October 21, 1976 (cf. Fig. 54).

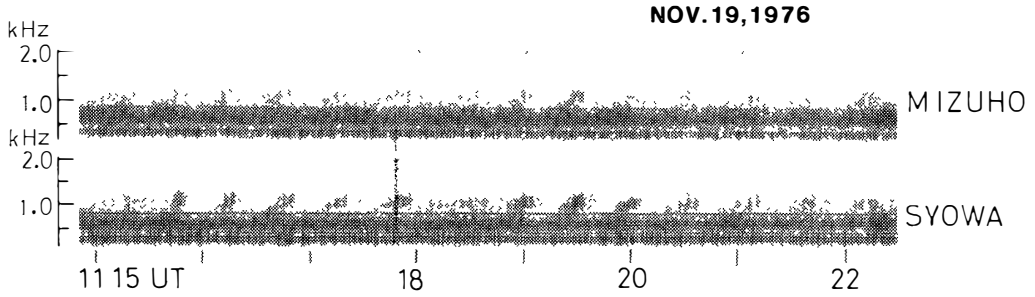

Fig. 56. Frequency-time spectra of QP emissions. The periods and the start time of QP emissions were same at both the stations.

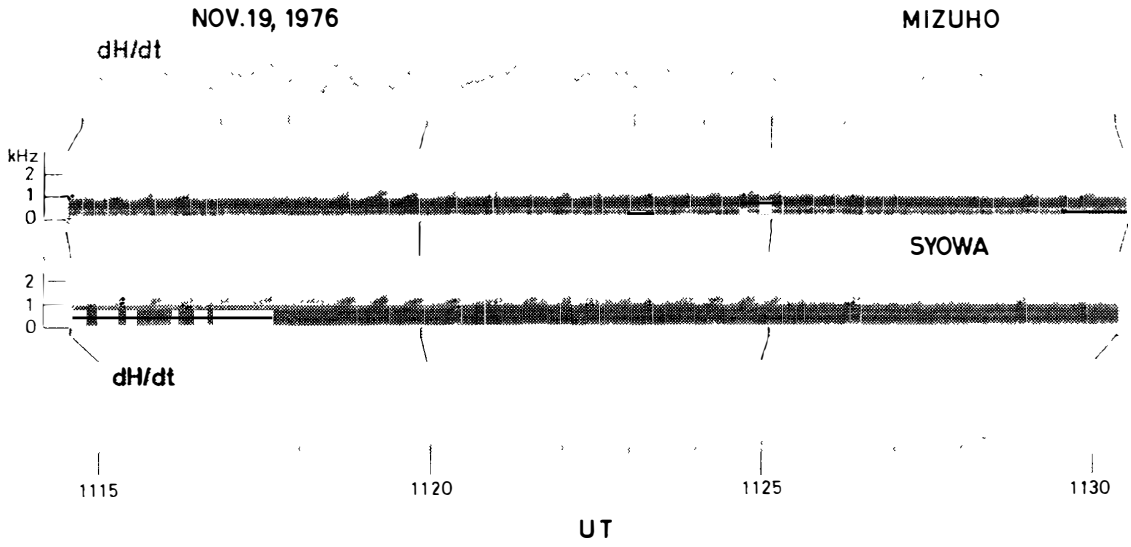

Fig. 57. Frequency-time spectra of QP emissions and magnetic pulsations observed at Mizuho and Syowa Stations. It is found that QP emissions were associated with magnetic pulsations at both stations.

7.1.3. QP emissions

Fig. 56 shows frequency-time spectra of QP emisions at Syowa and Mizuho Stations on November 19, 1976. The period of QP emissions was 30 s, and the QP spectra showed a 'rising-tone' during one quasi-period. It is clear in Fig. 56 that the periods and fine structures of the QP spectra were almost the same at both stations. Fig. 57 shows the *f-t* spectra of QPs and the pulsations in the *H* component of magnetic field observed at Mizuho and Syowa Stations on November 19, 1976. This is a typical example of emissions with a period of about 30 s, which were associated with magnetic pulsations at both stations. Fig. 58 shows the average power spectra of QPs in the time interval 1115–1125 UT on November 19, 1976 for Syowa and Mizuho Station (*cf.* Fig. 56). It is found that the power in the lower frequency range (0.5–0.8 kHz) was 10 dB higher than the power in higher frequency range (1.0–1.4 kHz) at Mizuho, while the difference in intensities between the lower and higher frequency ranges at Syowa Station is much smaller. These results suggest that the QP emissions in lower frequency range are generated at a higher latitude.

The results mentioned in this section are consistent with the statistical results of arrival direction described in Section 6. Firstly, the low-frequency ELF chorus and Type 1 QP emissions in the 0.75 kHz band come mostly from the south (poleward side) in the daytime. Secondly, the generation regions of daytime ELF chorus emissions and Type 1 QP emissions appear to be in the outer magnetosphere.

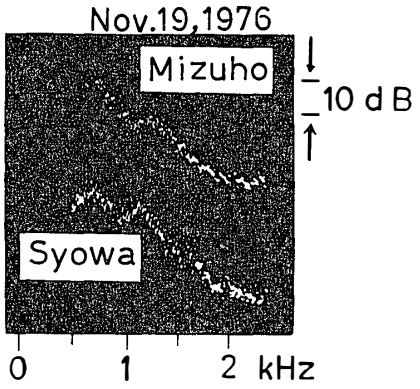

Fig. 58. Power spectra of QP emissions for the time interval 1115–1125 UT on November 19, 1976 (cf. Fig. 56). It is found that the intensity in the lower frequency range is greater at Mizuho Station than at Syowa Station.

7.2. Geomagnetic conjugacy of ELF-VLF emissions observed at Syowa Station, Antarctica and Husafell, Iceland

Conjugate observations of ELF-VLF emissions, magnetic pulsations, and auroras have been carried out at Syowa Station in Antarctica and at Husafell in Iceland from July 29 to September 18, 1977. Husafell is located about 60 km north of the conjugate point of Syowa Station. In this section we will examine the conjugate relationship of QP emissions using the data of intensity records

of ELF-VLF emissions, magnetic pulsations, and of the frequency-time spectrum.

The studies of conjugacy of QP emissions on the basis of data obtained at a pair of conjugate stations up to now are very limited. According to KITAMURA *et al.* (1969), who examined the data of VLF emissions obtained at Great Whale River and Byrd Station ($L\sim7$), the Type 1 QP seldom shows a emission conjugacy, whereas the Type 2 QPs are frequently observed at the conjugate-pair stations with a good conjugate relationship. KOROTOVA *et al.* (1975) reported that many QP emissions, associated with magnetic pulsations, were often observed at a fixed frequency around 2 kHz at two conjugate-pairs, Sogra-Kerguelen ($L=3.5$) and Dolgoschelie-Herd ($L=4.2$). CARSON *et al.* (1965) noted that each periodic element, which forms quasi-periodic structures, is observed alternatively with a time delay of one-hop whistler mode propagation at conjugate stations.

In this section, we will first reexamine the results by KITAMURA *et al.* (1969) that Type 1 QPs rarely show a good conjugacy and that Type 2 QPs usually show a good conjugacy. Conjugate relations of QP emissions will be examined in more detail by using the frequency-time spectrum.

7.2.1. Conjugacy of QP emissions seen on the band-limited intensity records

Fig. 59 shows a typical example of Type 1 QP emissions observed at Husafell and Syowa Station in the 0.75 and 1 kHz bands along with records of magnetic pulsations. QP emissions were seen to be associated with Pc 3 magnetic pulsations in the interval of 1340–1448 UT and with slowly varing magnetic variations in the intervals, 1350–1435 and 1445–1520 UT. It is clear that QP activity and

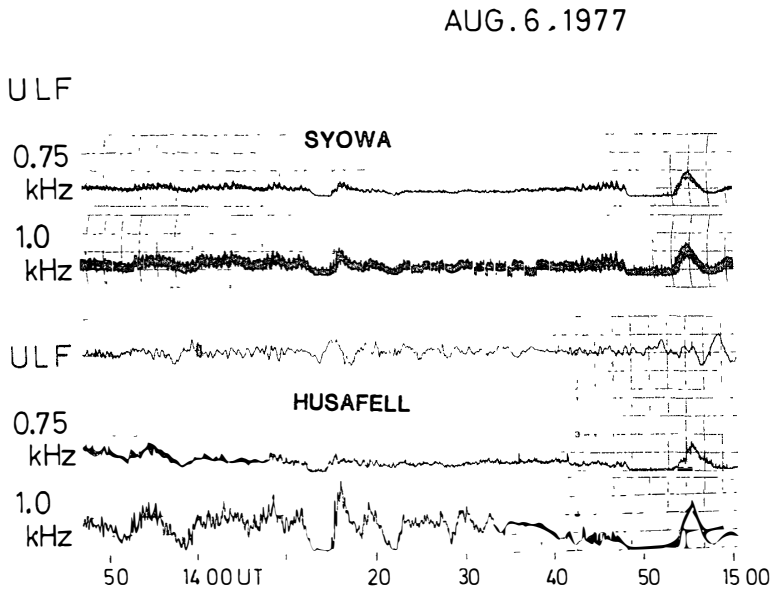

Fig. 59. Intensity records of QP emissions and magnetic pulsations observed at Husafell and Syowa Station on August 6, 1977. QP emissions were associated with Pc 3 magnetic pulsations during the time interval 1340–1448 UT and with long period magnetic pulsations ($t=120\sim250$ s) during the time intervals 1350–1435 and 1445–1520 UT.

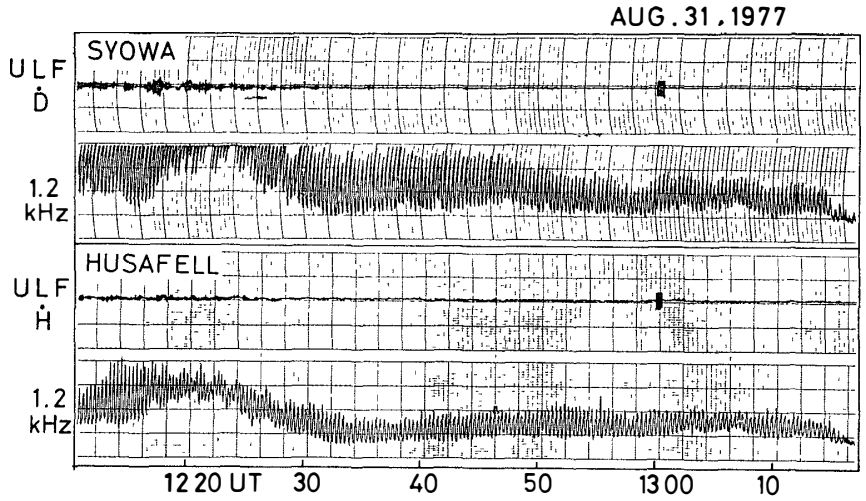

Fig. 60. An example of Type 2 QP emissions observed at Husafell and Syowa Stations on August 31, 1977. Emission activity of QPs was very strong at both stations. On the other hand, activity of magnetic pulsations corresponding to the active periods of QPs (T~30 s) were very weak at both stations.

magnetic pulsations occurred simultaneously at Husafell and Syowa Station, *i.e.*, Type 1 QPs and magnetic pulsations show a good conjugacy. Fig. 60 shows an example of Type 2 QPs that occurred on August 31, 1977. The activity of magnetic pulsations was very low both at Husafell and Syowa Station in this example. However, the activity of QP emissions was very high at both the stations. This example shows that Type 2 QP emissions have a peak to peak correlation between the two conjugate stations during a period of quiet magnetic activity.

QP events found on the intensity records at the conjugate-pair of stations in the period from July 31 to September 17, 1977 are listed in Table 4. In this period, 28 QP events were found in the intensity records. Most QPs occurred in the first half of August, related to high magnetic activity during this period. It is evident that most of QPs (including both Type 1 QPs and Type 2 QPs and magnetic pulsations show a good conjugacy except for the August 4 event. These results are inconsistent with those of KITAMURA *et al.* (1969) who reported that Type 1 QPs have a poor conjugacy. They accordingly suggested that the sources of the VLF emission may be local. However, the present results indicate that both types have a good conjugacy.

Our results that most QPs, including both Type 1 QPs and Type 2 QPs, show a good conjugacy, indicate that QP emissions are generated near the equatorial region in the outer magnetosphere and propagate to both the hemispheres along the field line of force which act as a wave duct, as suggested in Sections 5, 6, 7 and 8. So that, most of QP emissions show a good conjugacy when there is not a fade-out of emissions, caused by a strong absorption in the ionosphere of one

Table 4. Conjugacy of QP emissions.

Date	Start time (UT)	Stop time (UT)	QP period (s)	GP activity at Husafell	GP activity at Syowa Station	Type of QP emission	Conjugacy of QP activity
July 31	0855	1046	10–15	M	M	2	Yes
31	1820	1840	150	A	A	1	〃
Aug. 1	1150	1255	25–35	M	M	1	〃
4	0450	1540	80	A	M	1	〃
4	1155	1220	15–20	M	M	1	〃
4	1300	1350	50–70	W	W	(?)	?
4	1605	1735	25–35	W	W	(?)	?
5	1000	1430	20–60	A	A	1	Yes
6	0920	0925	30	A	A	1	〃
6	1340	1520	25–35	A	A	1	〃
8	0920	1000	12–18	W	N	?	〃
8	1105	1300	25–40	A	A	1	〃
9	0900	0930	10–15	W	W	2	〃
9	0950	1030	15–20	W	W	2	〃
10	1330	1340	35–45	W	W	2	〃
16	0850	1140	15–25	W	W	1 and 2	〃
18	0840	1510	20–40	A	A	1	〃
19	0750	0920	25–35	A	A	1	〃
19	1220	1510	30–40	A	A	1	〃
20	0905	0920	35–40	M	M	1	〃
20	1200	1520	50–70	M	M	1	〃
23	1040	1120	30–40	W	W	2	〃
26	0710	0750	10–15	M	M	1 and 2	〃
31	0940	1520	15–25	W	W	2	〃
Sep. 3	0800	1120	15–20	A	A	1	〃
3	1605	1740	50–70	M	M	2(?)	〃
14	0940	1530	20–40	M	M	1	〃
17	1910	2020	25–30	N	N	2	〃

A: Active, M: Modelate, W: Weak, N: Nothing.

hemisphere or caused by a extinction of the magnetosphere-ionosphere wave duct in one hemisphere.

7.2.2. Comparison of frequency-time spectra

In this section we will examine the conjugate relationship of QP emissions that occurred on August 18, 1977, as a typical example of a disturbed period. August 18 was one of the most active days for magnetic pulsations and VLF emissions in the 52 days period of conjugate-pair observations. Fig. 61 shows examples of intensity records of QP emissions associated with Pc 3 magnetic

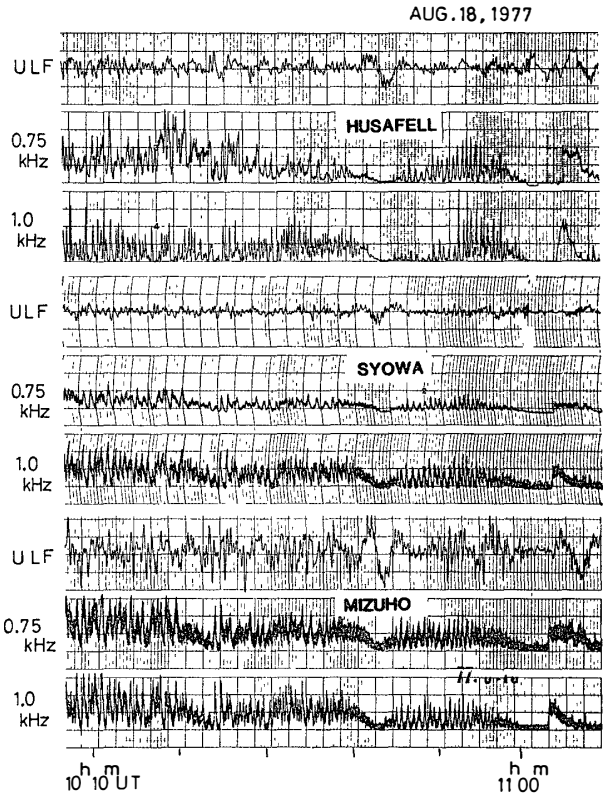

Fig. 61. Examples of intensity records of QP emissions associated with Pc 3 magnetic pulsations observed at Husafell, Syowa and Mizuho Stations on August 18, 1977.

pulsations observed at Husafell, Syowa and Mizuho Stations during the interval of 1007–1109 UT on August 18, 1977. It is clear that QP emissions in the frequency bands 0.75 kHz and 1.0 kHz and Pc 3 magnetic pulsations were simultaneously observed at Husafell in the northern hemisphere and at Syowa and Mizuho Stations in the southern hemisphere. Figs. 62a and b show frequency-time spectra of QP emissions in the two periods of 1013:20–1017:00 and 1051:50–1055:15 UT which are included in Fig. 61. The QP emissions with periods of 20–40 s were simultaneously observed with roughly the same *f-t* spectra at both hemispheres. However, a considerable difference in the frequency dependence of intensity is noted between the conjugate stations. The intensity of the lower frequency range (0.7–0.9 kHz) was higher at Syowa Station than at Husafell while the reverse was observed in the higher frequency range (1.2–1.4 kHz). It is also seen that the periodic emissions are quasi-periodically modulated during the time interval of 1015:56–1016:05 UT as seen in Fig. 62a. Fig. 63 shows time expanded *f-t* spectra for the periodic emissions. It is found that each element of periodic emissions appeared alternately at conjugate stations with the time delay of a one-hop whistler mode propagation. This result is the same as for the conjugate observation at sub-auroral latitudes (L=4.1) of CARSON

et al. (1965). In contrast to the element of periodic emissions, the element of the QP emission appears almost simultaneously at the conjugate stations. Fig. 64 shows a time expanded *f-t* spectrum of a QP emission which consists of a rising tone as well as a diffuse band with a constant frequency. It is seen that the rising-tone element of the QP emission occurs simultaneously at the conjugate points. These facts suggest that the generation region of QPs is around the magnetic equator and that the emissions propagate simultaneously toward both the hemisphere along magnetic field lines.

Fig. 65 shows a sudden enhancement of ELF emissions accompanied by a positive sudden impulse in the magnetic field (described in Section 5). The onset of sudden enhancement of ELF emissions in both the hemispheres coincides, however, the intensified frequencies are not necessarily the same. A higher frequency component (1.2–1.4 kHz) was more intense at Husafell than at Syowa Station for 1103:20–1105:40 UT and a lower frequency emission (0.5–0.8 kHz) was more intense at Syowa Station than at Husafell after 1104:00 UT. The difference in frequency dependence of the enhanced band between Syowa Station and Husafell is very similar to that of the QP emissions, shown in Fig. 62b, which were observed just before the sudden enhancement of ELF emissions at 1103:20 UT. This fact suggests that generation and propagation conditions for the sudden enhancement of the emissions is nearly the same as those of previous QP emissions. Furthermore, it suggests that the quasi-periodic modulation associated with Pc 3 magnetic pulsations and the sudden enhancement of ELF emissions accompanied by a sudden impulse in geomagnetic field are essentially due to the same mechanism, *i.e.*, both Type 1 QPs and sudden enhancement of ELF emissions would result from modulation of the emission source by magnetic field variations in the magnetosphere.

7.2.3. *Conjugacy of the auroral chorus*

Next, we examine the geomagnetic conjugacy of auroral chorus emissions seen in frequency-time spectra on August 18, 1977. The auroral chorus is frequently observed during the recovery phase of a magnetic substorm from post-midnight to early morning and is very often associated with pulsating auroras and Pi C magnetic pulsations (HAYASHI and KOKUBUN, 1971; OGUTI and WATANABE, 1976).

Fig. 66 shows examples of the *f-t* spectra of auroral chorus observed at the conjugate-pair stations for 0656:10–0700:00 UT on August 18, 1977. The frequency-time spectra at Syowa Station indicate emission of diffuse noise with a constant frequency of 0.4–0.8 kHz. No diffuse emission was seen in this frequency band at Husafell, Iceland on the other hand, a group of strong discrete risers was dominant in the frequency band of 0.5–2.5 kHz. Discrete elements at Syowa Station were so weak that we could not distinguish any. This example

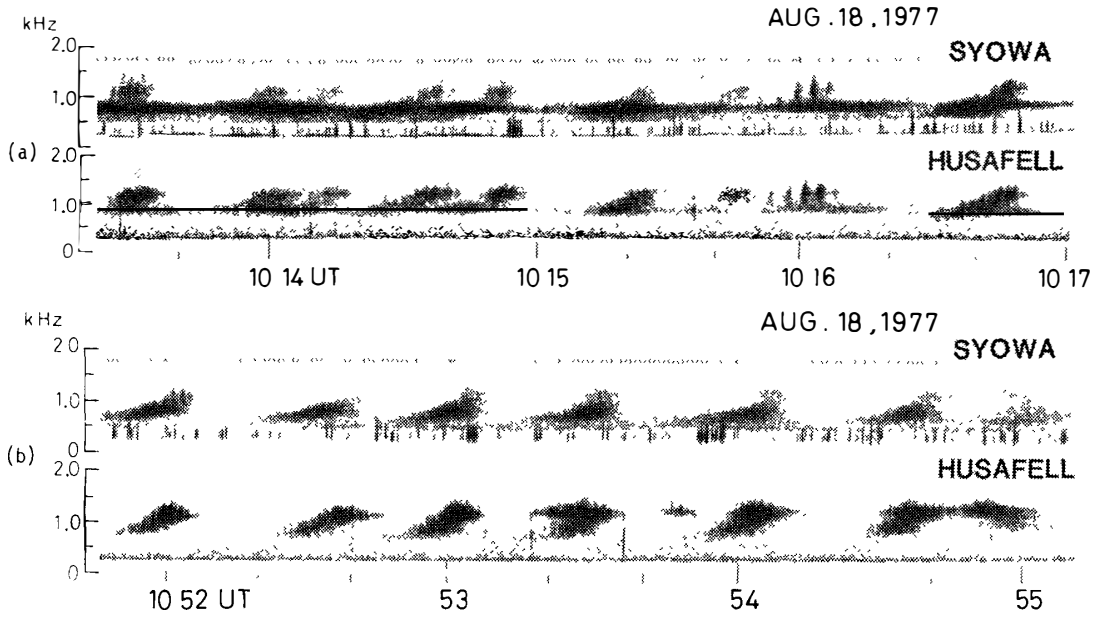

Fig. 62. Frequency-time spectra of QP emissions for the two time intervals, 1013:20–1017:00 UT (a) and 1051:50–1055:15 UT (b) in Fig. 61. It is found that the emission intensity in the frequency range below 1 kHz is larger at Syowa Station than at Husafell, and in the higher frequency range, the reverse occurs.

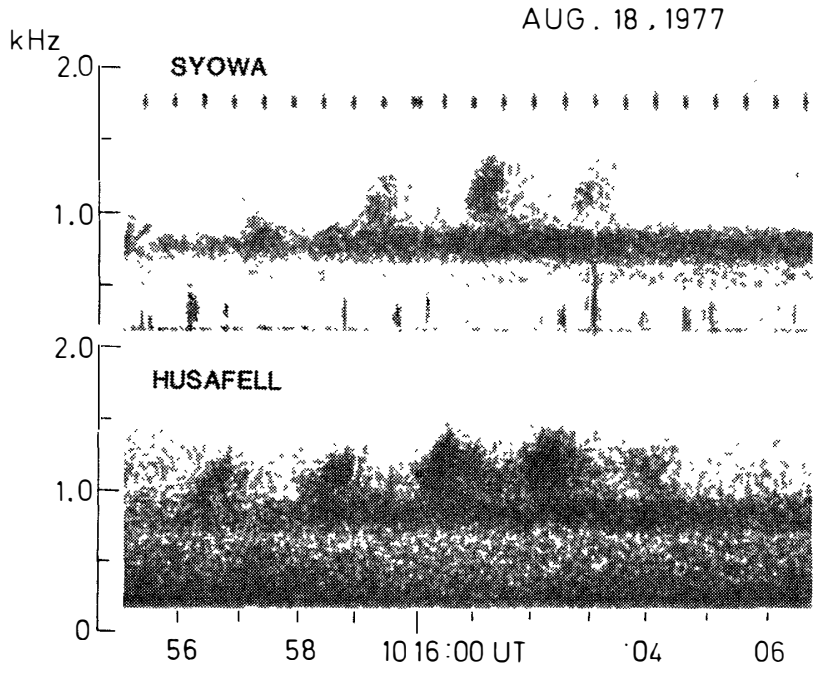

Fig. 63. Expanded frequency-time spectra of periodic emissions in the time interval 1015:55–1016:07 UT. It is found that periodic emissions are alternately observed in the two hemispheres.

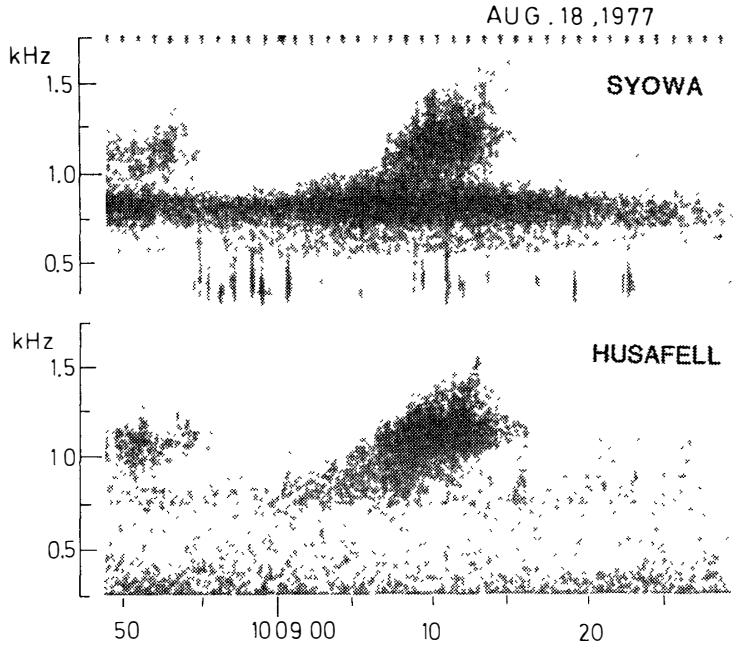

Fig. 64. Expanded frequency-time spectra of QP emissions during the time interval 1008:48–1009:30 UT. It is found that QP emissions are simultaneously observed in both the hemispheres.

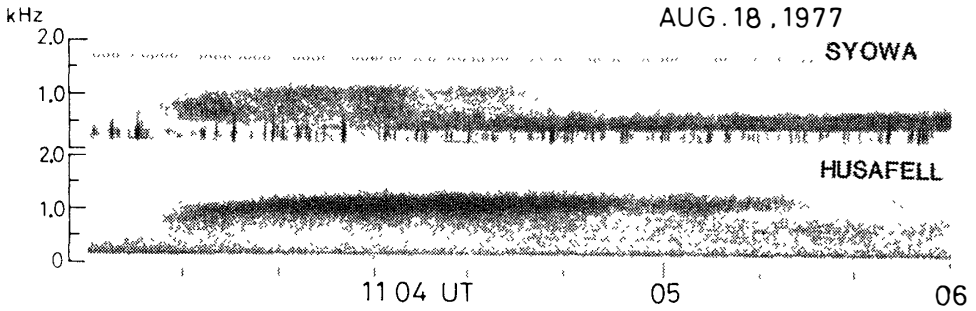

Fig. 65. Examples of frequency-time spectra of ELF emissions excited by a positive sudden impulse. ELF emissions began simultaneously at the conjugate-pair stations. However, the intensities in the higher frequency range were higher at Husafell than at Syowa Station (1103:20–1105:30 UT) and the intensities in the lower frequency range were higher at Syowa Station than at Husafell (1104.00–1106.00 UT).

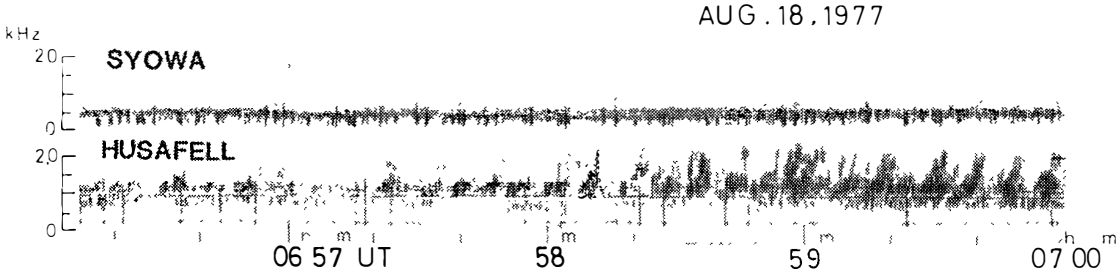

Fig. 66. Examples of frequency-time spectra of ELF chorus emissions in the early morning. It is found that the emission intensity is higher at Husafell than at Syowa Station.

clearly indicates that the conjugate relationship of auroral chorus observed in the early morning is more complicated than that of daytime chorus.

7.2.4. Conjugacy of the auroral hiss

Next, we discuss briefly the conjugacy of auroral hiss emissions. Auroral hiss is well known to be associated with the appearance of an auroral arc (MAKITA and FUKUNISHI, 1973; OGUTI, 1975). Using the data obtained at Syowa Station, KOKUBUN *et al.* (1972) and MAKITA and FUKUNISHI (1973) reported that the occurrence of auroral hiss has a clear seasonal variation. Auroral hiss is mostly observed with an occurrence probability of more than 70%, in the winter season from April to September and is rarely observed (with the occurrence less than 10%) in the summer season from November to February. It is interesting to examine the conjugacy of auroral hiss in connection with the seasonal variation of hiss emissions.

Fig. 67 shows the amplitude records of magnetic pulsations, and emission

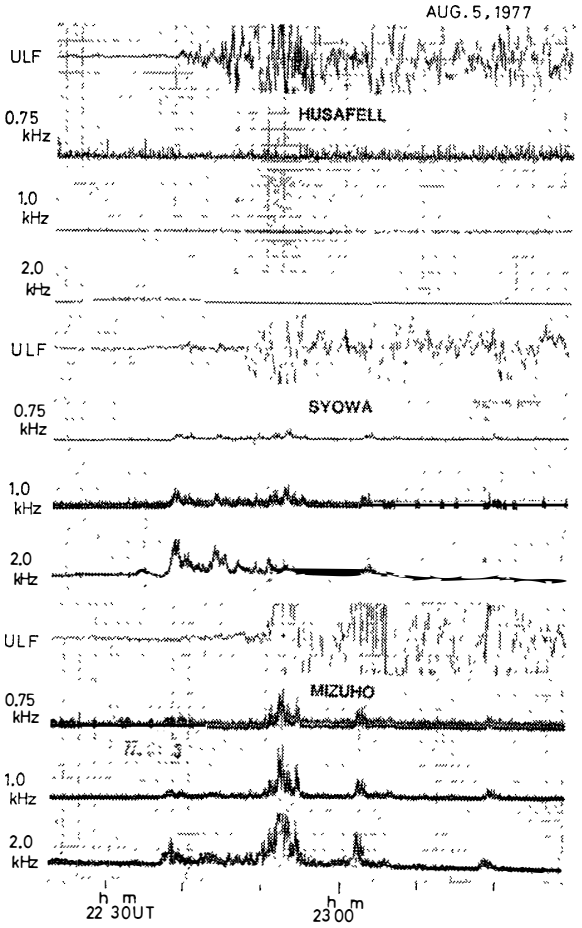

Fig. 67. Intensity records of auroral hiss emissions and magnetic pulsations observed at Husafell, Syowa and Mizuho Stations. It is found that the intensity is much higher at Syowa and Mizuho Stations in the southern hemisphere than at Husafell in the northern hemisphere.

intensity in the frequency bands 0.75, 1.0, 2.0 kHz at Husafell in Iceland, and at Syowa and Mizuho Stations in Antarctica for the period 2222–2328 UT on August 5, 1977. It is clear that auroral hiss emissions in all frequency bands are enhanced at Syowa and Mizuho Stations, associated with the enhancements of magnetic disturbance in the time intervals 2230–2306 and 2318–2322 UT. However, no emissions appeared at Husafell in the northern hemisphere.

Non-conjugacy of auroral hiss, such as shown in Fig. 67 is consistent with the seasonal variation of the occurrence of auroral hiss, because the occurrence probability is larger in winter.

In this section, we described the geomagnetic conjugacy of QP emissions, auroral chorus, and auroral hiss observed at a good conjugate-pair of stations, Husafell, Iceland and Syowa Station, Antarctica. As mentioned above, there are considerable difference in ELF-VLF emissions at conjugate stations. In order to explain the physical process involved in conjugate relationships we must examine the differences between geophysical conditions in the northern and the southern hemispheres. For example, the total intensity of magnetic field is about 45000 γ at Syowa Station and 52000 γ at Husafell, and the dip angle of the magnetic lines of force is 65° at Syowa Station and 75° at Husafell. Furthermore, the sunlit time in the ionosphere is very different at the two stations.

8. Relationships Between QP Emissions and Magnetic Pulsations

It was shown in a previous section that the QP emissions can be classified into two types, Type 1 and Type 2 QP emissions. Type 1 QPs are associated with magnetic pulsations whose intensities are larger than $\sim 0.05\,\gamma$/s, and the 10 min average periods of QPs and magnetic pulsations are nearly the same, within 10%. In the case of Type 2 QPs the periodicity is more regular than in the case of Type 1 QPs, and intensities of concurrent magnetic pulsations are usually weaker than $\sim 0.01\,\gamma$/s. We also classified QPs into Type 2, when 10 min average periods of QPs and concurrent magnetic pulsations were entirely different.

We found essential differences in the properties of the two types as mentioned in the previous sections. In this section, we will examine in more detail the quantitative relationship between QP emissions and magnetic pulsations by using dynamic power spectral analysis and correlation analysis. This will give the quantitative relationships of spectral structures for both the types of QP emissions.

8.1. Comparison of dynamic spectra for intensities of QP emissions and magnetic pulsations

In this section, we will make comparisons between dynamic spectra of the intensities of QP emissions and magnetic pulsations using a real-time FFT spectral analyzer.

8.1.1. Dynamic spectra for intensities of QP emissions and magnetic pulsations

Intensity records of selected frequency bands of QP emissions and magnetic pulsations are first analyzed by a real-time FFT spectral analyzer to show the general features of the relationship between QP fluctuations and magnetic pulsations. Fig. 68 shows examples of *f-t* spectra for the $\dot{D}$ component of magnetic pulsations and quasi-periodic variations of ELF emission intensity at the center frequency bands of 0.56 and 0.9 kHz on January 9, 1975. Magnetic pulsations with a broad frequency band from 0.02 Hz to 0.06 Hz were observed for a long time from 06 UT to 14 UT. QP emissions were active in the time interval of 1030–1330 UT. ELF emission activity was weak before 1030 UT. The periodicity

of both magnetic pulsations and QPs show a broad frequency structure with a frequency band from 0.02 Hz to 0.06 Hz in the time interval of 1030–1200 UT. After 1200 UT, the band width of both magnetic pulsations and QPs reduced to a narrow band and the center frequency shifted from 0.04 Hz to 0.02 Hz. This figure demonstrates that Type 1 QP emissions are closely associated with magnetic pulsations with the same period and activity.

The left panel of Fig. 69 represents the relation between the amplitude of magnetic pulsation and the peak-to-peak amplitude of QPs in the 0.75 kHz frequency band. This plot is made for five minute average values in the time interval of 1030–1330 UT on January 9, 1975. It is seen in this illustration that QP modulations tend to become larger with increase in pulsation amplitude, suggesting that the QP emission results from an adiabatic modulation of preexisting emission by magnetic pulsations. The right panel of Fig. 69 gives the relation between the peak-to-peak amplitude of QPs and the average (band-integrated) intensity of ELF emissions. There is a distinct relationship that the amplitudes of the QPs become larger with increase in background emission intensity.

Fig. 70 shows the other example that QP emissions are closely correlated with magnetic pulsations. The left panel shows intensity records of magnetic pulsations ($\dot{D}$) and ELF emissions at the center frequency of 0.75 kHz obtained at Syowa Station on January 15, 1975. The right panel shows frequency-time spectra of magnetic pulsations and intensity modulations at 0.75 kHz. It is evident from the figure that the QP periods changed in accordance with those of magnetic pulsations. Both the frequencies of the intensity modulation of QPs and magnetic pulsations were from 0.01 Hz to 0.03 Hz before 0915 UT, and subsequently shifted to higher frequencies up to 0.06 Hz in a similar fashion. The variation in modulation frequency of the QPs was the same as that in the frequency of magnetic pulsations. Thus, QP events given in Figs. 68 and 70 yield evidence that QPs are really associated with magnetic pulsations.

8.1.2. Dynamic spectra of Type 2 QP emissions

The time variation of the modulation frequency of Type 2 QP emissions is first examined to illustrate the regularity in the repetition period. Fig. 71 shows frequency-time spectra of emissions observed at Mizuho Station on Decemebr 19, 1976. The geomagnetic condition during this event was quiet, (Kp=1+), and the pulsation activity was also low. It was confirmed from the dynamic spectrum analysis using a real-time spectrum analyzer that no clear peak in pulsation spectrum was noticed in the frequency range corresponding to the modulation frequency of QPs. It is clearly seen in the expanded f-t spectra during the time interval A (1150–1154 UT) that the recurrent periodicity is very regular and the emission frequency increases with time during one quasi-period. Fig. 72 indicates the frequency-time spectrum for the envelope of a filtered band, centered on

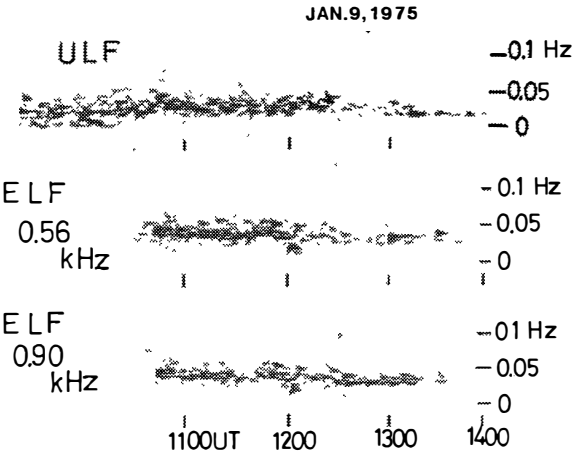

Fig. 68. Dynamic spectra for the Ḋ component of magnetic pulsations and emission intensities at frequency bands of 0.56 and 0.9 kHz (band width ~50 Hz) for 1030–1400 UT on January 9, 1975, observed at Syowa Station.

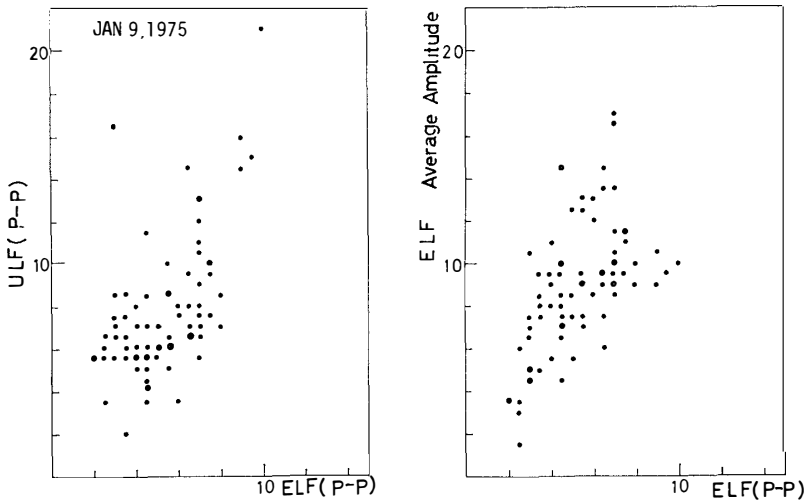

Fig. 69. Relation between the amplitude of magnetic pulsations and the peak-to-peak amplitude of QP modulations in the 0.75 kHz band (left), and the relation between the peak-to-peak amplitude of QP modulations and the average (band-integrated) intensity of ELF emissions (right). These plots are made for five-minute average values on arbitrary unit in the time interval of 1030–1330 UT on January 9, 1975.

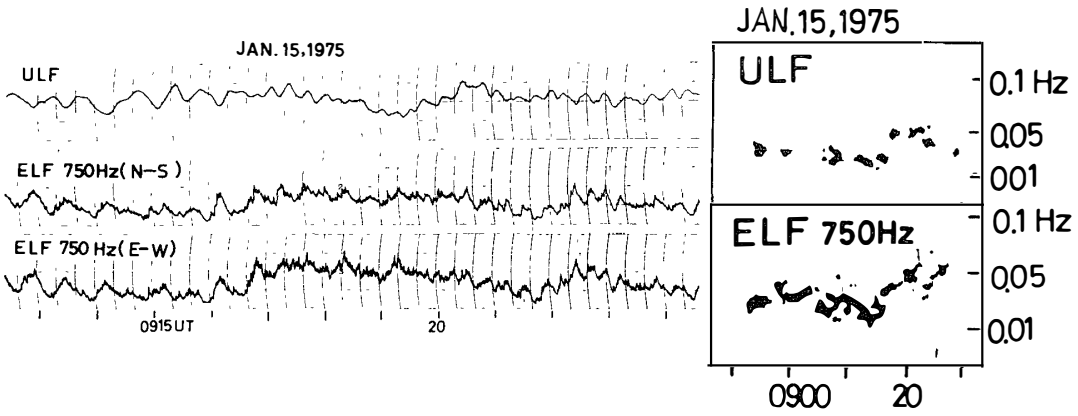

Fig. 70. Intensity records of magnetic pulsations (Ḋ) and ELF emissions at the center frequency of 0.75 kHz (left), and their frequency-time spectra (right) at Syowa Station on January 15, 1975.

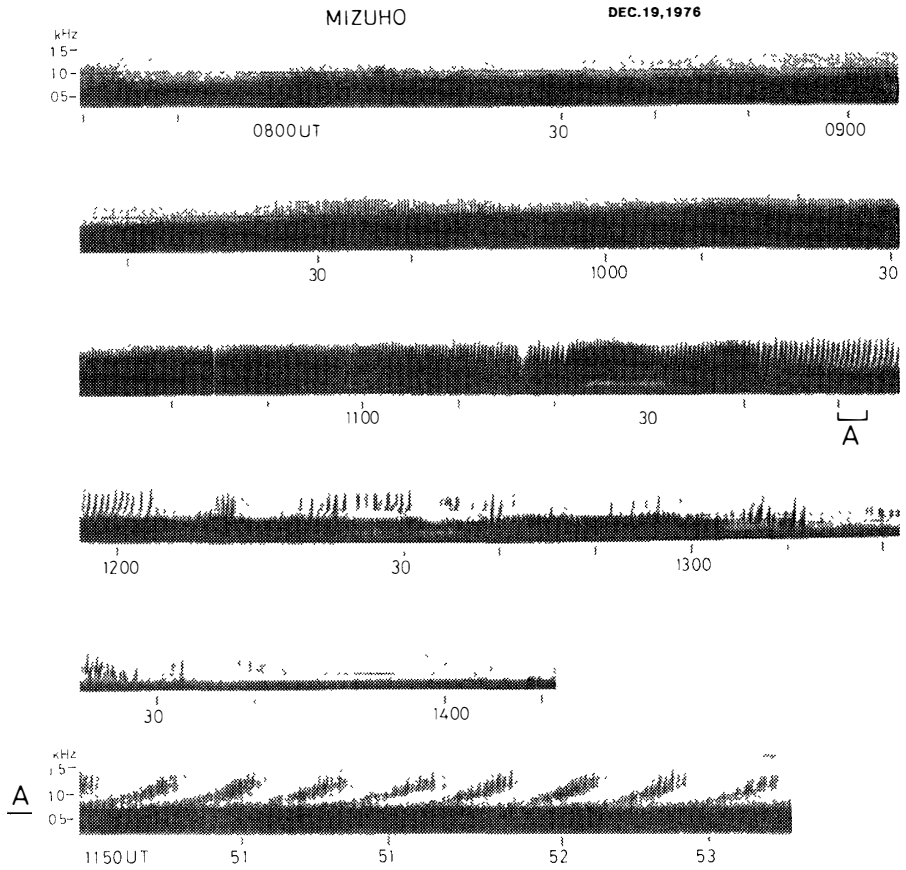

Fig. 71. Frequency-time spectra of Type 2 QP emissions observed at Mizuho Station in the time interval of 0740–1410 UT on December 19, 1976. The bottom panel shows the expanded f-t spectra during the time interval A(1150–1154 UT).

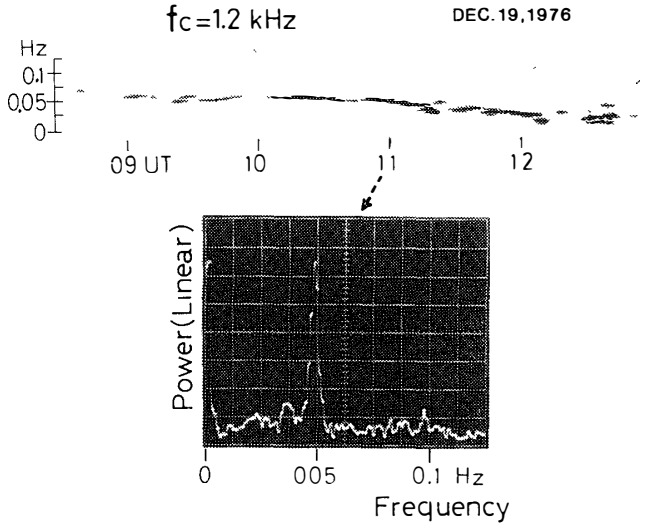

Fig. 72. Frequency-time spectra for the envelop of a filtered band, centered on 1.2 kHz, for 09–13 UT and a display of power spectrum in linear scale at 11h UT. Modulation frequency of QPs slowly decreased from 0.07 Hz to 0.025 Hz.

1.2 kHz, for 09–13 UT and a display of power spectrum in linear scale at 11h UT. As seen in Fig. 72, the band width of modulation frequency was very narrow (the Q value was larger than 12) in contrast to the broad band nature of Type 1 QPs. It is worth noting that the modulation frequency of QPs in Fig. 72 slowly decreased from 0.07 Hz to 0.025 Hz, *i.e.*, the period became longer from morning to noon. This characteristic of Type 2 QPs is frequently observed, as mentioned in Section 3.

8.2. Correlation between Type 1 QP emissions and Pc 3–4 magnetic pulsations

As shown previously, comparisons of dynamic spectra indicate that the intensity and period of QP emissions change with the amplitude and period of corresponding magnetic pulsations. However, a clear one-to-one correspondence, such as shown in Fig. 8, is not always seen between peaks of pulsation wave forms and emission intensities through the whole course of a Type 1 QP event. Geomagnetic pulsation events generally consist of series of trains with several wave cycles and are frequently overlapped by different frequency components. Furthermore, the difference in propagation speed between ULF and VLF waves should also affect the phase relation between the phenomena. Therefore, comparisons of dynamic spectra are not sufficient to know detailed relationships between QP emissions and magnetic pulsations.

In the following two sections, the cross correlation between QP emissions and magnetic pulsations is examined. Analog data of VLF emissions, the $\dot{H}$ and the $\dot{D}$ components of magnetic pulsations, simultaneously recorded on the same magnetic tapes, were converted to digital data. The spectral analysis was done by the use of the Conversational Analysis Program (CSAP) system developed by IWABUCHI *et al.* (1978). Power spectrum, relative phase, cross spectrum and coherency are calculated for both magnetic pulsations and QP emissions. Polarization parameters are also calculated for the magnetic pulsations by using this spectral analysis system. Three kinds of spectral analysis methods, Blackman-Turkey (BT), Fast-Fourier-Transform (FFT), and Auto-Regressive-Method (MEM-AR) with Akaike FPE criterion (AKAIKE, 1971) are available in this system.

QP emissions associated with magnetic pulsations (Type 1 QPs) with periods of 15–60 s, mostly around 30 s, are frequently observed at high latitudes. From many emission events, several cases were examined in detail to determine the correlation between QP emissions and Pc 3–4 magnetic pulsations.

8.2.1. Power spectrum and coherency

We first present an example of QP emissions observed concurrently with well-defined Pc 3 pulsations in Fig. 73 to illustrate the close relationships between QP emissions and magnetic pulsations. As seen from the top panel, modulations

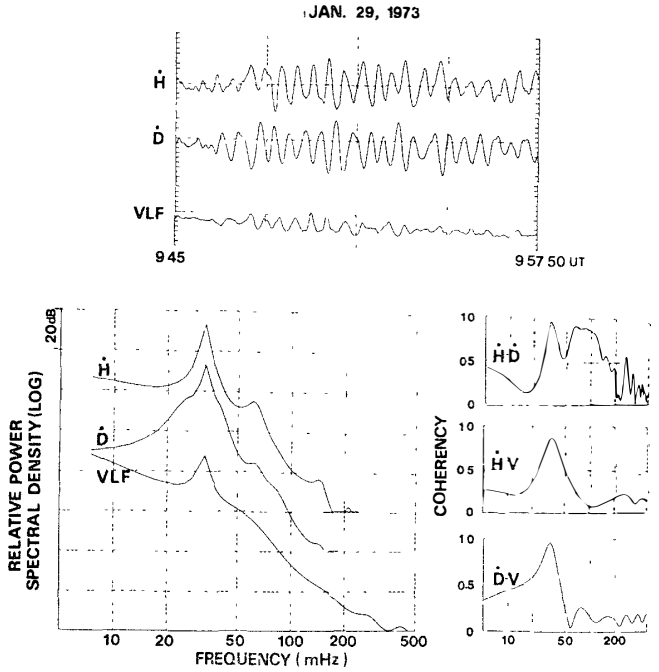

Fig. 73. QP emissions associated with Pc 3 pulsations, observed at Syowa Station on January 29, 1973. The top panel shows time-amplitude records of the $\dot{H}$ and the $\dot{D}$ components of pulsations and intensity variations of QP emissions in the frequency range of 0.5–1.4 kHz. Relative spectral densities and coherencies are illustrated in the bottom.

in the signal strength of emissions appeared almost simultaneously in association with the activation of Pc 3 pulsations. The period of QP emissions is 31 s, exactly the same as that of the main peak in pulsation spectra, indicating a close relation between the phenomena. The coherency analysis indicated that the polarization of Pc 3 waves is almost linear and right handed and the coherency between QPs and Pc 3 pulsations is as large as 0.8–0.9. It is interesting to note here that the coherency of QPs with the $\dot{D}$ component is slightly larger than that with the $\dot{H}$ component. A similar feature is found for more complicated examples, shown in the following.

Fig. 74a shows the intensity records for the $\dot{H}$ and the $\dot{D}$ components of magnetic pulsations and intensity variations of emissions between 0.3 and 1.4 kHz observed at Syowa Station from 0830 to 1030 UT on January 27, 1973. Frequency-time spectra for QP emissions are given with time-amplitude records of the $\dot{D}$ component in Fig. 74b. The figures indicate that intensities of emissions were closely correlated with the concurrent magnetic pulsations with periods of 40–50 s in the time intervals of 0835–0855 UT and 1015–1030 UT, and with shorter periods of 25–30 s in the time interval of 0905–1010 UT. Fig. 75a shows relative power spectra for intensity modulation of QP, and the $\dot{H}$ and the $\dot{D}$ components of magnetic pulsations calculated by the MEM-AR method in the time interval of 0830–1030 UT. Each spectrum was analyzed for every 20 min of

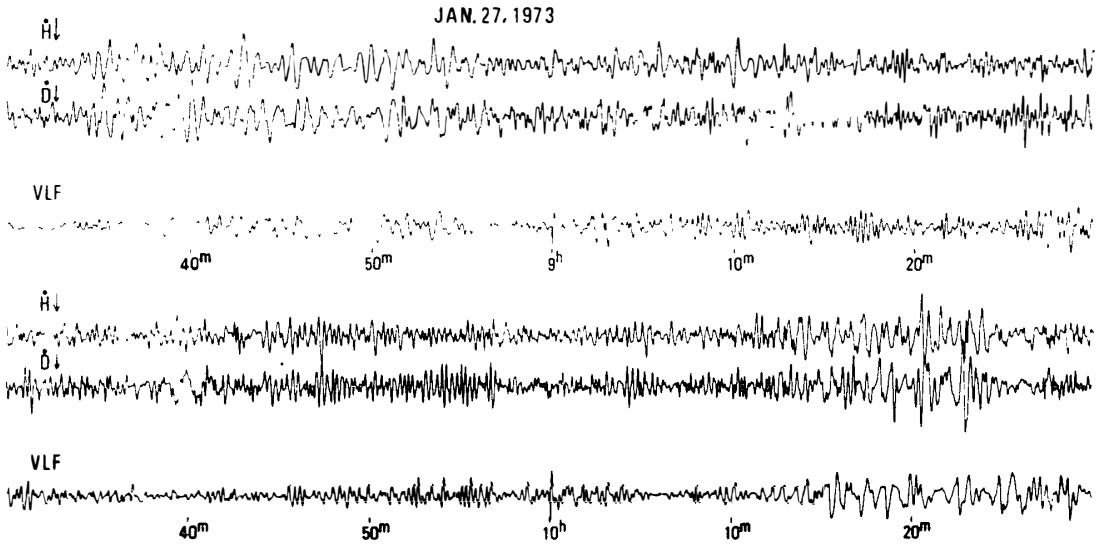

Fig. 74a. Intensity records for the $\dot{H}$ and $\dot{D}$ components of magnetic pulsations and 0.3–1.4 kHz band ELF emissions high-pass filtered ($f \geq 0.014$ Hz) for 0830–1030 UT on January 27, 1973, observed at Syowa Station.

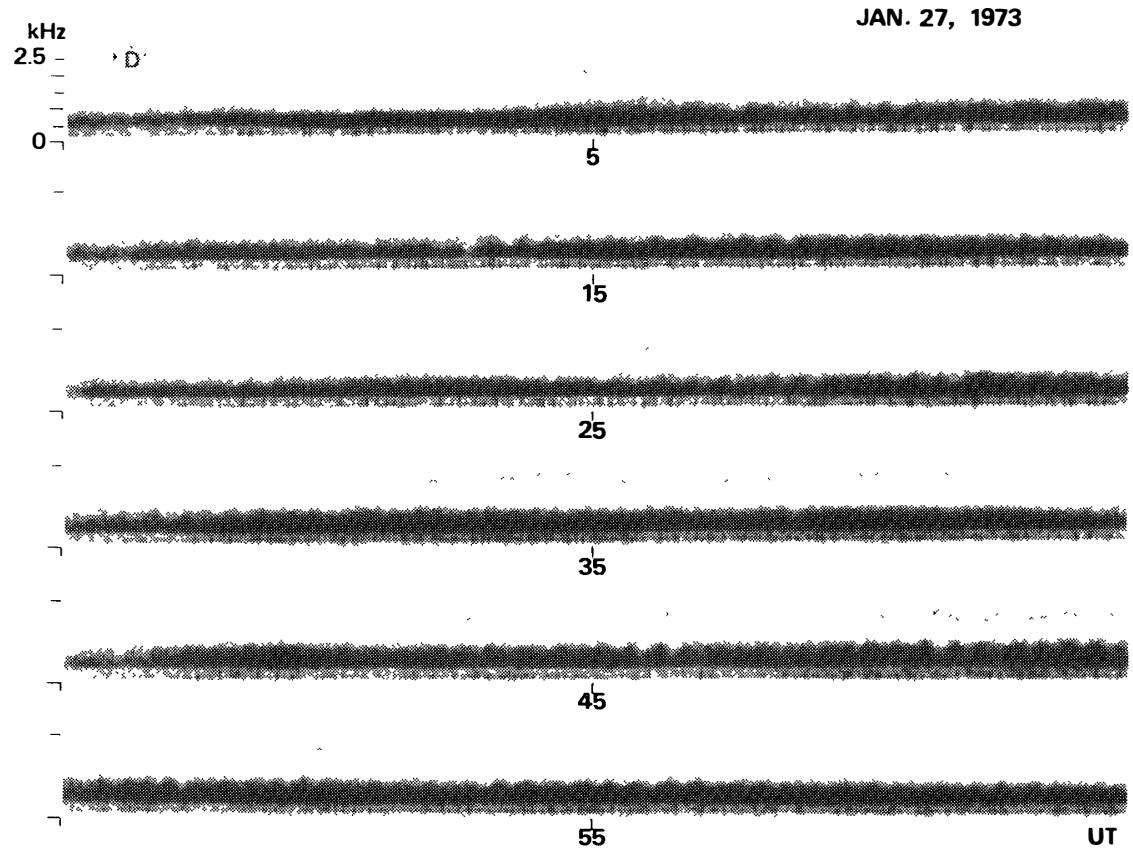

Fig. 74b. Frequency-time spectra of QP emissions and pulsation wave forms in a fine time resolution during 0900–1000 UT on January 27, 1973.

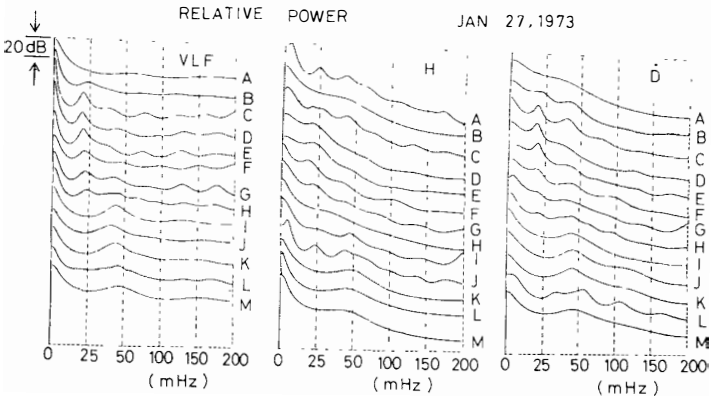

Fig. 75a. Relative power spectrum for QP emissions, the $\dot{H}$ and the $\dot{D}$ components of magnetic pulsations analyzed by Maximum Entropy Method in the time interval of 0830–1030 UT on January 27, 1973. Each spectrum was analyzed for every 20 min interval. The samples overlap by half their length.

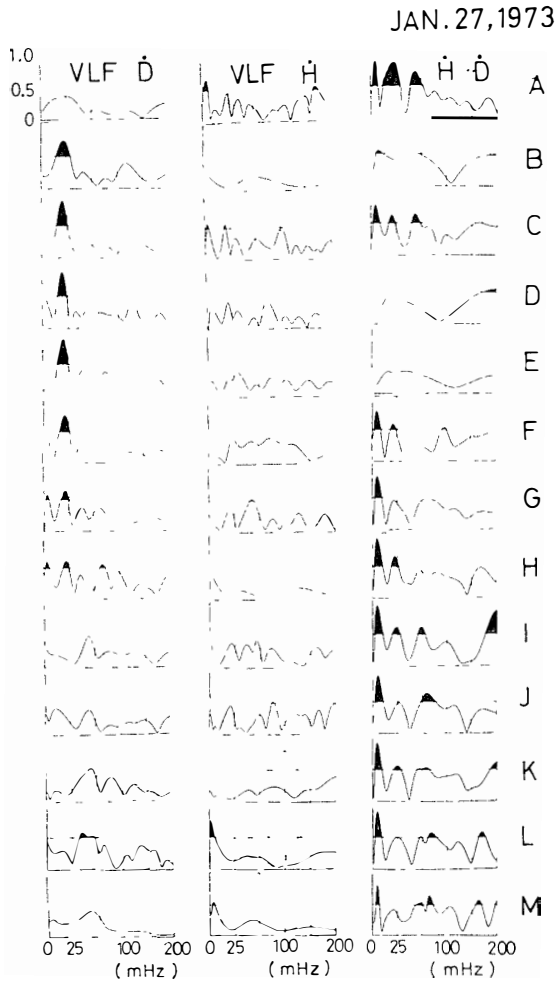

Fig. 75b. Coherency between QP emissions and magnetic pulsations.

data and the separation between successive spectra is 10 min. It is seen in the power spectra of QP modulations that there are two well defined spectral peaks around 20 mHz in B–H and around 40 mHz in G–M, respectively. On the contrary, the $\dot{H}$ component of magnetic pulsation only shows small spectral peaks at 20 mHz and 40 mHz. In the power spectra of the $\dot{D}$ component more distinct peaks around 20 mHz and 40 mHz are found, corresponding to peaks in the QPs spectra.

The coherency between QPs and magnetic pulsations is shown in Fig. 75b. As expected from the comparison of spectral peaks, the coherency between QPs and the $\dot{D}$ component is better than that between QPs and the $\dot{H}$ component. For the coherency of QPs and $\dot{D}$, it is seen that the coherency is larger than 0.5 around 20 mHz band for B–H, and is larger than 0.4 around 40 mHz and 5–10 mHz bands for I–M and G, H. The coherency between QPs and $\dot{H}$ larger than 0.5 was noticed only in spectra, A, C, L and M in the lower frequency range (f~10 mHz). The coherency between $\dot{H}$ and $\dot{D}$ is larger than 0.7 in the frequency range less than 10 mHz, but it was not so large around 20 mHz and 40 mHz.

Fig. 76a shows another example of QPs associated with Pc 3–4 magnetic pulsations observed on January 29, 1973. Frequency-time spectra of the QP emissions in the time interval of ~1034–1244 UT are shown in Fig. 76b. Power

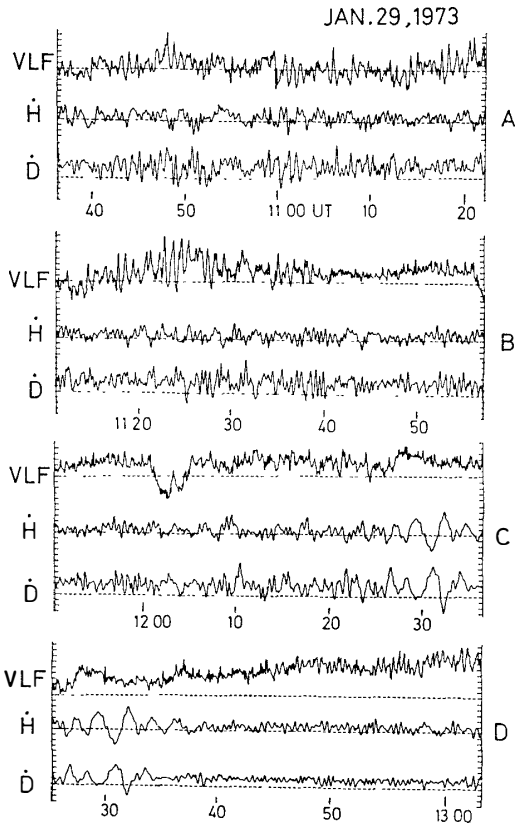

Fig. 76a. Intensity records of magnetic pulsations and VLF emissions in the time interval of 1036–1333 UT on January 29, 1973, observed at Syowa Station. Data intervals to calcurate power spectra and coherency were divided into four periods from A to D.

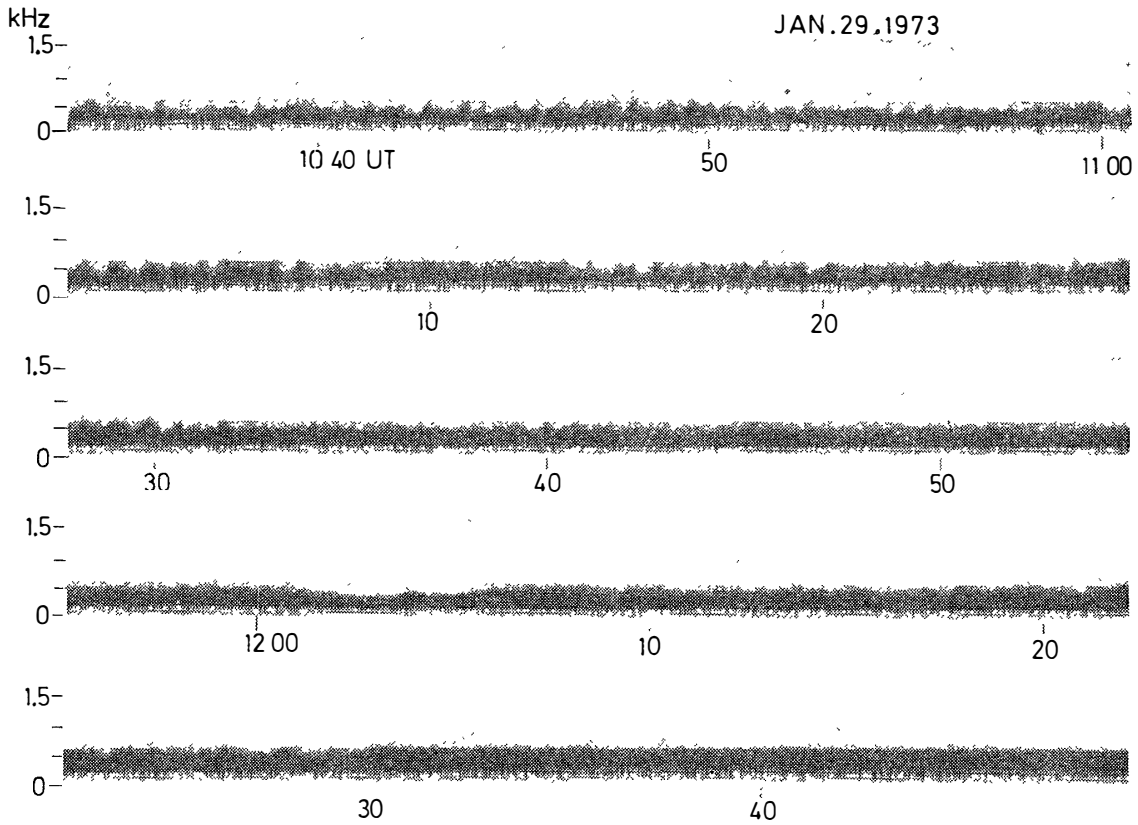

Fig. 76b. Frequency-time spectra of QP emissions in the time interval of ~1034–1249 UT on January 29, 1973.

spectra and coherency were calculated for four time intervals, A, B, C and D from 1036 to 1333 UT (Fig. 77). In Fig. 77a, a sharp spectral peak is seen at 20 mHz in the QPs spectra A and B, and small spectral peaks are also noticed in the frequency range from 20 mHz to 40 mHz in A, B, C and D. For the $\dot{H}$ component of magnetic pulsations, there are sharp peaks at the frequency around 6 mHz, and other peaks from 20 mHz to 40 mHz in the spectra A–D. It is evident that spectral peaks in $\dot{H}$ do not necessarily correspond to peaks in QPs, especially in the frequency range around 20 mHz. However, spectral structures of the $\dot{D}$ component in the frequency range from 20 mHz to 40 mHz are very similar to those of QPs, suggesting that the coherency between QPs and $\dot{D}$ is larger in comparison with that between QPs and $\dot{H}$. In fact, Fig. 77b illustrates the good coherency between QPs and the $\dot{D}$ component. In this figure, it is evident that QPs and $\dot{D}$ are much more coherent than QPs and $\dot{H}$. These two events mentioned above showed the same characteristics, that is, QP emissions are more correlated with the $\dot{D}$ component of magnetic pulsation than with the $\dot{H}$ component.

8.2.2. Phase differences between QP emissions and magnetic pulsations

The phase difference between the intensity variations of QPs and magnetic

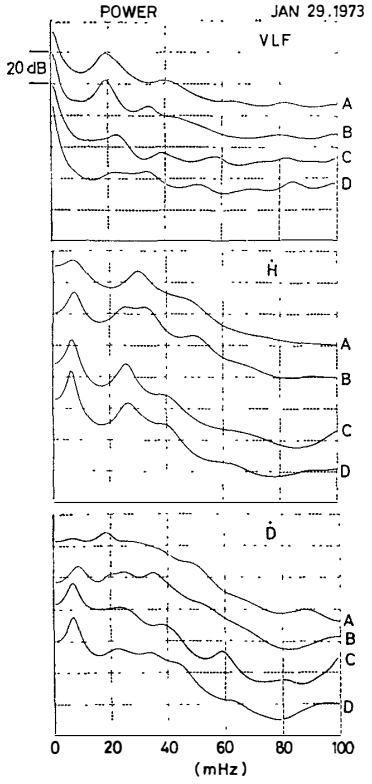

Fig. 77a. Relative power spectra for QP emission, the $\dot{H}$ and the $\dot{D}$ components of magnetic pulsations obtained by the Maximum Entropy Method, on January 29, 1973.

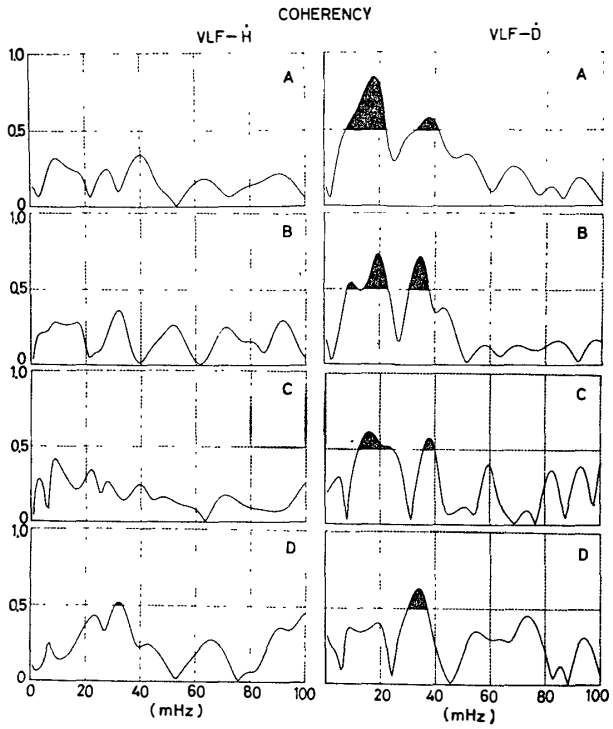

Fig. 77b. Coherency between QP emissions and magnetic pulsations.

pulsations is important information for understanding the generation or modulation mechanism of QP emissions, since the interaction region may be located near the equatorial plane in the magnetosphere. A difference in arrival time should exist between QP emissions and magnetic pulsations on the ground if the interaction between ULF and whistler waves occurs considerably far from the ground. Whistler mode waves (ELF-VLF emissions) and hydromagnetic waves (magnetic pulsations) have different propagation speeds, *i.e.*, the propagation speed of the whistler wave is much faster than that of the HM wave. The difference in propagation speed between the two modes must affect the phase relation. That is to say, the phase difference must be larger as the pulsation period is shorter.

For example, if the pulsation period is the same as the time lag of hydromagnetic wave propagation behind that of ELF-VLF emissions, the phase difference between QP fluctuations and magnetic pulsations on the ground must be the same as the phase difference in the interaction region, but actually it must have 2π added. If the pulsation period is a half of the difference in propagation time,

the phase difference on the ground must be identical to the original phase, but 4π must be added here. Therefore, a linear relationship is expected between the actual phase difference and the pulsation period, *i.e.*, the phase becomes larger as the pulsation period becomes shorter. It is worth noting that the rate of increase in phase difference with increase in period is proportional to the difference in propagation time between ELF-VLF emissions and hydromagnetic waves from the interaction region to the receiving region. Furthermore, the phase difference between QP modulations and magnetic pulsations, extrapolated to the point, where the modulation frequency is equal to zero, shows the phase relation between QP fluctuations and magnetic pulsations in the interaction region in the magnetosphere if QPs are modulated by magnetic pulsations with the same phase lag in the whole period range of pulsations in the interaction region between ULF and ELF-VLF waves. We must also take into account the phase difference of 90° corresponding to the induction effects by an induction magnetometer.

The difference in propagation time of the two records from the interaction region to the ground, ΔT(s), is given by

$$\Delta T = -\frac{1}{2\pi} \cdot \frac{\mathrm{d}\theta}{\mathrm{d}f},$$

where $\mathrm{d}\theta/\mathrm{d}f$ is the rate of increase of phase difference (θ in radian) between QP fluctuations and magnetic pulsations with a modulation frequency (f in Hz) of QPs. ΔT is approximately equal to the propagation time of magnetic pulsations from the interaction region to the ground because the propagation speed of HM waves is much slower than that of whistler mode waves.

Fig. 78a shows the relative phase between QPs and magnetic pulsations in the eleven spectra shown in Fig. 75 when the coherency is larger than 0.3. The phase delay of $\dot{D}$ behind $\dot{H}$ of magnetic pulsations is seen around $-90°$ in the frequency around 5 mHz. The phase delay of $\dot{D}$ by $-90°$ indicates that these magnetic pulsations had left handed polarization viewed along the line of force. On the other hand, it is evident that Pc 3–4 magnetic pulsations were linearly polarized, *i.e.*, the relative phase is approximately 180° around 25 mHz and 50 mHz.

Although the relative phase between QPs and magnetic pulsations appears to be widely scattered, especially between QPs and $\dot{H}$, a systematic relation can be obtained for the relative phase of QPs and $\dot{D}$ when the uncertainty of phase measurement by $2\pi n$ is taken into account. Fig. 78b indicates the phase relation between QP fluctuations and the $\dot{D}$ component of magnetic pulsations rearranged from Fig. 78a which is made up for the uncertainties of $2\pi n$ (n is an integer) in phase difference, considering the discussion mentioned previously. A striking linear relation versus frequency is seen in the phase difference between fluctuations

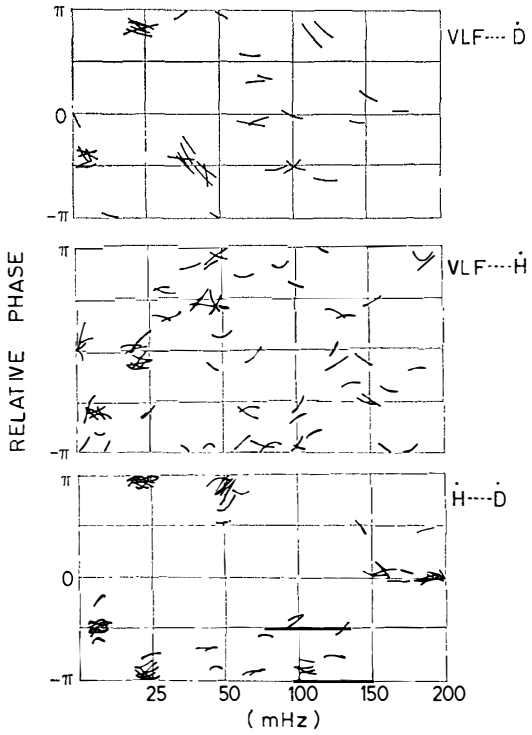

Fig. 78a. Relative phase between QPs and magnetic pulsations plotted for frequencies where the values of coherency are larger than 0.3 in the time interval from A to M on January 27, 1973 shown in Fig. 75.

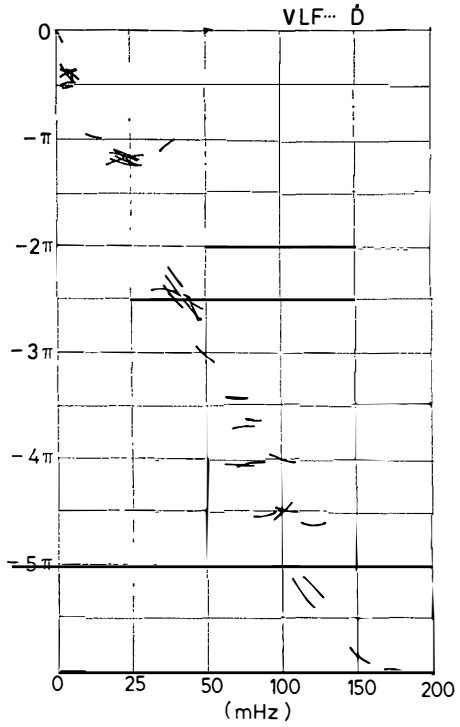

Fig. 78b. Phase relation between QP emissions and the Ḋ component of magnetic pulsations rearranged from Fig. 78a with the assumption that phase difference becomes larger associated with modulation frequency increase.

and magnetic pulsations as we expected. For this particular example, ΔT is given by,

$$\Delta T = -\frac{1}{2\pi}\cdot\frac{d\theta}{df} \sim 22 \text{ (s)}.$$

Hence the traveling time of magnetic pulsations from the interaction region to the ground is expected to be approximately 22 s.

Fig. 79 shows another example of the relation between the phase difference and the modulation frequency rearranged the same as Fig. 78b except for the event on January 29, 1973. In this figure the relative phases in spectra with the coherency of larger than 0.4 for QPs and $\dot{D}$ are plotted. The time difference ΔT is obtained as before,

$$\Delta T = -\frac{1}{2\pi}\cdot\frac{d\theta}{df} \sim 21 \text{ (s)}.$$

The estimated time difference in this example is nearly the same as the time difference in the previous example on January 27, 1973.

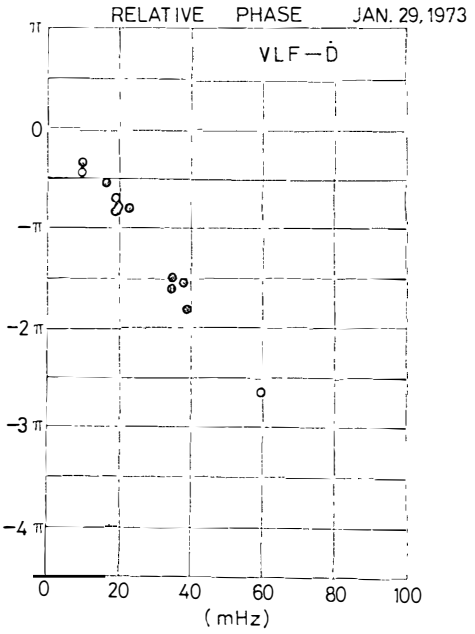

Fig. 79. Example of the relation between phase lag and modulation frequency rearranged with the same assumption as Fig. 78b except for the event on January 29, 1973 shown in Fig. 76. In this illustration coherency larger than 0.4 between QP and $\dot{D}$ was plotted.

The time lag of hydromagnetic waves behind ELF-VLF waves thus obtained is consistent with those deduced by other modulation phenomena, such as SSC- or SI-triggered ELF-VLF emissions and simultaneous magnetic variations (KOKUBUN *et al.*, 1969; HAYASHI *et al.*, 1978). The time lag of magnetic pulsation was interpreted as the difference in propagation speed between ELF-VLF emissions and hydromagnetic waves which trigger the increase in ELF-VLF waves in the equatorial region of the magnetosphere (HAYASHI *et al.*, 1968). In Fig. 38b was given an example, showing a time lag of magnetic variations behind ELF-VLF waves during a SI event. In this event, abrupt changes of ELF-VLF intensity were also observed onboard GEOS-1 (CORNILLEAU-WHERLIN *et al.*, 1978). Therefore, our results of time lag, 20–25 s, strongly suggest that QP emissions are generated by the modulation due to magnetic pulsations in the equatorial region of the magnetosphere.

It is also worth noting that the relative phase between QP fluctuations and the $\dot{D}$ component of magnetic pulsations are roughly the same in the interaction region in the broad frequency ranges of 20–50 mHz for Fig. 78b, and 10–60 mHz for Fig. 79 because there is the linear relation between phase lag and modulation frequency. Therefore, we can conclude that the relative phase difference between QP fluctuations and the $\dot{D}$ component of magnetic pulsations is roughly the same at the interaction region in the outer magnetosphere in the period ranges Pc 3–4.

The phase relation between QP fluctuations and the $\dot{H}$ component of magnetic pulsations was found to be widely scattered. It also had weak coherency as shown in Figs. 75b and 77b, so that we could not find any systematic phase relation. The coherency analysis was also made for several QP events other than those

shown in Figs. 73, 75 and 77. It was found that a better coherency between QPs and $\dot{D}$ is observed for roughly two thirds of cases examined. In cases that the coherency between QPs and $\dot{H}$ is better than that between QPs and $\dot{D}$ values of coherency function between QPs and $\dot{D}$ were not so small as those between QPs and $\dot{H}$.

8.3. QP emissions associated with short period ($T\sim$ 3–10 s) magnetic pulsations

Short period QP emissions with the period of 3–10 s have never been studied up to now. We examine in this section the correlation between such QP emissions associated with magnetic pulsations.

Fig. 80 shows *f-t* spectra of QP emissions and the intensity records of magnetic pulsations in the $\dot{H}$ and $\dot{D}$ components observed at Husafell in Iceland on August 15, 1977. In this figure, QPs with a rising tone and with a period of about 8 s are observed. We can see a peak-to-peak correspondence between the enhancement of emission intensity and the increase in the $\dot{H}$ component of magnetic pulsations with the phase lag of about 180° (note that the $\dot{H}$ component increases downward). Fig. 81a shows the intensity record of QP emissions at the center frequency of 1 kHz along with magnetic pulsations (upper panel), and relative power spectra of VLF and ULF data obtained by FFT method (lower panel). The spectral peaks of QPs and pulsations are identified at the same frequency, around 130 mHz. The relative power peaks at 130 mHz for the $\dot{H}$, $\dot{D}$ and QPs are about 40 dB and 35 dB higher than the noise level, respectively. At this frequancy an extremely good coherency, approximately equal to 1.0, is seen between QPs-$\dot{H}$, QPs-$\dot{D}$ and $\dot{H}$-$\dot{D}$ as shown in Fig. 81b. Such an excellent coherency indicates that there exists a one-to-one correlation between QP and magnetic pulsations in this example. Thus, it is worth noting that the QPs had good coherency with short period $\dot{H}$ component of magnetic pulsations instead of the poor coherency for Pc 3–4 periodic range of $\dot{H}$ as mentioned in previous section.

Fig. 82a shows another interesting fact. That is, that periodic emissions with a period of ~3 s had good coherency with magnetic pulsations that occurred on January 26, 1973. The figure shows the intensity records of the $\dot{D}$ component of magnetic pulsations, frequency-time spectra of QP emissions and intensity records of QPs at the center frequency of 2.5 kHz. As seen in *f-t* spectra, the periodic emissions with the period of about 3 s appear to be grouped into 15–20 s quasi-periodic emissions. In the ULF data, the short period pulsations with the 3 s period were very weak in contrast to that of the quasi-periodic emissions. For example, Fig. 82b illustrates relative power spectra and coherency between QPs and magnetic pulsations for the same example. The power spectrum of intensity in ELF shows clear peaks at 62 mHz and at 300 mHz. The latter peak indicates the recurrence of periodic emissions, and the former peak shows the successive occurrence of quasi-periodic emissions consisting of the periodic

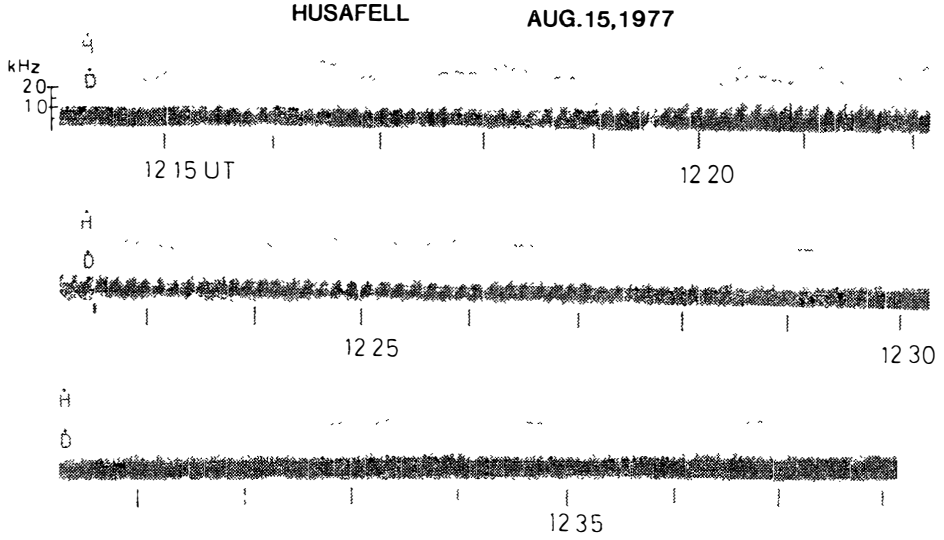

Fig. 80. Frequency-time spectra of QP emissions and the intensity records of the $\dot{H}$ and $\dot{D}$ components of magnetic pulsations with fine time resolution, for August 15, 1977.

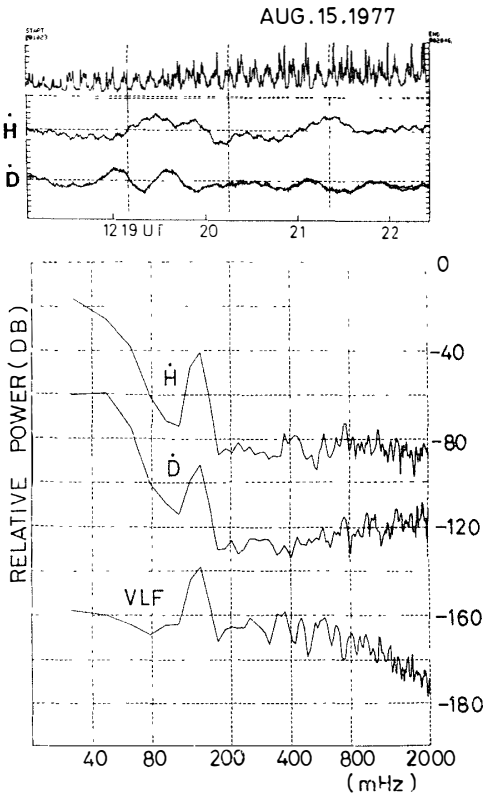

Fig. 81a. Intensity records of QP emissions at a center frequency of 1 kHz and magnetic pulsations (upper panel). The relative power spectrum of VLF and magnetic pulsations analyzed by FFT method (lower panel).

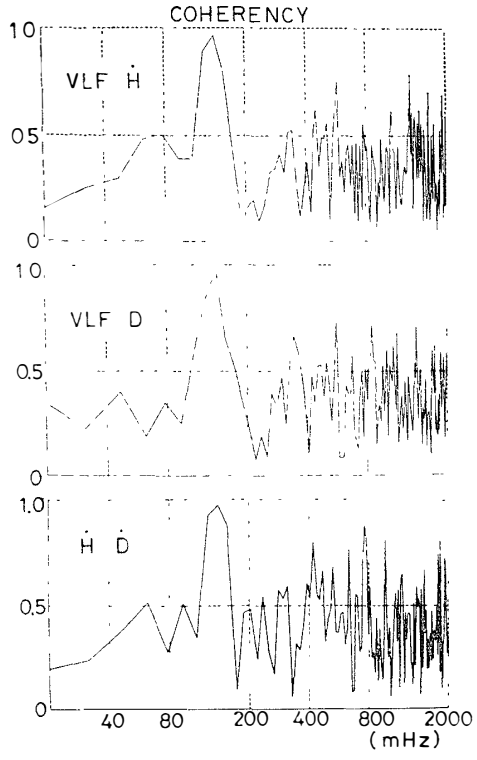

Fig. 81b. Coherencies between QPs-$\dot{H}$, QPs-$\dot{D}$ and $\dot{H}$-$\dot{D}$. The value of coherency reached approximately to 1.0 at the frequency 130 mHz.

emissions. In comparison, the magnetic pulsations also had a spectral peak at ~300 mHz corresponding to the spectral peak of the periodic emissions. Furthermore, a good coherency (more than 0.5) is found at ~300 mHz. Although the relative power at ~300 mHz was two or three orders of magnitude less than the power at ~60 mHz in ULF data, the relative power of the intensity fluctuation

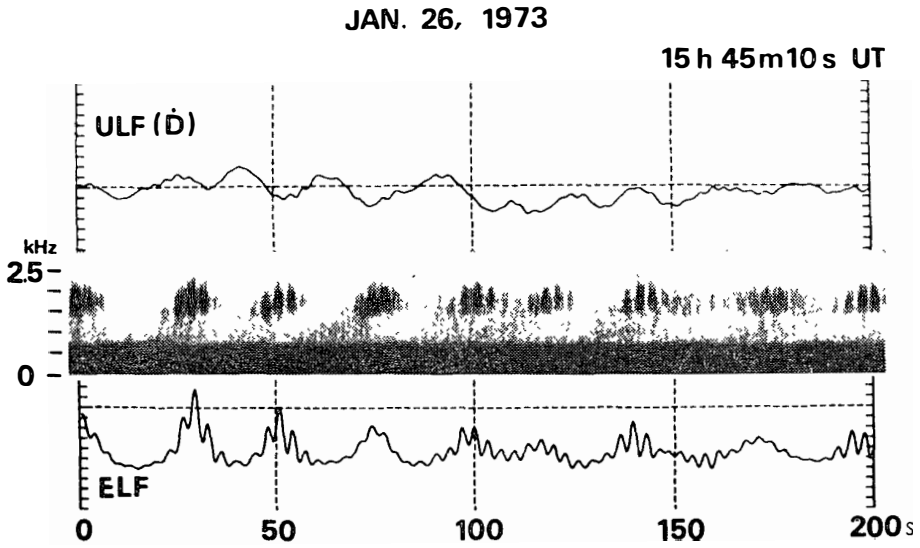

Fig. 82a. Intensity record of the Ḋ component of magnetic pulsations, frequency-time spectra of QPs, and intensity record of QPs at a center frequency of 2.5 kHz.

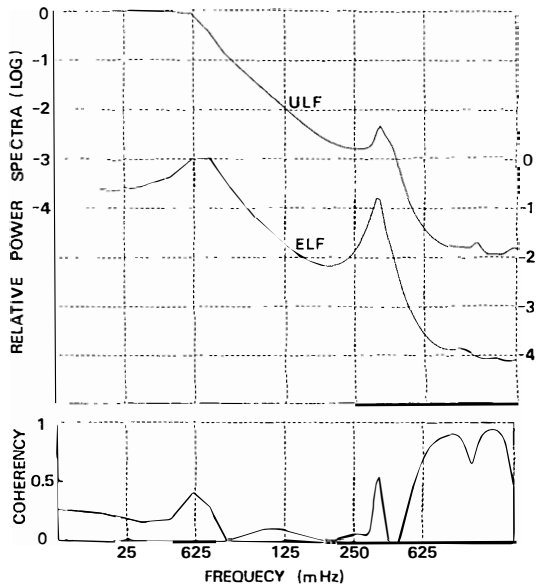

Fig. 82b. Relative power spectra (upper) and coherency between QPs and magnetic pulsations (lower). Magnetic pulsations showed a power peak at about 300 mHz corresponding to the spectral peak of periodic emissions.

in the periodic emission (~300 mHz) is only one order of magnitude less than that of QP emission (~60 mHz).

Fig. 83 shows another example of a good correlation between short period QPs and magnetic pulsations, occurring on August 18, 1977 at Husafell. The top panel shows intensity records of VLF and the $\dot{H}$ component of magnetic pulsations for the time interval 0850:50–0859:20 UT. Middle panel shows evidence that there are power peaks in the short period range at frequencies around 250–400 mHz both in VLF and ULF. The coherency between QPs and ULF in this example is more than 0.7 in the frequency range around 250–400 mHz. Good coherency in the frequency range of 40–150 mHz was also noticed.

Although events mentioned above occur infrequently, we could find some correlation between short period QP emissions and magnetic pulsations (T~3–10 s), which have never been reported before.

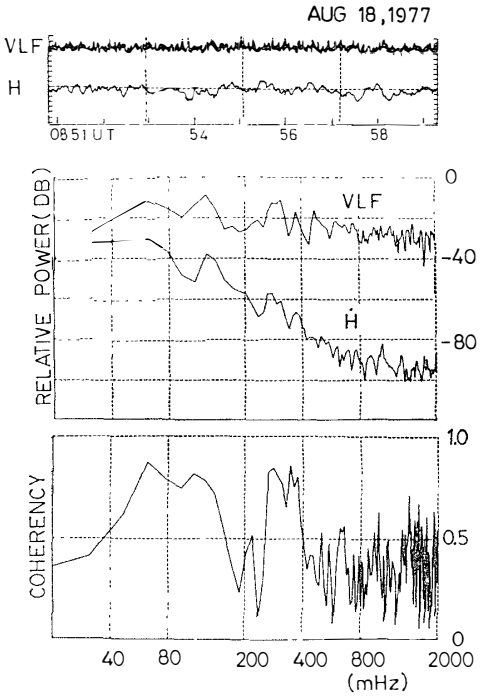

Fig. 83. Intensity records of VLF emissions and the $\dot{H}$ component of magnetic pulsations (upper). Relative power spectra of VLF and magnetic pulsations (middle) and coherency between QPs and magnetic pulsations (lower). There were good coherency, more than 0.75, between QPs and ULF at the frequency bands around 250-400 mHz and 40–150 mHz.

8.4. Spectral characteristics of magnetic variations during Type 2 QP events

As mentioned previously, it is important to examine spectral characteristics of magnetic variations during Type 2 QP events to give a basis on the classification of QP emissions. Spectrum and coherency analyses were made for several QP emission events, which were classified as Type 2 from comparisons of chart records and spectral forms of QP emissions. It was found that pulsation spectra have no corresponding peak to the spectral peak of intensity modulations of QPs in most of the cases examined, especially in cases observed under magnetically

quiet conditions. However, a small but significant frequency component, which corresponded to the spectral peak of QP emissions, was sometimes observed in pulsation spectra.

Fig. 84 shows an example of *f-t* spectra of Type 2 QPs observed at Husafell on August 31, 1977. On August 31, QP emissions occurred for more than five hours from 0940 UT at the conjugate pair of stations, Husafell and Syowa Station (see Table 4). *Kp* indices during this period were 1+ and 0+. The figure shows a typical feature of fine structures in Type 2 QP spectra that each QP element consists of diffuse and discrete emissions and that the mean frequency increases during one period (KITAMURA *et al.*, 1969; SATO *et al.*, 1974). The top panel of Fig. 85 represents the intensity record of VLF emissions around 1.0 kHz and the $\dot{H}$ and $\dot{D}$ components of magnetic field. As seen in this figure,

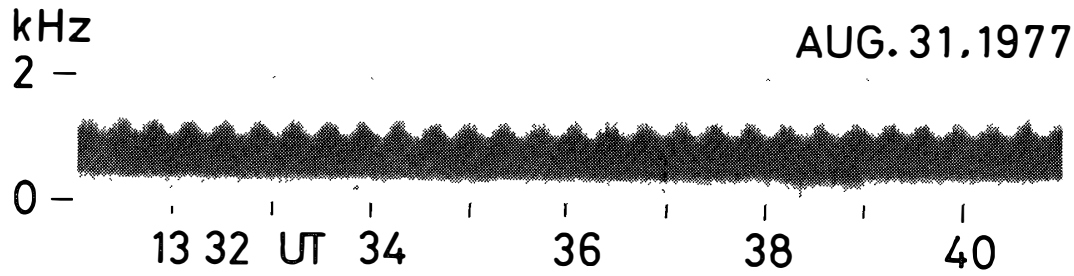

Fig. 84. An example of f-t spectra of Type 2 QP emissions observed at Husafell on August 31, 1977.

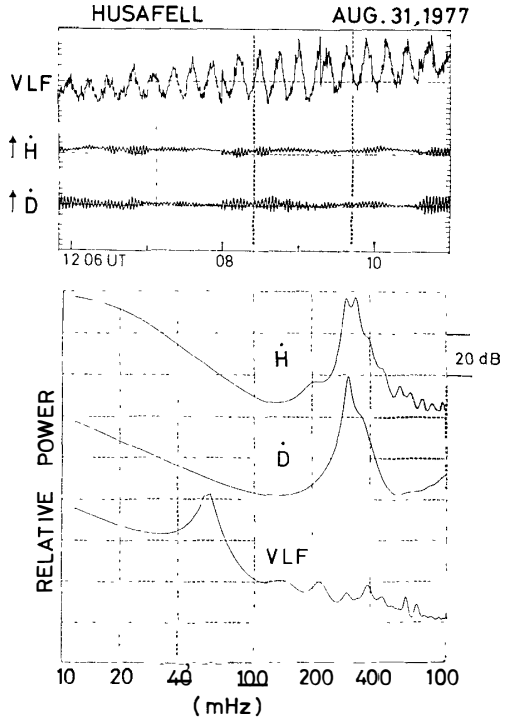

Fig. 85. Intensity records of VLF emissions around 1 kHz and $\dot{H}$ and $\dot{D}$ components of magnetic variations (top panel), and relative power spectra for VLF and ULF (bottom panel) on August 31, 1977.

intensity variations of VLF emissions are very regular with the period of ~20 s, while regular Pc 1 pulsations are only seen in ULF data. Power spectra given in the bottom panel of Fig. 85 evidently indicate this feature. The QPs spectrum has a very sharp peak at ~50 mHz. No corresponding peak is found around 50 mHz in ULF spectra. Peaks in ULF spectra only show the existence of Pc 1 pulsations with a period of ~3 s. Thus, this example yields evidence of the existence of QP emissions without associated pulsations. It was also confirmed from the spectral analysis that most of Type 2 QP emissions, observed especially during quiet conditions, are not really associated with magnetic pulsations.

Next, we will discuss interesting examples which indicate that a small but significant frequency component common to the spectral peak in QPs spectra is observed in pulsation spectra. Fig. 86 displays *f-t* spectra of QP emissions, observed at Syowa Station, in the time interval of 1445–1500 UT on January 6,

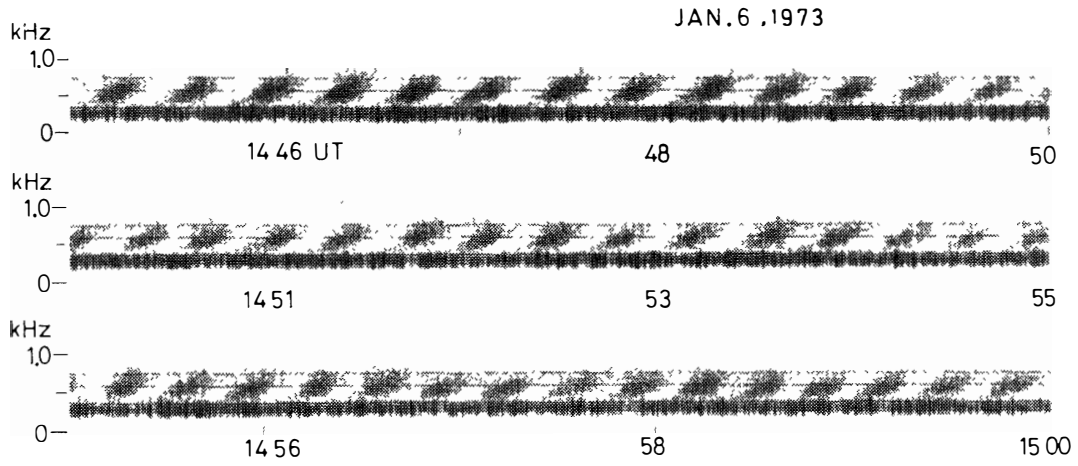

Fig. 86. Frequency-time spectra of QP emissions observed at Syowa Station in the time interval of 1445–1500 UT on January 6, 1973.

1973. This event occurred during a period of moderate magnetic activity with $Kp=3$. The QP elements show a very regular periodicity and the form of each element shows a typical feature of Type 2 QP emissions. In the upper panel of Fig. 87 is shown the envelope of VLF emissions of a filtered band, center at 0.7 kHz, and the $\dot{H}$ component of magnetic pulsations. VLF intensity variations are very regular as expected, while ULF variations are not so regular with a dominant period longer than that of VLF. Power spectra in the middle panel of Fig. 87 show these features more evidently. A sharp peak of VLF spectrum at ~45 mHz indicates a regularity of VLF periodicity, while a dominant peak of ULF spectrum is at ~25 mHz. It is interesting to note that a small but significant peak in ULF spectrum appears at the same frequency as the VLF spectral peak. The coherency also peaks at ~45 mHz, although it is not so large. These features indicate that the spectral component around ~45 mHz is related to VLF emissions,

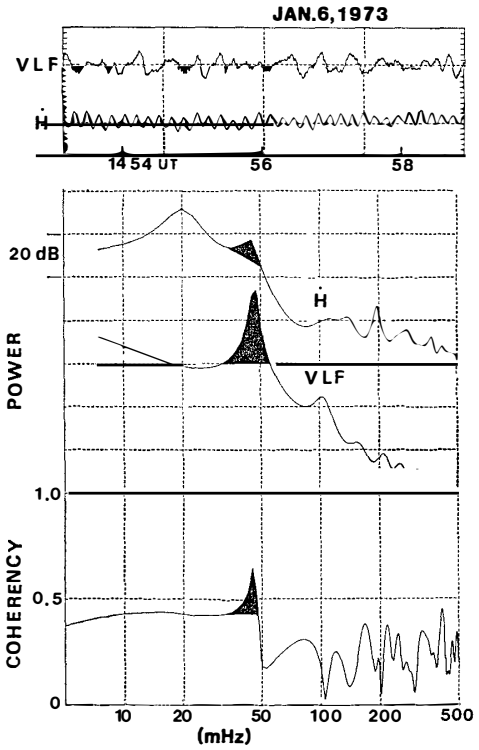

Fig. 87. Intensity records of VLF emissions in the center frequency around 0.7 kHz and the $\dot{H}$ component of magnetic variations (upper panel). Relative power spectra for VLF and ULF (middle) and coherency between QPs and ULF (lower panel).

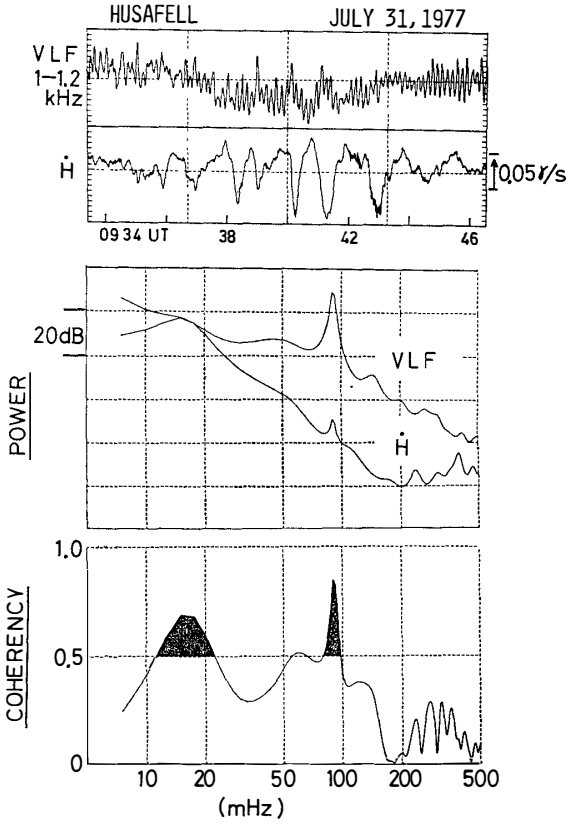

Fig. 88. Intensity records of VLF emissions at 1.0–1.2 kHz band and the $\dot{H}$ component of magnetic variations observed at Husafell in the time interval of ~0933:44–0946:20 UT on July 31, 1977 (upper panel). Relative power spectra for VLF and ULF (middle) and coherency between QPs and ULF (lower panel).

while there is no spectral peak at ~25 mHz in VLF data where ULF waves have maximum power.

Another example, observed at Husafell on July 31, 1977, is shown in Fig. 88. QP emissions with a regular periodicity occurred from 0856 to 1046 UT on this day. *Kp* index during this period was 2. Each QP element consists of diffuse risers and discrete emissions (see Fig. 92). The period was fairly regular and changed slowly from 11 to 15 s during this event. We could not find the corresponding component to QP emissions in ULF records from visual inspection. However, spectral analyses reveal that the ULF spectrum has a peak at the same frequency as the peak in QP spectrum, although a close correlation, such as shown in Fig. 88, was not observed through the whole course of event, but at certain intervals of QP event. A sharp peak at 91 mHz in VLF spectrum shows regularity

of emission periodicity. In pulsation spectrum the broad and dominant peak is around 15 mHz, which reflects less regular variations seen in the upper panel of Fig. 88. A peak of coherency around 15 mHz seems to indicate that spike-like variations of the magnetic field is related to variations of background VLF emissions. Similar to the previous example shown in Fig. 87, a small peak is also noted on a decreasing slope of ULF spectrum. The frequency of this peak is exactly the same as that of VLF peak and the coherency between VLF and ULF is large as 0.85. Although the spectral density of this ULF peak is two order to magnitude less than the maximum around ~15 mHz, a high coherency value indicates that there exist spectral components in ULF, closely correlated with a periodic variation of VLF emissions.

8.5. Geomagnetic conjugacy of QP emissions and magnetic pulsations

The characteristics of geomagnetic conjugacy of QP emissions by analysis of *f-t* spectra and amplitude records have already been examined in Section 7. We examine here the correlation between QP emissions and magnetic pulsations observed at conjugate-pair stations using the same analysis method as in previous section.

8.5.1. Geomagnetic conjugacy of Type 1 QP emissions

As for the conjugacy of the Type 1 QP emissions, a very limited number of data have been examined so far. KITAMURA *et al.* (1969), who examined the data from a conjugate pair of stations, Great Whale River and Byrd, reported that Type 1 QPs have seldom shown conjugacy. They found the lack of conjugacy in four out of five cases, and suggested that the source of the VLF emissions may be local. However, it is necessary to examine further whether or not the lack of conjugacy is a general feature of Type 1 QP emissions. In this section we will discuss the conjugate relationship of Type 1 QP emissions and associated magnetic pulsations, based on the data obtained by observation at Syowa Station-Husafell conjugate stations which was carried out as the IMS project in conjugation with the GEOS observation.

In contrast to the result by KITAMURA *et al.* (1969), the examination of the data obtained during 52 consecutive days from July 29, 1977, revealed that the daytime ELF-VLF emissions, including the Type 1 QP emissions, show good conjugacy, although the lack of conjugacy is often noted in cases of discrete-burst type emissions observed especially in the early morning. In this period 27 QP events were identified from the chart record (see Table 4). Most of events, except for one, were found to show a good conjugacy in contrast to the result reported by KITAMURA *et al.* (1969).

In order to demonstrate the conjugacy of these phenomena in great detail, the result of the coherency analysis for a particular example observed on August

19, 1977, is shown in the following. As the data are registered on analog magnetic tapes, we should carefully check timing errors which are mostly due to slowly varying fluctuations in tape speed. To adjust these timing errors, an interpolation is made for digitalized data by using hour marks overlapping original records. A time accuracy of less than one second among different sets of data at the two stations is obtained as a result. Fig. 89a shows intensity records of the $\dot{H}$ and the $\dot{D}$ components of magnetic pulsations and ELF-VLF emissions at 0.6–0.8 kHz band observed at Syowa Station and Husafell in the time interval of 1230–1301 UT on August 19, 1977. The similarity in amplitude fluctuations of VLF emissions with the period of 20–50 s was coincidently seen between the stations. Magnetic pulsations with a period of Pc 3–4 ranges were also observed simultaneously at the conjugate-pair stations. Fig. 89b shows the relative power spectra obtained by the MEM-AR method for the interval shown in Fig. 89a.

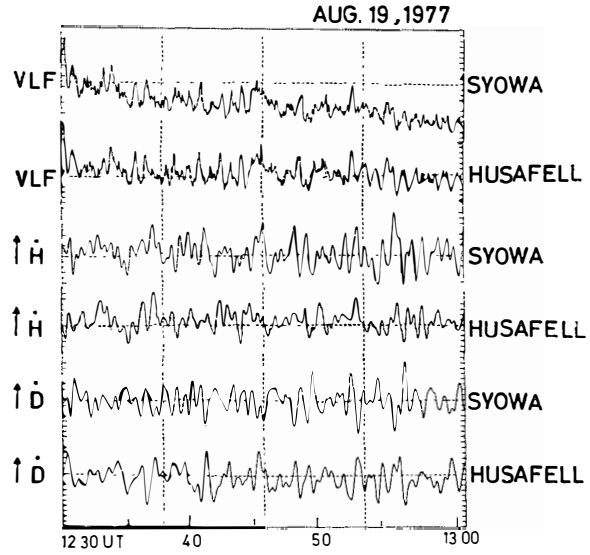

Fig. 89a. Intensity records of the $\dot{H}$ and the $\dot{D}$ components of magnetic pulsations and VLF emissions at 0.6–0.8 kHz band observed at Syowa Station, Antarctica and Husafell, Iceland in the time interval of 1230–1300 UT on August 19, 1977.

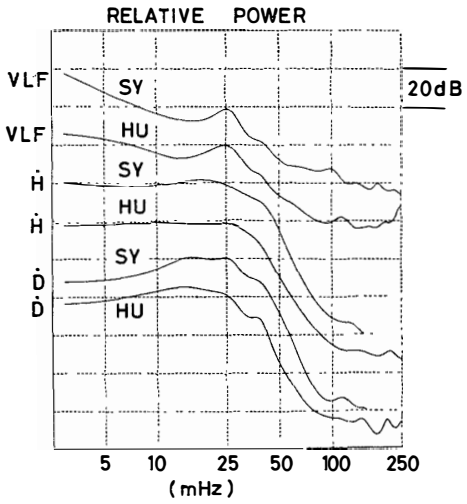

Fig. 89b. Relative power spectra for VLF emissions and magnetic pulsations analyzed by the Maximun Entropy Method.

Fluctuations of VLF emissions have a distinct power peak around 25 mHz, and also a weak one around 40 mHz. Power spectra of the $\dot{H}$ and the $\dot{D}$ components of magnetic pulsations show broad peaks in the frequency range 10–50 mHz at both stations.

Fig. 90a represents the coherency between VLF emissions and magnetic pulsations. The coherency between QPs and the $\dot{H}$ component of magnetic pulsation at Syowa Station is maximum around ~25 mHz and has the value of ~0.5.

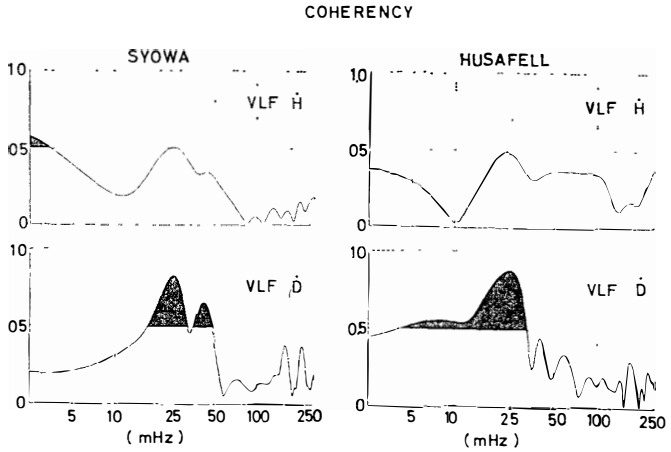

Fig. 90a. Coherency between QP emissions and magnetic pulsations observed at conjugate-pair stations on August 19, 1977.

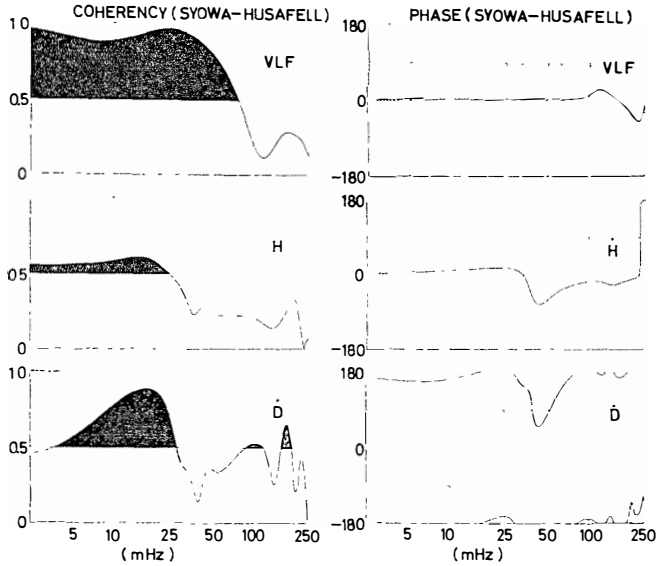

Fig. 90b. Coherency and phase relation between Syowa Station and Husafell for the data of VLF emissions, the $\dot{H}$ and the $\dot{D}$ components of magnetic pulsations.

On the other hand, the coherency between QPs and $\dot{D}$ at Syowa Station has peaks of ~0.8 and ~0.65 at frequencies of ~25 mHz and ~40 mHz. These two coherency maxima can be noticed from the power spectra of VLF and $\dot{D}$ in Fig. 89b. The coherency between QPs and $\dot{D}$ is larger than that between QPs and $\dot{H}$ which is the same characteristic as mentioned in the previous section. The same characteristics as those observed at Syowa Station are seen in coherency at Husafell.

Fig. 90b shows the coherency and phase relations between the same components of magnetic pulsations and emissions. VLF emissions show good coherency in the frequency range less than ~70 mHz including the peak frequency of Type 1 QPs at 25 mHz, indicating that a good geomagnetic conjugacy holds

not only for the quasi-periodic component, but also for slowly varying components as seen in the intensity record (Fig. 89a). The phase lag is approximately zero in the frequency range less than ~70 mHz. These results indicate that Type 1 QP emissions are generated near the equatorial plane in the outer magnetosphere, and then propagate simultaneously to both hemispheres along the field line of force. As for the coherency of magnetic pulsations, the $\dot{D}$ component of magnetic pulsations has a larger coherency than the $\dot{H}$ component. The phase relation of magnetic pulsations between two stations is almost in-phase in the $\dot{H}$ component and out of phase in the $\dot{D}$ component, respectively. The result suggests that magnetic pulsations in the Pc 3–4 ranges have odd-mode wave characteristics (SUGIURA and WILSON, 1964; LANZEROTTI and FUKUNISHI, 1974; FUKUNISHI, 1979). It is worth noting that the $\dot{D}$ component of magnetic pulsations has good coherency not only with QP emissions but also with conjugate-pair data in the Pc 3–4 period ranges in comparison to the $\dot{H}$ component of magnetic pulsations, suggesting that properties of the $\dot{D}$ component of magnetic pulsations are conserved in the propagating process from the outer magnetosphere to the conjugate-pair stations on the ground. It is also found that the geomagnetic conjugacy of $\dot{D}$ was good at the frequency range of 25 mHz where coherency of QPs-$\dot{D}$ was good at both the conjugate-pair stations. On the other hand, the conjugacy was not so good at the frequency range of ~40 mHz where coherency of QPs-$\dot{D}$ at Syowa Station was good and at Husafell was poor.

Fig. 91 shows the phase relation between VLF and the $\dot{D}$ component of magnetic pulsations in the frequency range where the coherency is larger than 0.5. These phase relations indicate that the phase is approximately 180 degrees different from Syowa Station to Husafell in almost all frequency ranges. This is due to the phase lag in $\dot{D}$ at conjugate stations as shown in Fig. 90b. The propagation time lag between QP and magnetic pulsations from the interaction region to the ground is estimated using the same method as mentioned in the previous section,

$$\Delta T = -\frac{1}{2\pi} \cdot \frac{d\theta}{df} \sim 26 \text{ (s)} .$$

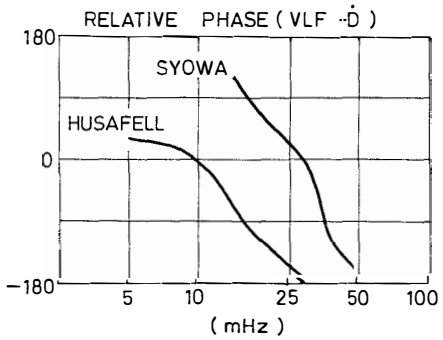

Fig. 91. Phase relation between QP emissions and the $\dot{D}$ component of magnetic pulsations in the frequency range where the coherency is larger than 0.5 at each station.

This result shows that propagation time lag between QP and magnetic pulsations is approximately the same (~26 s) at the conjugate-pair stations. It is thus concluded that the interaction between the whistler turbulence and magnetic pulsations takes place near the equatorial plane in the outer magnetosphere.

8.5.2. Geomagnetic conjugacy of Type 2 QP emissions

In this section we will examine the conjugacy of Type 2 QP emissions to confirm the previous results and also discuss characteristics of magnetic pulsations during Type 2 QP events.

From the examination of conjugate date obtained for 52 days, nine events

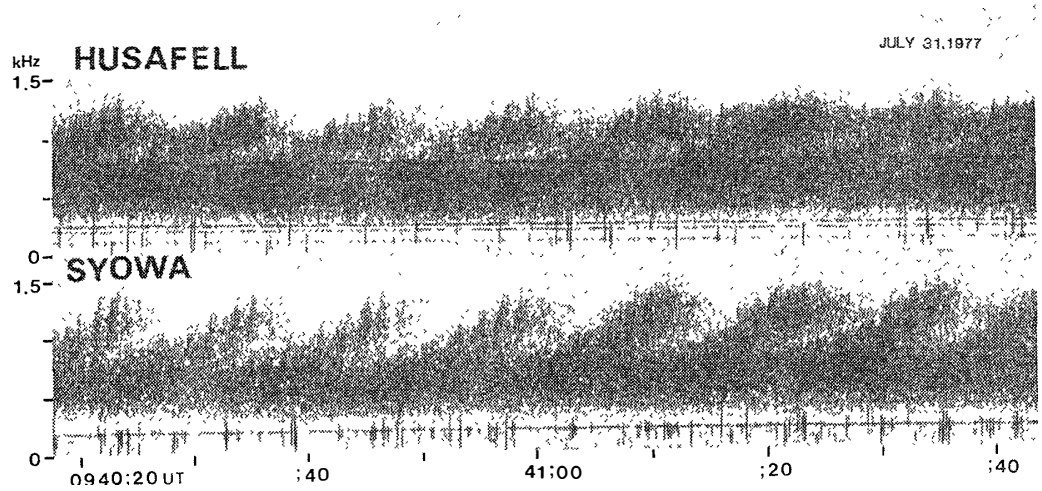

Fig. 92. Frequency-time spectra of Type 2 QP emissions observed at conjugate-pair stations, Syowa Station and Husafell in the time interval of 0940:18–1941:43 UT on July 31, 1977.

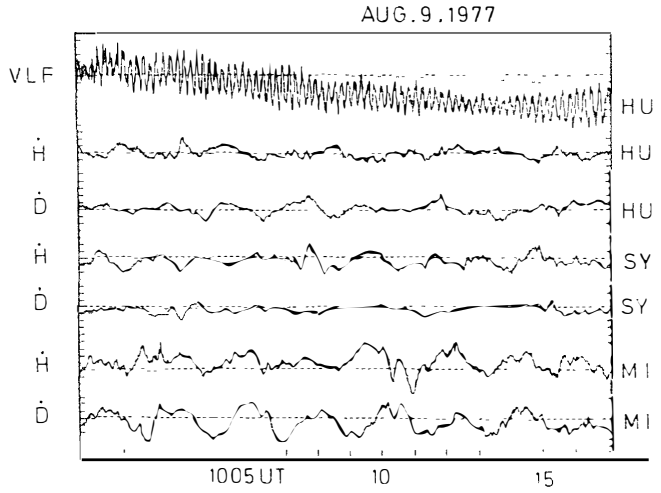

Fig. 93a. Intensity records of VLF emissions, the Ḣ and Ḋ component magnetic variations in the time interval of 1000:47–1017:10 UT on August 9, 1977, observed at Husafell-Syowa Station conjugate pair, and also Mizuho Station, Antarctica.

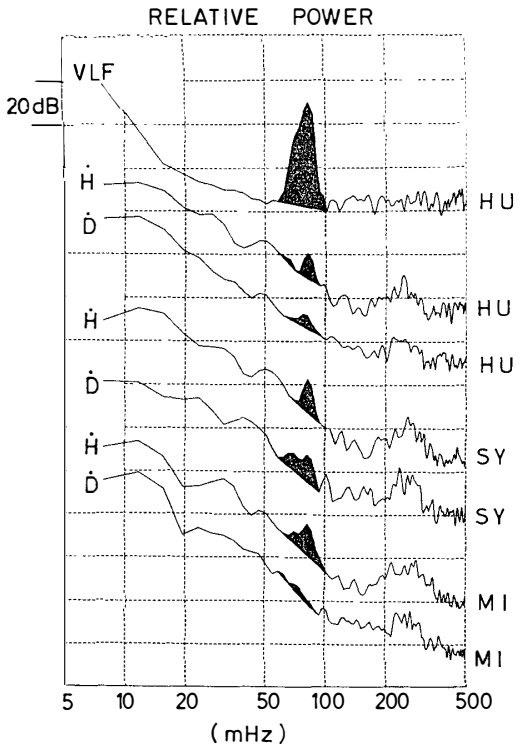

Fig. 93b. Relative power spectra of fluctuations of QPs at Husafell and magnetic variations observed at three stations, Husafell, Syowa and Mizuho Stations.

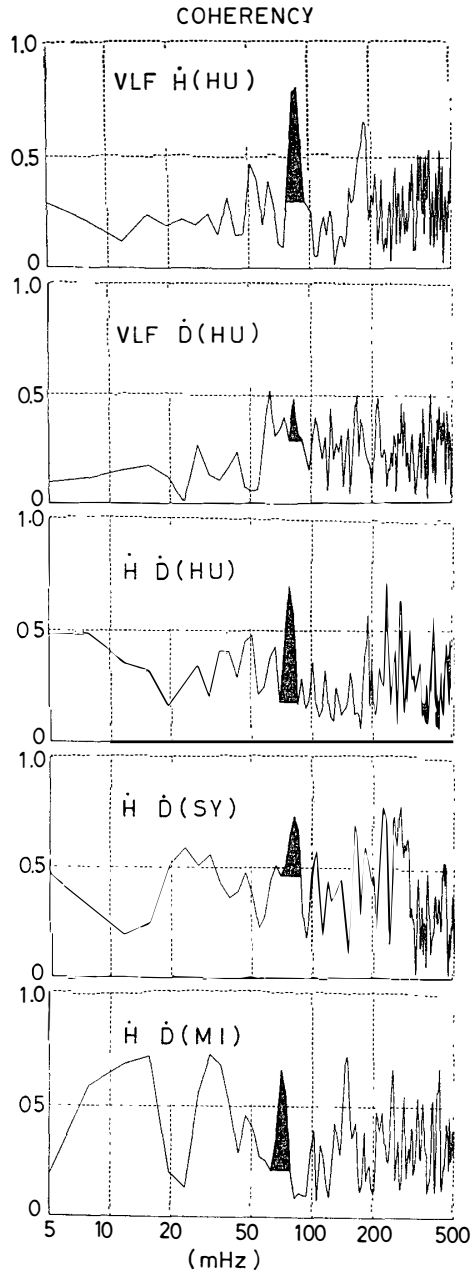

Fig. 93c. Coherency between QPs fluctuations and magnetic variations and the $\dot{H}$ and the $\dot{D}$ components of magnetic pulsations observed at Husafell, Iceland. The $\dot{H}$ component is more coherent with QPs than the $\dot{D}$ component.

were identified as Type 2 QP events (Table 4). It was found that QP structures with rising elements almost simultaneously occur at the two stations for all of nine cases. Example of spectrograms are shown in Fig. 92. Fig. 92 represents

spectrograms of QPs observed for a part of the interval shown in Fig. 88. The regularity in repetition period and spectral form is evidently seen in these figures.

Spectral characteristics of magnetic pulsations during seven QP events shown in Table 4 were examined. Peaks in magnetic spectra corresponding to the modulation frequency of QP emissions were found for three cases out of the seven events. As for the July 31 event, it was already discussed in the last section. We will discuss QP emissions observed on August 9, in the following. Fig. 93a shows the intensity records of VLF emissions, the $\dot{H}$ and $\dot{D}$ components of magnetic variations in the period of 1000:47–1017:10 UT on August 9, 1977, observed at Husafell–Syowa Station conjugate pair, and also Mizuho Station, Antarctica. *Kp* index during this period was 2. The intensity records of VLF emissions show a very regular periodicity, while magnetic pulsations are not so regular with longer period components, as compared with VLF emissions. Although it is hard to identify the periodicity of magnetic pulsations in the time-amplitude records, the spectral analyses revealed that there exists a small but significant peak in pulsation spectrum, related to the peak in VLF spectrum (Fig. 93b).

The power spectrum of QPs has a sharp peak around 80 mHz, indicating the regularity of periodicity similar to other examples. On the other hand maximum spectral densities are observed around 12 mHz in pulsation spectra and spectra rapidly decrease with frequency increase in proportion to approximately f^{-3}. The interesting feature to be noted is that there are peaks common to all of spectra around 80 mHz, especially in the $\dot{H}$ component. These peaks are significant,

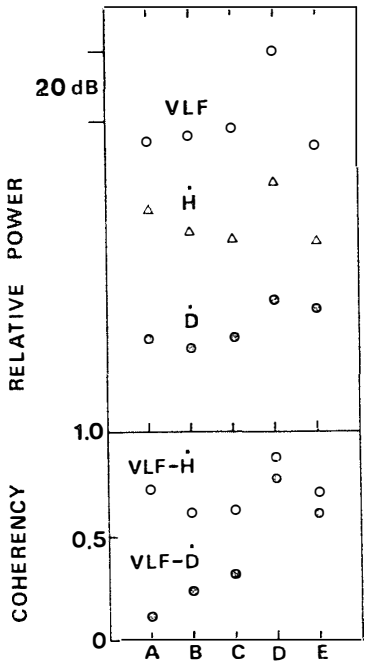

Fig. 94. Peak powers of VLF variations along with corresponding peak values in the $\dot{H}$ and $\dot{D}$ components (top panel) and coherencies between QPs and ULF (bottom panel) for the period from 0958 to 1028 UT on August 9, 1977.

considering that similar features are noted at the three stations.

The coherency analysis of data obtained at Husafell shows that spectral components of pulsation around 80 mHz are closely correlated with QP modulations (Fig. 93c). It is worth noting that the $\dot{H}$ component is more coherent with QPs than the $\dot{D}$ component. In order to examine relationships of pulsations and VLF intensity variations during this event in greater detail, data from 0958 to 1028 UT were divided into five segments and spectral calculations were made for each segment. In the top panel of Fig. 94 are shown peak powers of VLF intensities along with corresponding peak values in the $\dot{H}$ and $\dot{D}$ components. Both $\dot{H}$ and $\dot{D}$ peak values change in accordance with VLF peaks. Coherencies indicate that the $\dot{H}$ component is again more correlated with VLF than the $\dot{D}$ component. A significant coherency between $\dot{D}$ and QPs is only noted around the intensity maximum of VLF. Thus, these features show that spectral components of pulsations around 80 mHz are related to periodic modulations of VLF emissions.

9. Discussion

We have examined various aspects of QP emissions in order to study their interaction region and generation mechanism. QP emissions are classified into two types, Type 1 QP emissions and Type 2 QP emissions. There are essentially different characteristics between Type 1 and Type 2 QPs in occurrences, spectral features, periodicity and the quantitative relation to magnetic pulsations, suggesting that these two types of QP emissions are controlled by different physical processes in the magnetosphere.

We shall discuss here the generation regions and modulation mechanisms of QP emissions, and the spectral forms of QP emissions.

9.1. Generation region and modulation mechanism of Type 1 QP emissions

The statistical features of Type 1 QP emissions have been reported in Section 3, and by SATO *et al.* (1974). Since the classification of types of QP emissions has, however, been made from the comparisons of chart records in their study, more sophisticated analysis is necessary to establish the relevance of their classification and the detailed relationships between QP emissions and magnetic pulsations. In Section 8 we examined several examples of the Type 1 QP events by spectrum and coherency analyses to demonstrate close relationships between the phenomena. As shown in Section 8.1, comparisons of dynamic spectra indicate that the intensity and period of QP emissions concurrently change with the amplitude and period of magnetic pulsations during the course of a long duration event. It is often found that the modulation amplitude of QPs tends to be larger as the increase in amplitude of magnetic pulsations.

The conjugacy of Type 1 QP events has been also discussed, because data examined so far are very limited (KITAMURA *et al.*, 1969). KITAMURA *et al.* (1969) examined data from a pair of stations, Great Whale River (66.5°, 349.5° in geomagnetic coordinates, $L \simeq 6.3$) and Byrd Station ($-70.5°$, 336.8°, $L \simeq 9.1$). The difference in L value is as large as $\Delta L \simeq 3$ for this pair, while it is very small ($\Delta L \simeq 0.2$) for Syowa Station–Husafell pair. In contrast to the results reported by KITAMURA *et al.* (1969), the conjugate observations at Syowa Station and

Husafell reveal that the Type 1 QP emissions show good conjugacy. This discrepancy of observations suggests that the radial scale of the interaction region between whistler mode waves and hydromagnetic waves is less than 3 earth's radii.

The present observation showed that each QP element is simultaneously observed at the conjugate stations within an accuracy of one second. This symmetry indicates that the interaction between whistler mode waves and hydromagnetic waves occurs near the equator in the outer magnetosphere, where various types of whistler mode waves are generated as observed by satellites (RUSSELL *et al.*, 1969; DUNKELL and HELLIWELL, 1969; TSURUTANI and SMITH, 1977). The $\dot{H}$ component of associated magnetic pulsations is in phase at the conjugate station, while the $\dot{D}$ component is out of phase. This is a feature expected of the odd mode waves in terms of the field line resonance concept.

The coherency analysis shows that the intensity variations of QP emissions are generally more correlated with the $\dot{D}$ component of associated magnetic pulsations in the Pc 3–4 range than with the H component. This gives us an inference on the mode of ULF waves which play a major role in the interaction with whistler mode waves in the magnetosphere, by referring to the theoretical consideration by HUGHES (1974) and satellite observations of Pc 3 waves by ARTHUR *et al.* (1977). HUGHES (1974) has shown that the azimuth of a magnetic pulsation is rotated through a right angle in propagating through the ionosphere to the ground. A better coherency between QP emissions and the $\dot{D}$ component would indicate that the radial class of Pc 3 waves (ARTHUR *et al.*, 1977) plays a dominant role in the interaction with whistler mode turbulence. ARTHUR *et al.* (1977) reported that a radial class of Pc 3 waves at synchronous altitude has more compressional components as compared with an azimuthal class of Pc 3 waves. Thus, it is strongly suggested that the Type 1 QP emissions are caused by the interaction between whistler turbulence and compressional hydromagnetic waves in the outer magnetosphere.

Similar arguments have already been presented in Sections 5 and 8 by HAYASHI *et al.* (1968) and SATO *et al.* (1974), in connection with the effect of the storm sudden commencement and world wide magnetic variations of the SI type. They have shown that the triggering or enhancement of VLF emissions is observed in association with the SSC or world-wide increase in the H component in low latitudes and that a negative variation causes an intensity decreases or fade out of emissions.

Another significant result obtained from the coherency analysis is that the propagation time of ULF waves from the interaction region is inferred from the phase difference between the intensity variation of QPs and the $\dot{D}$ component of associated pulsations. Estimated times are 20–30 s, almost the same at the conjugate stations. It is worth noting here that the time delay of magnetic pulsations behind QP emissions is almost the same as that in case of SSC or

SI-triggered emission events. These results support that the interaction region between QP fluctuations and magnetic pulsations is near the equatorial plane in the outer magnetosphere. If we adopt mean whistler velocity and Alfvén velocity to be 6×10^4 km/s and 2×10^3 km/s, respectively, 25 s in the difference of the arrival times can be expected to be 5×10^4 km for the path length from the interaction region to the ground.

On the other hand, the phase relation of magnetic pulsations at the conjugate stations shows a feature expected of odd mode waves, as mentioned previously. If magnetic pulsations, which correlate QP emissions, are originated from the standing oscillation of field lines, the period of the fundamental oscillation would be 80–120 s, taking into account the traveling time inferred from the coherency analysis, and is much larger than observed periods. This suggests that magnetic pulsations are a higher harmonic oscillation, possibly the third harmonics, or they originates from the other mechanism, such as suggested by TAMAO (1978). He has shown that trapping oscillations of the fast mode in the trough between the two peaks in the Alfvén wave profile, one at the plasmapause and the other at the peak of the ring-current proton distribution, would be a candidate for Pc 3 range pulsations observed in high latitudes.

The interaction between the whistler mode waves and ULF waves has recently attracted the attention of theorists (CORONITI and KENNEL, 1970; KIMURA, 1974; CHEN, 1974; HAUGSTAD, 1975, 1976; SHUKULA and SPATSCHEK, 1976; BESPALOV and TRAKHTENGERTS, 1976; BESPALOV, 1977). CORONITI and KENNEL (1970) first presented a theoretical discussion of the modulations of whistler turbulences, which demonstrates that geomagnetic pulsations can modify the distribution of energetic electrons in the magnetosphere so as to trigger whistler mode wave variations and produce electron precipitation into the atmosphere. HAUGSTAD (1975, 1976) has made some modification of this theory and claimed that this theory accounts for periodic changes in the upper cut-off frequency of QP emissions, as reported by SATO *et al.* (1974).

In the theory by CORONITI and KENNEL (1970) the nature of the interactions has been based on the concept of the modulations of VLF growth rate by ULF waves. Another approach to the problem has been given by CHEN (1974), taking into account the convection loss rate and wave-wave interaction. He predicts that the modulation of VLF waves is either in phase or out of phase depending on the spectrum of the back ground VLF waves. BESPALOV (1977) has further discussed the interaction between VLF and ULF waves, combining both the effects discussed by CORONITI and KENNEL (1970) and CHEN (1974). In the theories mentioned above whistler turbulences are assumed to be modulated by externally excited ULF compressional waves. On the other hand, HAGEGE *et al.* (1973) considered the interaction of whistler turbulence with low-frequency drift waves to explain the storm time Pc 5 in the magnetosphere. Although these theoretical

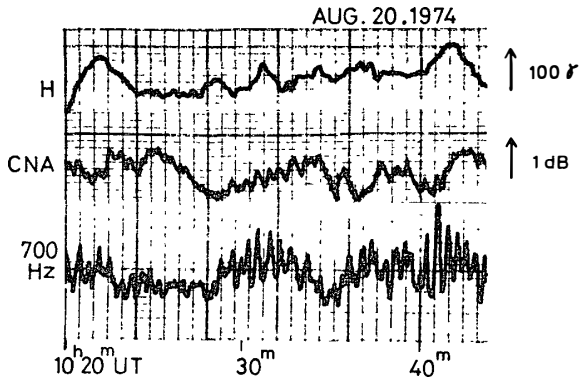

Fig. 95. Intensity record of the H component of magnetic variations, cosmic noise absorption, and VLF emission intensity.

considerations have emphasized a wide variety of possible explanations for the interaction between whistler mode turbulence and ULF waves, the feature common to these theories is that the whistler turbulence strongly interacts with compressional ULF waves. This is consistent with the inference from the previous discussion.

Fig. 95 shows an example of quasi-periodic variations in cosmic noise absorption along with the intensity record of QP emissions to the *H* component of the magnetic field, observed at Syowa Station. It is evident in this figure that periodic fluctuations in riometer records are closely correlated with variations of periods of ~40 s in both the 700 Hz band intensity and the *H* component, indicating that high energy electrons, associated with QP emissions, precipitate quasi-periodically. Although cosmic noise absorption events such as shown above are not so often observed at Syowa Station, probably because of limited sensitivity and response of the riometer, this example gives us some evidence of interaction mechanisms, such as first discussed by CORONITI and KENNEL (1970). It is very desirable to make observations in the future by using a higher sensitivity riometer, such as done by LANZEROTTI *et al.* (1978) to clarify the interaction mechanism between ULF and VLF waves.

9.2. Generation region and modulation mechanism of Type 2 QP emissions

Characteristics of intensity modulations of Type QP emission and of concurrent magnetic variations were examined in detail. The results are summarized as follows:

1) The frequency of intensity modulations of Type 2 QPs is stable as compared with that of Type 1 QPs, although it slowly changes in the course of an event. The *Q* value of a spectral peak usually attains to more than 10. Thus, it may be more appropriate to call this phenomenon "Regular period ELF-VLF pulsations".

2) In most cases magnetic variations during Type 2 QP events, which occur under magnetically quiet condition, have no spectral peak corresponding to the

peak in QPs spectrum as expected from the original definition of Type 2 QP emissions.

3) However, a small but significant peak in pulsation spectrum is occasionally noted, when the Type 2 QP event occurs in moderately disturbed condition. A high correlation between magnetic pulsations and QPs is not observed in the whole course but at certain intervals of an QP event. The peak value of the pulsation spectrum, in such a case, is generally two order of magnitude less than the maximum power of background magnetic fluctuations. The amplitude of pulsations is order of 0.01 nT/s. The $\dot{H}$ component tends to be more correlated with the VLF intensity than the $\dot{D}$ component, as far as cases examined here are concerned, while the $\dot{D}$ component tends to be more coherent to the VLF intensity in case of Type 1 QP emissions as shown in Section 8.2. It is worth noting that the period of Type 2 QPs associated with weak pulsations ranges in 10–20 s.

These results appear to give a basis on the relevance of classification of QP emissions by SATO *et al.* (1974), although weak pulsations are sometimes detected at a certain interval of Type 2 QP event.

One of the puzzling features of Type 2 QP emissions is their regularity in repetition of rising frequency structures. The problem is what determines this regular recurrence. There is a possibility that the periodic modulation originates from a certain ULF wave, which may be electrostatic and accelerates electrons to produce whistler mode waves. It is also possible that the modulation agent is a localized hydromagnetic wave which is not observable on the ground. HUGHES and SOUTHWOOD (1976) have theoretically shown that a localized hydromagnetic wave of scale size ~50 km at the ionospheric level is almost screened by the ionosphere and then is not observed on the ground. Since ground-based observations can not give direct evidence for the existence of an electrostatic wave or a localized hydromagnetic wave, coordinated observations from the ground and from satellite are needed to clarify these possibilities.

An occasional association of a weak pulsation could be interpreted, taking into account electron precipitation induced by whistle mode waves. Before discussing this point, an interesting example of a correlation between periodic emissions and weak magnetic pulsations was given in Fig. 82a. QP elements were composed of periodic emissions with the frequency of ~0.3 Hz. The repetition period of QP groups of risers was not so regular and a high correlation between QP intensity modulations and magnetic pulsations was noted at certain intervals during the event. A weak coherency around 50 mHz seen in Fig. 82b indicates this feature. An interesting feature to be noted in Fig. 82b is that there is a small peak on the decreasing slope of magnetic variation spectrum, which corresponds to the peak of periodic emission spectrum. The coherency also shows a significant peak at 0.32 Hz. Although a high coherency between emission intensity and

magnetic variations, such as shown in this figure, was not observed in the whole interval of the event, the feature shown in the figure indicates that there exist magnetic pulsations closely correlated with periodic emissions.

HELLIWELL and BRICE (1964) and HELLIWELL (1965) have reported evidence to show that periodic emissions are caused by the echoing of whistler mode wave packets alternately between the hemispheres along the line of force. Thus, this example strongly suggests that the periodic variation of VLF emissions of which the period is not determined by a modulation agent, such as hydromagnetic waves, but by the propagating characteristic of whistler mode waves, can produce associated magnetic variations observed on the ground.

Considerable evidence for energetic electron precipitation induced by whistler mode waves have recently been reported by ROSENBERG *et al.* (1971) and HELLIWELL *et al.* (1979). ROSENBERG *et al.* (1971) found a one-to-one correlation between bursts of whistler-triggered discrete VLF emissions propagating at L=4.2 and bursts of >30 keV X-rays observed at balloon altitudes. One-to-one correlations have also been observed between bursts of VLF noise in the ~2–4 kHz range and optical emissions at 4278 Å (HELLIWELL *et al.*, 1979). They have reported that the correlated VLF emissions usually consist of clusters of discrete risers or chorus ranging in duration from ~1–10 s and that the precipitated energy fluxes are estimated to be in the range 0.04–0.1 erg $cm^{-2} \cdot s^{-1}$. On one case they reported, the VLF activity consisted of group of discrete risers with a period of ~10 s.

These observations strongly suggest that weak magnetic pulsations, occasionally associated with Type 2 QP emissions and periodic emissions shown in Fig. 82 are caused by ionospheric conductivity variations due to electron precipitation induced by whistler mode waves. If this is the case the magnitude of magnetic pulsations should depend on both conductivity enhancement and the ambient electric field. In case that ambient electric field is small, magnetic variations would be below the detection level of magnetometers, even though a strong emission activity is observed. As shown previously, the Type 2 QP correlated pulsations tend to be detected when the Type 2 QP occurs during moderately active condition. This fact is likely to support the hypothesis that conductivity variations are the origin of magnetic pulsation.

It has been proposed by several workers, including CAMPBELL (1967), MCPHERRON *et al.* (1968), MORIOKA and SAITO (1971) and REID (1976) that ionospheric conductivity fluctuations caused by particle precipitations are the origin of Pi type magnetic pulsations observed on the ground. BELL (1976) has theoretically discussed the ULF wave generation through particle precipitations induced by a periodic injection of artificial VLF waves and has shown that detectable magnetic pulsations can be produced by the injection of VLF periodic pulses. Pi 1 pulsations of amplitude 0.1–1 nT/s are usually observed associated with

optical emission fluctuations of ~0.5 kR at 4278 Å. According to the observations by HELLIWELL *et al.* (1979), intensity variations of 4278 Å in wave induced events are 10–50 R in amplitude. Therefore, weak magnetic pulsations of ~0.01 nT/s, observed during Type 2 QP event, could be produced by wave induced particle precipitations, although the scale size of QP emission is not yet known.

9.3. Models of spectral form for QP emissions

QP emissions have been classified into five types based on frequency-time spectra; 'non-dispersive', 'rising-tone', 'falling-tone', 'mixed' and 'burst' types. Interaction regions and interaction mechanisms between QP fluctuations and magnetic pulsations were discussed in this paper. QPs are observed simultaneously at conjugate-pair stations with good conjugacy and the coherency between the $\dot{D}$ component of magnetic pulsations and the intensity fluctuations of QPs is higher than that between the $\dot{H}$ component and QPs. It is also found that the propagation time of magnetic pulsations (HM waves) from the interaction region between magnetic pulsations and QPs to the ground is ~20–30 s. From these results we suggested that QP emissions are modulated by compressional mode Pc 3–4 magnetic pulsations near the equatorial plane in the outer magnetosphere.

In this section we will interprete the frequency-time spectra of QP emissions, mostly for Type 1 QP emissions by using a phenomenological model. The start points of our model are as follows;

1) The intensity and frequency of ELF-VLF emissions are modulated by compressional mode magnetic pulsations.

2) Interaction region between ELF-VLF emissions and magnetic pulsations is near the equatorial region in the outer magnetosphere.

3) The frequency of the intensity peak of ELF-VLF emissions in the magnetosphere is proportional to $\sim(1/4)\Omega^-$, where Ω^- is the local electron gyrofrequency (TSURUTANI and SMITH, 1977).

4) Emissions are observed simultaneously at stations apart from each other about a few hundred kilometers (HELLIWELL, 1965). Therefore, it is suggested that emissions generated in different regions in the magnetosphere can be observed at the same station on the ground.

9.3.1. Model of 'rising-tone' and 'falling-tone' emissions

In order to interprete the spectral forms of 'rising-tone' and 'falling-tone' QP emissions, we assume that compressional mode magnetic pulsations propagate in the radial direction from the magnetopause toward the earth when 'rising-tone' QPs are observed on the ground.

Schematic picture for the generation of 'rising-tone' type QPs is shown in Fig. 96.

1) Stage 1; ULF wave with compressional component does not exist in

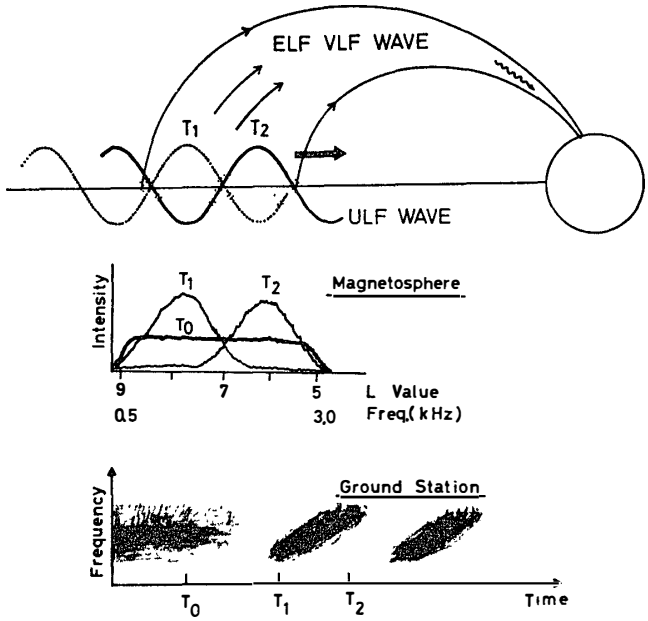

Fig. 96. Schematic picture for a model of generation mechanism of 'rising-tone' type QPs.

the magnetosphere.

ELF-VLF emissions are generated near the equatorial region in the outer magnetosphere (L~6–8). Assuming that the emission frequency is proportional to a quarter of local electron gyrofrequency, the emission frequency is ~0.3 kHz at L=8 and ~1.0 kHz at L=6. These emissions propagate through wave ducts along geomagnetic field lines to the ground. So that, continuous ELF-VLF emissions are observed on the ground.

2) Stage 2–3; ULF wave with compressional component propagates in radial direction from the magnetopause toward the earth.

When ULF wave propagates in radial direction, ELF-VLF emissions can be modulated by the compressional component of ULF waves through the electron-cyclotron instability mechanism suggested by KENNEL and PETCHEK (1966). That is, the intensity of ELF-VLF emissions increases in the region where the ambient magnetic field intensity increases, while the intensity of ELF-VLF emissions decreases or fades out in the region where the magnetic field intensity decreases. Therefore, at the time T_1 when a positive phase of compressional ULF wave is located in the region with larger L values, emissions are excited there, while the emissions are suppressed in the region with smaller L values where the negative phase of compressional ULF wave is located. As a result, emissions with lower frequency are excited in the larger L value region in the magnetosphere. At the time T_2 when magnetic pulsations propagate in radial direction to the region with smaller L values, positive phase of compressional magnetic pulsations exists at smaller L values. Therefore, emissions are excited in higher frequency range, while emissions in the lower frequency range are

suppressed. These emissions are observed on the ground. As a result, frequency-time spectra of ELF-VLF emissions show 'rising-tone' type of QP emissions.

Many other observational results support this modulation model due to propagating ULF waves. Type 1 QP emissions observed at Syowa Station often correlate closely to magnetic pulsations observed at middle and low latitude stations (Section 5). This result suggests that Pc 3–4 magnetic pulsations propagate from the outer magnetosphere to the inner magnetosphere. Furthermore, Type 1 QP emissions were sometimes observed simultaneously at widely separated two stations, Sogra (geomag. lat. 56.4, long. 131.7) in USSR and Syowa Station (−70.7, 79.4) in Antarctica. A typical event was observed on December 2, 1977 (KLEIMENOVA, private communication, 1978). This result also indicates that compressional magnetic pulsation exists simultaneously in wide region and propagates to lower L value, and this magnetic pulsation modulates ULF intensities generated at both high and middle latitudes.

On the direction finder analysis of Type 1 QP emissions, it is observed that only north-south component of arrival direction fluctuates associated with 'rising-tone' Type 1 QP emissions (Section 6). This result strongly indicates that 'rising-tone' QP emissions are generated by the compressional mode magnetic pulsations which propagate to radial direction.

Recently, many authors have been studying the relation between solar wind parameters and magnetic pulsations on the ground or in the magnetosphere, and found some remarkable correlations between Pc 3–4 magnetic pulsations (T∼10–150 s) and solar wind parameters (TROITSKAYA *et al.*, 1971; GREENSTAD and OLSON, 1976; ARTHUR and MCPHERRON, 1977). These results suggest that daytime Pc 3–4 magnetic pulsations originate from the propagation of MHD waves excited near the bow shock through the magnetosheath to the magnetopause and into the magnetosphere. Their suggestion is consistent with our simple model assuming that Pc 3–4 magnetic pulsation propagates in radial direction toward the lower L value region.

In our model, 'falling-tone' types of QPs is interpreted that the QP emissions are modulated by compressional mode magnetic pulsations propagating toward the higher L value region. In the auroral zone, some types of poleward propagating auroras are observed in the morning sector (OGUTI and WATANABE, 1976). Furthermore, radar aurora behaves quasi-periodically poleward propagation in the morning sector (KANEDA *et al.*, 1964; MCDIARMID and MCNAMARA, 1972). TAMAO (1977) suggested theoretically that enhanced compressional mode Pc 3 magnetic pulsations which propagate outward from the coupling resonance region would account for propagating auroral pulsation in the morning sector.

9.3.2. Model of 'non-dispersive' type QP emissions

'Non-dispersive' type QP emissions are observed in the daytime and associated

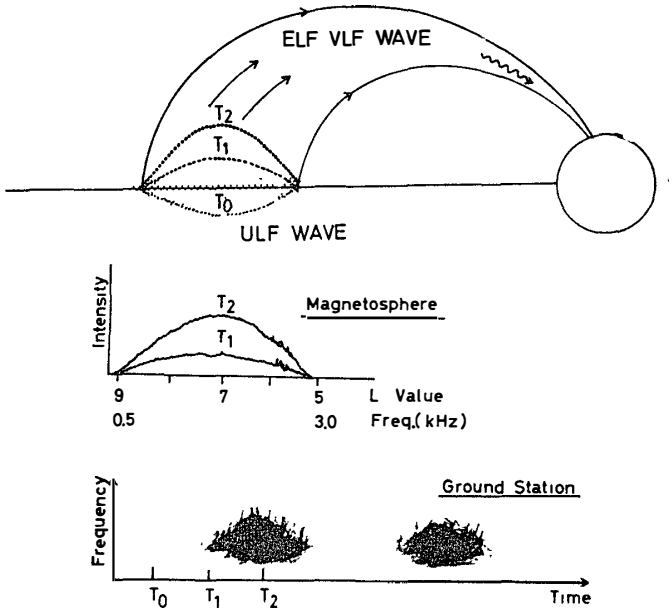

Fig. 97. Schematic picture for a model of generation mechanism of 'non-dispersive' type QPs.

with long period magnetic pulsation (T~40–150 s). This type of QPs will be also interpreted by using the same analogy as discussed above. The generation and propagation conditions for background ELF-VLF emissions are the same as the previous mode. Only properties of magnetic pulsations are different, *i.e.*, we assume that standing hydromagnetic waves along the magnetic field lines which have an effective compressional component interact with ELF-VLF emissions. Schematic illustration of this model is shown in Fig. 97. Intensity fluctuation of compressional component associated with standing mode waves is assumed to occur simultaneously in the wide L-value ($L \simeq 6$–8) region near the equatorial plane where ELF-VLF emissions are generated. In this case, the intensity of ELF-VLF emissions whose frequencies are in proportion to local electron gyrofrequency is modulated simultaneously in the wide L-value region. Therefore, 'non-dispersive' type QP emissions are observed on the ground.

Our assumption for standing mode wave will not be unnatural, because many authors reported that long period magnetic pulsations (Pc 4–5) are standing waves rather than propagating waves in radial direction (*e.g.*, SUGIURA and WILSON, 1964; LANZEROTTI and FUKUNISHI, 1974; KOKUBUN *et al.*, 1976; CUMMINGS *et al.*, 1978).

As discussed above, we have interpreted frequency-time spectra of Type 1 QP emissions by using a simple model. This model will also apply to not only 'rising-tone' and 'falling-tone' but also to 'hybrid' types. Furthermore, it is possible that Type 2 QP emissions are modulated by compressional mode magnetic pulsations which are not easily detectable on the ground because most of Type 2

QPs belong to the 'rising-tone' type, as is shown in Table 2 and magnetic pulsations which are detectable on the ground are generally standing oscillations of local resonant field lines (shear Alfvén mode) excited by compressional (fast) mode MHD waves (SOUTHWOOD, 1974; CHEN and HASEGAWA, 1974; LANZEROTTI and FUKUNISHI, 1974). If the coupling condition between shear Alfvén waves and fast mode waves is not satisfied in the outer magnetosphere, standing oscillations can not be excited. Therefore, in this case, it is possible that magnetic pulsations are not observed on the ground, even if compressional waves exist in the magnetosphere. Another possibility is that the wave length of MHD waves associated with Type 2 QPs is much shorter than that of Type 1 QPs. In this case, MHD waves in the magnetosphere are shielded by the ionosphere and are not observed on the ground (HUGHES and SOUTHWOOD, 1976).

Perhaps, there will be other possibility to interprete *f-t* spectra of QP emissions. However, our model will be most simple and reasonable in our understanding of present magnetospheric physics.

10. Conclusions and Future Research

10.1. Summary and conclusions

We have examined the characteristics of QP emissions and their relationships to magnetic pulsations. The ELF-VLF and ULF data used here are those obtained at Syowa Station in Antarctica, Mizuho Station ~270 km south of Syowa Station and at Husafell in Iceland, the geomagnetic conjugate point of Syowa Station. From a few hundred QPs data, QP emissions are classified into two types, Type 1 and Type 2, on the basis of the amplitude of magnetic pulsations and on the periodicity. Type 1 QP emissions are associated with magnetic pulsations, and Type 2 QP emissions are not associated with magnetic pulsations or, if they exist, their intensities are usually very weak. However, the periodicity of Type 2 QPs is more regular than that of Type 1 QPs.

We were able to find essential differences in the properties of the two types, and have discussed in detail the interaction region and interaction mechanisms and also have proposed a simple model to explain the frequency-time spectra of QP emissions. We come to the following conclusion.

10.1.1. Type 1 QP emissions

1) Most of the QPs are observed on the dayside with a maximum occurrence around noon during the moderate geomagnetic activity ($Kp \sim 2$). QPs periods range from 15 s to few minutes, but are mostly around 30 s, and diurnal variation of QP period tends to increase gradually from morning to evening. Emission frequencies range from 0.3 to 1.5 kHz, and the emission spectra are mostly of the polar chorus type.

2) Background intensities of QPs are modulated associated with SSC or SI type worldwide geomagnetic field variations. This property strongly suggests that the emissions (ELF-VLF emissions) are generated near the equatorial plane in the outer magnetosphere by electron-cyclotron resonance.

3) Intensities and periods in QP fluctuations change concurrently with the intensity and period of magnetic pulsations, and modulation amplitude of the QPs is larger when the intensity of ELF-VLF emissions is higher.

4) Type 1 QP emissions observed at Syowa Station are seen to be almost synchronously associated with magnetic pulsations in the 20–60 s in period range observed at middle and low latitude stations, strongly suggesting that Type 1 QP emissions are modulated by compressional mode Pc 3–4 magnetic pulsations in the magnetosphere.

5) Magnetic pulsations likely propagate from the interaction region between ULF and ELF-VLF waves to the ground along the line of force with a time lag behind the QPs arrival of approximately by 20–30 s because of difference in propagation speed between ELF-VLF waves (whistle mode) and ULF waves (Alfvén mode). This property also observed at conjugate-pair stations. It indicates that QP fluctuations interact with magnetic pulsations near the equatorial plane in the outer magnetosphere.

6) The relative phases between QP fluctuations and $\dot{D}$ are roughly constant in the Pc 3–4 period range, 10–100 s, at the interaction region between ULF and ELF-VLF waves.

7) The coherency between QP fluctuations and the $\dot{D}$ component of magnetic pulsations is greater than that between QPs and the $\dot{H}$ component. This property is observed at conjugate-pair stations. The simple interpretation of these properties is that radial (N-S) oscillations of Pc 3 magnetic pulsations which have a significant compressional component near the equatorial plane in the outer magnetosphere (ARTHUR *et al.*, 1977) appear in the $\dot{D}$ (E-W) component of magnetic pulsations on the ground, because the azimuth of magnetic pulsations rotats through a right angle in propagating through the ionosphere-atmosphere, as theoretically predicted by HUGHES (1974).

8) The phase relation of Pc 3–4 magnetic pulsations which interact with QP fluctuations is approximately in-phase in $\dot{H}$ and out of phase in $\dot{D}$ at conjugate-pair stations, suggesting that the Pc 3–4 magnetic pulsations are odd-mode waves.

9) A simple model to explain the frequency-time spectra of QP emissions is proposed. 'Rising-tone' and 'falling-tone' types of QPs interact with compressional mode magnetic pulsations which propagate in the radial direction to the equatorward and the poleward, respectively. The 'non-dispersive' type of QPs interacts with long period ($T\sim$40–150 s) standing mode magnetic pulsations which have effective compressional components. Our model is simple, but reasonable in view of our present understanding of magnetospheric physics.

10) Short period QP fluctuations or periodic emissions ($T\sim$3–4 s) are sometimes associated with magnetic pulsations with the same period.

10.1.2. Type 2 QP emissions

1) The Type 2 QP emissions are observed between 09 and 20 LMT, with a maximum around noon and a secondary one in the afternoon-evening period, and occur during quiet geomagnetic times ($Kp\sim$1) after geomagnetic storms.

The QPs period ranges from 10 to 60 s, mostly around 20 s, and tends to increase gradually from morning to evening. The Type 2 QPs period is shorter than Type 1 QPs, but the emission frequencies are slightly higher than that of Type 1 QPs.

2) The background intensities of QP emissions are modulated by SSC or SI type worldwide geomagnetic field variations, suggesting that background emissions of the QPs are generated near the equatorial plane in the magnetosphere by electron-cyclotron resonance, the same mechanism as for Type 1 QPs. The QPs period modulates becoming shorter or longer associated with positive or negative worldwide geomagnetic changes, respectively.

3) Most of the *f-t* spectra of Type 2 QPs are the 'rising-tone' type, and when the QPs type changes from Type 1 to Type 2, *f-t* spectra change form 'non-dispersive' to 'rising-tone' type.

4) The QPs show good geomagnetic conjugacy and are observed simultaneously at conjugate-pair stations as are Type 1 QPs.

5) The power spectra of the Type 2 QP fluctuations show a pronounced spectral peak in contrast to that of Type 1 QPs.

6) Most of the Type 2 QPs occurs during very quiet magnetic pulsation periods, so that we can not find a correlation between Type 2 QPs and magnetic pulsations even if high accuracy spectral analysis is carried out. However, some special Type 2 QPs events which occur on ULF waves during moderately active intervals have some associations with magnetic pulsations and show a small spectral peak at the frequency corresponding to the frequency of the sharp spectral peak in Type 2 QP fluctuations. However, the relative power of the ULF waves at this frequency is more than one order to magnitude less than the maximum power of the ULF waves.

7) The periods of Type 2 QPs are mostly shorter than those of magnetic pulsations which have a maximum power in the Pc 3–4 range, and there is no spectral peak in the VLF data during the Type 2 QPs occurrence at the frequency where ULF waves have maximum power.

8) Correspondence of magnetic pulsations with Type 2 QPs is observed at conjugate-pair stations, Husafell and Syowa Station, and also observed at Mizuho Station, 270 km south of Syowa Station.

9) Coherency between Type 2 QP fluctuations and $\dot{H}$ is much larger than that between QPs and $\dot{D}$ with the same properties, at all the three stations, Husafell, Syowa and Mizuho Stations. This is in contrast to the coherency between Type 1 QPs and magnetic pulsations.

10) To explain the periodicity of Type 2 QPs, two mechanisms will be presented. First, QPs are modulated by compressional mode magnetic pulsations in the magnetosphere with very regular periodicity which are not easily detectable at the ground, where they are mostly evanescent mode magnetic pulsations on

the ground. Therefore, the magnetic pulsations which have a small spectral peak corresponding to the sharp spectral peak of Type 2 QPs at the ground indicate the leakage of the pure compressional magnetic pulsations from the magnetosphere. Second, the periodicity of QPs is controlled by some other type of waves, not hydromagnetic waves. Therefore, the weak spectral peaks in ULF waves at the frequency corresponding to the period of Type 2 QPs is caused by the effects of small local fluctuations in the auroral electrojet due to the change in the ionospheric conductivity associated with periodic electron precipitations.

Investigation of QP emissions and related magnetic pulsations have included statistical analysis, special events, and qualitative correlation analysis based on the ground data including station nets, and geomagnetic conjugate-pair stations. These have presented much useful information on the interaction mechanism of ELF-VLF and ULF waves in the magnetosphere and especially, the wave-wave interaction in the magnetosphere. Furthermore, the investigations of the relationships between ELF-VLF emissions and magnetic pulsations contribute to the physical behavior of magnetic pulsations which are still largely unknown.

10.2. Suggestions for future research

1) There is a need for study of satellite data on the modulation of energetic fluxes, ELF-VLF emissions, and electric and magnetic field fluctuations.

2) There is a need for coordinated measurements by satellites of energetic flux ELF-VLF emissions, and electric and magnetic fluctuations at different longitudes, latitudes, and altitudes, to determine the propagation characteristics of these waves and particles.

3) There is a need for coordinated simultaneous measurements by station nets on the ground and by the synchronous orbit satellite to examine the propagating properties of waves from the magnetosphere to the ground through the ionosphere.

4) There is a need for simultaneous measurements of ELF-VLF emissions, magnetic pulsations and by a high resolution riometer, by operating station nets on the ground at different longitudes and latitudes in order to examine the propagation characteristics of waves and particles which propagate in radial and in azimuthal directions.

5) Experimental and analytical studies on particle precipitations and their effects on electrojet in the ionosphere, induced by QP emissions are needed.

6) Direct observations of Type 2 QP emissions and their related phenomena, *i.e.*, ULF waves, electric field fluctuations, cold plasma density, and energetic particles, are needed in the magnetosphere in order to determine the modulation mechanisms of Type 2 QP emissions.

Acknowledgments

The author wishes to express his gratitude to Prof. T. OGUTI and Dr. S. KOKUBUN for their continuous encouragement and countless suggestions throughout the course of this research.

The author would also like to thank Profs. T. NAGATA, T. HIRASAWA, and Dr. H. FUKUNISHI of National Institute of Polar Research for their encouragement and useful comments.

It is a pleasure to acknowledge all members of the 15th wintering party of the Japanese Antarctic Research Expedition, especially, the leader N. MURAKOSHI, for their kind support in making the observations at Syowa Station, Antarctica. As for the observations in Antarctica, the author is greatly indebted to Dr. K. HAYASHI for the preparation of the instruments of direction finding of ELF-VLF waves.

The author would like to thank Prof. I. KIMURA, Drs. T. TAMAO, T. SATO, K. TSURUDA, K. HAYASHI, K. MAKITA and Mr. R. FUJII for their valuable discussions. The author also wants to thank Profs. N. FUKUSHIMA, T. OBAYASHI and Dr. A. NISHIDA for their kind encouragement. His thanks are also due to Mrs. M. IWABUCHI for her kind help with the computer spectral analysis.

The author wants also to thank to the members of CRPE, France, for their helpful cooperation at Husafell in Iceland.

The author is grateful all persons involved in the preparation of the manuscript and especially to Mrs. N. SHIMURA for her excellent and conscientious typing.

References

AKAIKE, H. (1971): Autoregressive model fitting for control. Ann. Inst. Statist. Math., **23**, 163–180.

ALLCOCK, G. MCK. (1957): A study of audio-frequency radio phenomenon known as "dawn chorus". Aust. J. Phys., **10**, 268–298.

ARTHUR, C.W. and MCPHERRON, R.L. (1977): Interplanetary magnetic field conditions associated with synchronous orbit observations of Pc 3 magnetic pulsations. J. Geophys. Res., **82**, 5138–5142.

ARTHUR, C.W., MCPHERRON, R.L. and HUGHES, W.J. (1977): A satistical study of Pc 3 magnetic pulsations at synchronous orbit, ATS 6. J. Geophys. Res., **82**, 1149–1157.

BARRINGTON, R.E., HARTS, T.R. and HARVEY, R.W. (1971): Distribution of ELF, VLF and LF noise at high latitudes as observed by Alouette 2. J. Geophys. Res., **76**, 5278–5291.

BELL, T.F. (1976): ULF wave generation through particle precipitation induced by VLF transmitters. J. Geophys. Res., **81**, 3316–3326.

BESPALOV, P.A. (1977): Modulation of VLF noise intensity by hydromagnetic oscillations. Geomagn. Aeron., **17**, 43–46.

BESPALOV, P.A. and TRAKHTENGERTS, V.YU. (1976): Dynamics of the cyclotron instability in a mirror system. Sov. J. Plasma Phys., **2**, 215–221.

BRICE, N. (1964a): Discrete VLF emissions from the upper atmosphere. Tech. Rep. No. 3412–3416, Stanford Electronics Lab., Stanford University, Calif.

BRICE, N. (1964b): Fundamentals of very low frequency emission generation mechanisms. J. Geophys. Res., **60**, 4515–4522.

BRICE, N.M. and SMITH, R.L. (1965): Lower hybrid resonance emissions. J. Geophys. Res., **70**, 71–80.

BURTIS, W.J. and HELLIWELL, R.A. (1976): Magnetospheric chorus: Ocurrence patterns and normalized frequency. Palnet. Space Sci., **24**, 1007–1024.

BURTON, E.T. (1930): Submarine cable interference. Nature, **126**, 55.

BURTON, E.T. and BOARDMANN, E.M. (1933): Audio-frequency atmospherics. Proc. IRE, **21**, 1476–1494.

BURTON, R.K. and HOLZER, R.E. (1974): The origin and propagation of chorus in the outer magnetosphere. J. Geophys. Res., **79**, 1014–1023.

CAMPBELL, W.H. (1964): A study of geomagnetic effects associated with auroral zone electron precipitation observed by balloons. J. Geophys. Res., **16**, 41–61.

CARPENTER, D.L. (1962): Electron-density variations in the magnetosphere deduced from whistler data. J. Geophys. Res., **67**, 3345–3360.

CARPENTER, D.L. (1963): Whistler evidence of a 'knee' in the magnetospheric ionization density profile. J. Geophys. Res., **68**, 1675–1682.

CARPENTER, D.L. (1966): Whistler studies of the plasmapause in the magnetosphere. 1. Temporal variations in the position of the knee and some evidence of plasma motions near the knee. J. Geophys. Res., **71**, 693–709.

CARSON, W.B., KOCH, J.A. and GALLET, R.M. (1965): Long period very low frequency emissions. J. Geophys. Res., **70**, 4293–4303.

CHAPPELL, C.R., HARRIS, K.K. and SHARP, G.W. (1971): The dayside of the plasmasphere. J. Geophys. Res., **76**, 7632–7646.

CHEN, L. (1974): Theory of ULF modulation of VLF emissions. Geophys. Res. Lett., **1**, 73–75.

CHEN, L. and HASEGAWA, A. (1974): A theory of long-period magnetic pulsations. 1. Steady state exitation of field line resonance. J. Geophys. Res., **79**, 1024–1032.

CORNILLEAU-WHEHRLIN, N., GENDRIN, R. and TIXIER, M. (1978): VLF waves: conjugate ground-satelliite relationships. Space Sci. Rev., **22**, 419–431.

CORONITY, F.V. and KENNEL, C.F. (1970): Electron precipitation pulsations. J. Geophys. Res., **75**, 1279–1288.

CUMMINGS, W.D., DEFOREST, S.E. and MCPHERRON, R.L. (1978): Measurements of the Poynting vector of standing hydromagnetic waves at geosynchronous orbit. J. Geophys. Res., **83**, 697–706.

DUNCKELL, N. and HELLIWELL, R.A. (1969): Whistler-mode emissions on the OGO 1 satellite. J. Geophys. Res., **74**, 6371–6385.

EGELAND, A., GUSTAFSSON, G., OLSEN, S., AARONS, J. and BARRONS, W. (1965): Auroral emissions centered at 700 cycles per second. J. Geophys. Res., **70**, 1079–1082.

FRANK, I.B., VAN ALLEN, J.A. and CRAVEN, J.D. (1964): Large diurnal variations of geomagnetically trapped and of precipitated electrons observed at low altitudes. J. Geophys. Res., **69**, 3155–3167.

FRITS, T.A. (1968): High-latitude outer-zone boundary region for 40 keV electrons during geomagnetically quiet period. J. Geophys. Res., **73**, 7245–7255.

FUKUNISHI, H. (1979): ULF wave observed at Syowa/Iceland conjugate pair. Magnetospheric Study 1979: Proceeding of the International Workshop on Selected Topics of Magnetospheric Physics. Tokyo, Japanese IMS Committee, 89.

GALLET, R.M. (1959): The very low frequency emissions generated in the earth's exosphere. Proc. Inst. Radio Electron. Eng. Aust., **47**, 211–231.

GENDRIN, R. (1975): Waves and wave-particle interactions in the magnetosphere. Space Sci. Rev., **18**, 145–200.

GREENSTAD, E.W. and OLSON, J.V. (1976): Pc 3, 4 activity and interplanetary field orientation. J. Geophys. Res., **81**, 5911–5920.

HAGEGE, K., LAVAL, G. and PELLAT, R.(1973): Interaction between high-frequency turbulence and magnetospheric micropulsations. J. Geophys. Res., **78**, 3806–3815.

HAUGSTAD, B.S. (1975): Modification of a theory of electron precipitation pulsations. J. Atmos. Terr. Phys., **37**, 257–272.

HAUGSTAD, B.S.(1976): Upper cut-off frequency changes in quasi-periodic VLF emission events. J. Atmos. Terr. Phys., **38**, 781–784.

HAYASHI, K. and KOKUBUN, S. (1971): VLF emissions during post breakup phase of polar substorm. Rep. Ionos. Space Res. Jpn, **25**, 369–382.

HAYASHI, K., KOKUBUN, S. and OGUTI, T. (1968): Polar chorus emission and worldwide geomagnetic variations. Rep. Ionos. Space Res. Jpn, **22**, 149–160.

HAYASHI, K., OGUTI, T., WATANABE, T., TSURUDA, K., KOKUBUN, S. and HORITA, R.E. (1978): Power harmonic radiation enhancement during the sudden commencement of a magnetic storm. Nature, **275**, 627–629.

HEACOCK, R.R. and HUNSUCKER, R.D. (1977): A study of concurrent magnetic field and particle precipitation pulsations, 0.005 to 0.5 Hz, recorded near College, Alaska. J. Atmos. Terr. Phys., **39**, 487–501.

HELLIWELL, R.A. (1965): Whistlers and Related Ionospheric Phenomena. Stanford Univ. Press, 23–82.

HELLIWELL, R.A. and BRICE, N.M. (1964): VLF emissions periods and whistler-mode group delays. J. Geophys. Res., **69**, 4704–4708.

HELLIWELL, R.A., CRARY, J.H., POPE, J.H. and SMITH, R.L. (1956): The 'nose' whistler—A new high latitude phenomenon. J. Geophys. Res., **61**, 139–142.

HELLIWELL, R.A., MENDE, S.B., DOOLITTLE, J.H., ARMSTRONG, W.C. and CARPENTER, D.L. (1979): Correlations between 4278 optical emissions and VLF waves events observed at L~4 in the Antarctica. Preprint, Radio Sci. Lab., Stanford Univ.

HO, D. (1972): Modifications of quasi-periodic emissions by whistlers, periodic emissions and hiss. Tech. Rep. 3465–1, Radioscience Stanford, Calif.

HO, D. (1973): Interaction between whistlers and quasi-periodic VLF emissions. J. Geophys.

Res., **78**, 7347–7356.

HOLZER, R.E., FARLEY, T.A., BURTON, R.K. and CHAPMAN, M.C. (1974): A correlated study of ELF waves and electron precipitation on Ogo 6. J. Geophys. Res., **79**, 1007–1013.

HUGHES, W.J. (1974): The effect of the atmosphere and ionosphere on long period magnetospheric micropulsations. Planet. Space Sci., **22**, 1157–1172.

HUGHES, W.J. and SOUTHWOOD, D.J.(1976): An illustration of geomagnetic pulsations structure by the ionosphere. J. Geophys. Res., **81**, 3241–3247.

IWABUCHI, M., FUJII, R. and UTSUMI, R. (1978): Gurafikku disupurei o mochiita kaiwa-gata kaiseki shisutemu (Conversational system of spectrum analysis by the use of graphic display). Nankyoku Shiryô (Antarct. Rec.), **62**, 29–70.

KANEDA, E., KOKUBUN, S., OGUTI, T. and NAGATA, T. (1964): Auroral radar echo associated with Pc-5. Rep. Ionos. Space Res. Jpn, **18**, 165–172.

KELLEY, M.C., TSURUTANI, B.T. and MOZER, F.S. (1975): Properties of ELF electromagnetic waves in and above the earth's ionosphere deduced from plasma wave experiments on the OVI-17 and Ogo 6 satellites. J. Geophys. Res., **80**, 4603–4611.

KENNEL, C.F. and PETSCHEK, H.E. (1966): Limit of stably trapped particle fluxes. J. Geophys. Res., **71**, 1–28.

KIMURA, I. (1967). On observations and theories of the VLF emissions. Planet. Space Sci., **15**, 1427–1462.

KIMURA, I. (1974): Interrelation between VLF and ULF emissions. Space Sci. Rev., **16**, 389–411.

KITAMURA, T., JACOBS, J.A., WATANABE, T. and FLINT, R.B.J. (1969): An investigation of quasi-periodic VLF emissions. J. Geophys. Res., **74**, 5652–5664.

KOKUBUN, S. (1971): Association between quasi-periodic VLF emission and micropulsation. Rep. Ionos. Space Res. Jpn, **25**, 383–388.

KOKUBUN, S., HAYASHI, K. and OGUTI, T. (1969): VLF emission study at Syowa Station, Antarctica—Polar chorus emission and world-wide geomagnetic variation. JARE Sci. Rep., Ser. A, **6**, 34p.

KOKUBUN, S., MAKITA, K. and HIRASAWA, T. (1972): VLF-LF hiss during polar substorm. Rep. Ionos. Space Res. Jpn, **26**, 138–148.

KOKUBUN, S., MCPHERRON, R.L. and RUSSELL, C.T. (1976): Ogo 5 observations of Pc 5 waves: Ground-magnetosphere correlations. J. Geophys. Res., **81**, 5141–5149.

KOROTOBA, G.I., KLEYMENOVA, N.G. and RASPOPOV, O.M. (1975): Modulation of VLF hiss by geomagnetic pulsations. Geomagn. Aeron., **15**, 149–151.

LANZEROTTI, L.J. and FUKUNISHI, H. (1974): Modes of magnetohydromagnetic waves in the magnetosphere. Rev. Geophys. Space Phys., **12**, 724–729.

LANZEROTTI, L.J., MACLENNAN, C.G. and EVANS, C. (1978): Association of ULF magnetic variations and changes in ionospheric conductivity during substorms. J. Geophys. Res., **83**, 2525–2532.

MAKITA, K. (1978): Study of auroral hiss emissions associated with the aurora. Ph. D. Thesis, Univ. of Tokyo.

MAKITA, K. and FUKUNISHI, H. (1973): Syowa Kiti ni okeru VLF emisshon kansoku (1970–1971). I. Ôrora·hisu to ôrora (Observation of VLF emissions at Syowa Station in 1970–1971. I. Relationship between the occurrence of auroral hiss emissions and the location of auroral arcs). Nankyoku Shiryô (Antarct. Rec.), **46**, 1–15.

MCDIARMID, I.B. and BURROWS, J.R. (1968): Local time asymmetries in the high-latitude boundary of the outer radiation zone for the different electron energies. Can. J. Phys., **46**, 49–57.

MCDIARMID, D.R. and MCNAMARA, A.G. (1972): Periodically varing radio aurora. Ann. Géophys., **28**, 433–441.

McPherron, R.L., Parks, G.K., Coroniti, F.V. and Ward, S.H. (1968): Studies of the magnetospheric substorm. 2. Correlated magnetic micropulsations and electron precipitation occurring during auroral substorms. J. Geophys. Res., **73**, 1697–1713.

Morioka, A. and Saito, T. (1971): Daytime irregular geomagnetic pulsation, Pid, and its relation to magnetospheric substorm. Rep. Ionos. Space Res. Jpn, **25**, 343–359.

Morozumi, H.M. (1965): Enhancement of VLF chorus and ULF at the time of SC. Rep. Ionos. Space Res. Jpn, **19**, 371–373.

Oguti, T. (1975): Hiss emitting auroral activity. J. Atmos. Terr. Phys., **37**, 761–768.

Oguti, T. and Watanabe, T. (1976): Quasi-periodic poleward propagation of on-off switching aurora and associated geomagnetic pulsations in the dawn. J. Atmos. Terr. Phys., **38**, 543–551.

Parker, E.N. (1967): The dynamical theory of gases and fields in interplanetary space. Solar-Terrestrial Physics, ed. by J.W. King and W.S. Newman. New York, Academic Press, 45–55.

Pope, J.H. (1963): A high-latitude investigation of natural-very-low-frequency electromagnetic radiation known as chorus. J. Geophys. Res., **68**, 83–99.

Reido, J.S. (1976): An ionospheric origin for Pi 1 micropulsations. Planet. Space Sci., **24**, 705–710.

Rosenberg, T.J., Helliwell, R.A. and Katsufrakis, J.P. (1971): Electron precipitation associated with discrete very-low-frequency emissions. J. Geophys. Res., **76**, 8445–8452.

Russell, C.T., Holzer, R.E. and Smith, E.J. (1969): OGO 3 observations of ELF noise in the magnetosphere. 1. Spatial extent and frequency of occurrence. J. Geophys. Res., **74**, 755–777.

Russell, C.T., McPherron, T.L. and Coleman, P.J., Jr. (1972): Fluctuation magnetic fields in the magnetosphere. Space Sci. Rev., **12**, 810–865.

Sato, N. and Hayashi, K. (1976): Kyokko-tai ni okeru ELF hôsha no tôrai hôkô kansoku (Direction finding of ELF emissions in auroral zone). Nankyoku Shiryô (Antarct. Rec.), **55**, 1–19.

Sato, N., Hayashi, K., Kokubun, S., Oguti, T. and Fukunishi, H. (1974): Relationships between quasi-periodic VLF emission and geomagnetic pulsation. J. Atmos. Terr. Phys., **36**, 1515–1526.

Sazhin, S. (1978): A model of quasi-periodic VLF emissions. Planet. Space Sci., **26**, 399–401.

Shukula, P.K. and Spatschek, K.H. (1976): On the modulation of whistler turbulence by magneto-acoustic perturbations. Geophys. Res. Lett., **3**, 225.

Southwood, D.J. (1974): Some features of field line resonances in the magnetosphere. Planet. Space Sci., **22**, 483–491.

Storey, L.R.O. (1953): An investigation of whistling atmospherics. Philos. Trans. R. Soc. London, Ser. A, **246**, 113–141.

Sugiura, M. and Wilson, C.R. (1964): Oscillation of the geomagnetic field lines and associated magnetic perturbations at conjugate points. J. Geophys. Res., **69**, 1211–1216.

Tamao, T. (1978): Coupling modes of hydromagnetic oscillations in non-uniform, finite pressure plasma: Two-fluids model. Planet. Space Sci., **26**, 1141–1159.

Taylor, W. and Gurnett, D.A. (1968): The morphology of VLF emission observed with the Injin 3 satellite. J. Geophys. Res., **73**, 5615–5625.

Thorne, R.M., Malloy, E.J. and Tsurutani, B.T. (1977): The local time variation of ELF emissions during periods of substorm activity. J. Geophys. Res., **82**, 1585–1590.

Troitskaya, V.A., Plyasova-Bakunina, T.A. and Gul'yel'mi, A.V. (1971): Relationship between Pc 2–4 pulsations and the interplanetary magnetic field. Dokl. Akad. Nauk SSSR, **197**, 1312.

TSURUDA, K. and HAYASHI, K. (1975): Direction finding technique for elliptically polarized VLF electromagnetic waves and its application to the low-latitude whistlers. J. Atmos. Terr. Phys., **37**, 1193–1202.

TSURUTANI, B.T. and SMITH, E.J. (1974): Postmidnight chorus: A substorm phenomenon. J. Geophys. Res., **79**, 118–127.

TSURUTANI, B.T. and SMITH, E.J. (1977): Two types of magnetospheric ELF chorus and their substorm dependences. J. Geophys. Res., **82**, 5112–5128.

UNGSTRUP, E. (1967): Very low frequency emission associated with aurora and particle precipitation. Aurora and Airglow, ed. by B.M. MCCORMAC. New York, Reinhold, 599–605.

UNGSTRUP, E. and JACKEROTT, L.M. (1963): Observation of chorus below 1500 cycles per second at Godhaven, Greenland from July 1957 to December 1961. J. Geophys. Res., **68**, 2141–2146.

WATTS, J.M., KOCH, J.A. and GALLET, R.M. (1963): Observations and results from the "hiss recorder", an instrument to continuously observe the VLF emissions. J. Res. Natl Bur. Stand., Sect. D, **67D**, 569–579.

(*Manuscript received September 15, 1979*;
Revised manuscript received June 25, 1980)